Tampere University of Technology
Institute of Communications Engineering

Tero Isotalo

Optimal Antenna Downtilting in WCDMA Based Networks

Master of Science Thesis

Subject Approved by Department Council 14.1.2004
Examiners: Prof. Jukka Lempiäinen
M.Sc. Jarno Niemelä

Contents

Abstract

Tampere University of Technology
Degree program in Electrical Engineering
Institute of Communications Engineering
Isotalo, Tero: Optimal Antenna Downtilting in WCDMA Based Networks
Master of Science thesis, 84 p.
Examiners: Prof. Jukka Lempiäinen, M.Sc. Jarno Niemelä
Funding: National Technology Agency of Finland (TEKES)
Department of Electrical Engineering
December 2004

The 3rd generation mobile communication systems are designed to provide sufficient capacity for services that require high bit rates. The WCDMA technology has been chosen for the technique of UMTS, the 3rd generation mobile system used in Europe. Proper radio network planning is a key in optimizing the network capacity and coverage, and controlling interference levels in the network, that is an important task of radio network planning in WCDMA systems. Base station antenna downtilting is an efficient method to direct antenna radiation more precisely to the cell area and to reduce interference to adjacent cells. Antenna downtilt has already been used in GSM networks, but general rules for defining and optimizing antenna downtilt angle in WCDMA systems with different topologies can not be found in literature.

In the thesis, the impact of the base station antenna downtilt on UMTS network performance is studied. The effect of downtilting technique has been evaluated by comparing the behavior of mechanical downtilt to electrical downtilt. The effect of base station antenna height, antenna vertical beamwidth, and site spacing on the optimum downtilt angle has been evaluated in a 3- and 6-sectored cellular network in a macrocellular environment. Both downlink and uplink performances are considered with a special attention to soft handover areas. The results are based on system-level simulations utilizing a Monte Carlo approach.

System capacity was improved and optimal downtilt angle was found in all simulation scenarios. Optimal angles were between 3.4° and 10.3° depending on the chosen macrocellular configuration. According to the results, the base station antenna vertical beamwidth has the greatest impact on the optimum downtilt angle. A wider antenna vertical beamwidth requires a larger downtilt angle in order to obtain the optimum system performance. In addition, compared to antenna vertical beamwidth, site spacing and base station antenna height affect optimum downtilt angle in a smaller scale. Electrical downtilt performs slightly better in most scenarios, but the differences in capacity and coverage are rather small. Moreover, it has been observed how soft handover areas can be shaped with antenna downtilt.

Tiivistelmä

Tampereen teknillinen yliopisto
Sähkötekniikan koulutusohjelma
Tietoliikennetekniikan laitos
Isotalo, Tero: Antennien optimaalinen tilttaus UMTS-radioverkossa
Diplomityö, 84 s.
Tarkastajat: Prof. Jukka Lempiäinen, DI Jarno Niemelä
Rahoittajat: TEKES
Sähkötekniikan osasto
Joulukuu 2004

Matkapuhelimet ovat levinneet koko kansan saataville kaikissa teollistuneissa maissa ympäri maailman. Samanaikaisesti Internetistä on tullut välttämättömyys ihmisten jokapäiväisessä elämässä niin kotona kuin työssä. Nämä kaksi teknologista saavutusta ovat yhdistymässä; sähköposti ja www-selaus ovat löytäneet tiensä myös matkapuhelimiin. Uusien palveluiden tulo matkapuhelimiin vaatii jatkuvasti lisää kapasiteettia matkapuhelinverkkoihin. GSM-verkot ovat toistaiseksi tarjonneet riittävästi kapasiteettia puhekäyttäjille. Perus-GSM:n datansiirtokapasiteetti on kohtalaisen heikko, mutta pakettikytkentäinen GPRS toi GSM:lle lisää kapasiteettia. Uusin GSM-tekniikkaan pohjautuva tekniikka on EDGE, jossa GSM:ään kehitetty uusi modulaatiotekniikka tarjoaa jo reilusti vanhoja modeemiyhteyksiä nopeamman yhteyden.

Uusi, mutta jo pitkään julkisuudessa ollut kolmannen sukupolven, matkapuhelinjärjestelmä on viemässä langattoman viestinnän uusille urille. Vaikka UMTS-puhelimet tulevat aluksi olemaan vain yrityskäyttäjien taskuissa, on internet tulossa myös tavallisien matkapuhelinkäyttäjien saataville. Ensimmäiset 3G-verkot ovat olleet käytössä ympäri maailmaa jo jonkin aikaa, ja viimein Suomeenkin on saatu 3G-verkot kaupalliseen käyttöön. Alkuvaiheessa liikennemäärät verkoissa eivät tule olemaan suuria. Käyttäjien ja liikennemäärien kasvaessa verkkojen kapasiteettiin aletaan kiinnittää enemmän huomiota, jolloin radioverkkojen suunnitteluun ja optimointiin pitää panostaa enemmän.

3G-verkkojen radiorajapinnaksi Euroopassa käytössä olevassa UMTS-järjestelmässä on valittu laajakaistainen koodijakoinen monipääsytekniikka, WCDMA. WCDMA-tekniikassa kaikki käyttäjät jakavat saman taajuuskaistan, ja eri käyttäjät erotellaan hajotuskoodien perusteella. WCDMA-järjestelmän kapasiteetti on voimakkaasti riippuvainen käytetyllä taajuuskaistalla olevien häiriöiden määrästä. Häiriötehon kasvu näkyy suoraan verkon kapasiteetin laskuna. Tämän vuoksi häiriöiden minimointi on yksi tärkeimmistä tehtävistä radioverkkojen suunnittelussa.

Antennin alastilttauksella tarkoitetaan antennin säteilytehon suuntaamista alaspäin, eli antennin pystysuuntaisen keilan suuntaamista kohti maata. Solukkoverkoissa

käytettävä antenni koostuu ryhmästä antennielementtejä, joiden määrällä säädellään antennin pysty- ja vaakasuuntaista keilanleveyttä. Tämän vuoksi antennia kutsutaan antenniryhmäksi. Mekaanisessa alastilttauksessa koko antenniryhmää käännetään fyysisesti alaspäin antennin pääkeilan suunnassa, jolloin antennin takakeila suunnataan ylöspäin, ja sivukeilojen suunta ei muutu ollenkaan. Sähköisessä alastilttauksessa antenniryhmän eri antennielementtien välistä vaihe-eroa säädellään, jolloin pystytään kääntämään antennin pystysuuntaista keilaa alaspäin kaikissa vaakasuunnissa. Vaihe-ero voidaan aikaansaada joko sähköistä viivettä lisäämällä, tai yksinkertaisesti siirtämällä antennielementtejä toisiinsa nähden.

Antennien alastilttaus on tehokas tapa estää antennin säteilytehon leviämistä solukkoverkon viereisiin soluihin, jolloin haluttuun soluun saadaan hyvä peitto, ja samalla häiriöt viereisiin soluihin pysyvät alhaisena. Antennien alastilttausta on käytetty jo GSM-verkoissa, mutta WCDMA-verkoissa antennien säteilyn suuntaamisella solun alueelle on vieläkin suurempi merkitys, koska häiriöiden määrä vaikuttaa voimakkaasti WCDMA-verkon suorituskykyyn. Antennien tilttausta WCDMA-verkoissa on tutkittu runsaasti, ja siitä löytyy tietoa kirjallisuudesta, mutta erilaisten tukiasema- ja antennikokoonpanojen vaikutusta optimaaliseen tilttauskulmaan ei ole tutkittu riittävästi, eikä optimaalisia tilttauskulmia eri kokoonpanoille ole esitetty.

Tässä on diplomityössä on tutkittu tukiasema-antennien alastilttauksen vaikutusta WCDMA-verkon kapasiteettiin eri tukiasema- ja antennikokoonpanoilla. Tukiasemien välisen etäisyyden, antennikorkeuden, antennin pystysuuntaisen keilanleveyden, sektorien määrän, sekä tilttausmenetelmän (sähköinen / mekaaninen) vaikutusta optimaaliseen tilttauskulmaan on tutkittu. Tutkimuksessa on käytetty kaupallista Nokia NetAct radioverkkosimulointiohjelmistoa. Simulaatiot perustuvat COST-231-Hata -etenenismallin käyttöön, sekä tilastolliseen Monte Carlo -analyysiin. Simuloinneissa on pyritty käyttämään parametreja, jotka vastaavat mahdollisimman paljon todellisia arvoja käytännön WCDMA-radioverkossa.

Diplomityössä analysoitiin ylä- että alalinkin suorituskykyä, kiinnittäen erityishuomiota WCDMA-verkossa tapahtuviin pehmeän solunvaihdon alueisiin. Kaikille simuloiduille kokoonpanoille löydettiin optimaalinen alastiltauskulma, ja systeemin kapasiteetti kasvoi optimaalisen alastilttauksen avulla kaikilla kokoonpanoilla. Optimaaliset alastilttauskulmat vaihtelevat välillä 3.4° - 10.3° kokoonpanosta riippuen . Simulaatiotulosten perusteella antennin pystysuuntaisella keilanleveydellä on suurin vaikutus optimaaliseen tilttauskulmaan, leveämpikeilainen antenni vaatii suuremman tilttauskulman. Myös antennikorkeus ja tukiasemien välinen etäisyys vaikuttavat; mitä korkeammalla antennit ovat ja mitä pienempi on tukiasemien välinen etäisyys, sitä suurempaa tilttauskulmaa tulee käyttää. Antennin sähköisellä tilttauksella saavutetaan parempi suorituskyky kuin mekaanisella, mutta erot ovat pieniä. Myös pehmeän solunvaihdon alueisiin pystytään vaikuttamaan antennien alastilttauksella.

List of Abbreviations

1G	1st generation
2G	2nd generation
2.5G	Enhanced 2nd generation
3G	3rd generation
3GPP	3rd Generation Partnership Project
4G	4th generation
ADSL	Asynchronous digital subscriber line
AS	Active set
BER	Bit error rate
BLER	Block error rate
BS	Base station
BSC	Base station controller
BSS	Base station subsystem
BTS	Base station
CAEDT	Continuously adjustable electrical downtilt
CCCH	Common control channel
CDMA	Code division multiple access
CN	Core network
CPICH	Common pilot channel
CS	Circuit switched
DL	Downlink
DPCCH	Dedicated physical control channel
DS	Direct sequence
EDGE	Enhanced data rates for GSM evolution
EDT	Electrical downtilt
EIRP	Effective isotropic radiated power
FDD	Frequency division duplex
FDMA	Frequency division multiple access
FFT	Fast Fourier transform

GGSN	Gateway GPRS support node
GMSC	gateway MSC
GPRS	General Packet Radio Service
GSM	Global System Mobile
HLR	Home location register
HO	Handover
HSCSD	High speed circuit switched data
HSDPA	High speed downlink packet access
IM	Interference margin
IMT-2000	International Mobile Telephony 2000
Iu	Interface between UTRAN and CN
Iub	Interface between RNC and Node B
ITU	International Telecommunication Union
KPI	Key performance indicator
LNA	Low-noise amplifier
LOS	Line-of-sight
ME	Mobile equipment
MDT	Mechanical downtilt
MRC	Maximal ratio combining
MS	Mobile station
MSC	Mobile services switching center
NB	Narrowband
NLOS	Non-line-of-sight
NMT	Nordic Mobile Telephone
Node B	BTS in UMTS
NRT	Non-realtime
OVSF	Orthogonal variable spreading factor
PC	Power Control
PCS	Personal Communications Service
PG	Processing gain
PRACH	Physical random access channel
PS	Packet switched
PSTN	Public switched telephone network
RET	Remote antenna downtilt
RNC	Radio network controller
RNP	Radio network planning
RRC	Radio resource control

Rx	Receive, receiver
SCH	Synchronization channel
SF	Spreading factor
SP	Service probability
SGSN	Serving GPRS support node
SHO	Soft Handover
SIR	Signal-to-interference ratio
TDD	Time division duplex
TDMA	Time division multiple access
Tx	Transmit, transmitter
TS	Traffic mix scenario
UE	User equipment
UL	Uplink
UMTS	Universal Mobile Terrestrial System
USIM	UMTS subscriber identity module
UTRA	UMTS terrestrial radio access
UTRAN	UMTS terrestrial radio access network
Uu	Interface between UE and UTRAN
VLR	Visitor location register
WCDMA	Wideband CDMA
WB	Wideband
WLAN	Wireless local area network

List of Symbols

Δf_c	Coherence bandwidth
η_{DL}	Downlink load factor
η_{UL}	Uplink load factor
δh	Uplink load factor
λ	Wavelength
ν_e	Electrical downtilt angle
ν_m	Mechanical downtilt angle
$\theta_{VER,BW}$	Antenna vertical beamwidth factor
θ_T	Topological factor
B	Chip rate
B	Breakpoint distance
C	Slope factor, Correction factor for h_{BTS} in Okumura-Hata
C_m	Area correction factor
d	Distance
E_b/N_0	Received energy per bit to noise energy ratio
E_c/I_0	Received energy per chip to interference ratio
f	Frequency
F	Noise figure
G_r	Received power
G_t	Transmitted power
h_{BTS}	Base station effective antenna height
h_{MS}	Mobile station antenna height
IM	Interference margin
IM_{DL}	Interference margin in downlink direction
IM_{UL}	Interference margin in uplink direction
k	Boltzman's constant
L	Path loss
N	Thermal noise density

PG	Processing gain
P_N	Noise power
P_r	Received power
P_t	Transmitted power
R	Data rate
S	Delay spread
T	Temperature
T	Time to trigger
W_b	Total bandwidth
W_c	Chip Rate

Chapter 1

Introduction

Traditional wired telephone expanded to commercial use in the beginning of 20th century. It enabled real-time interpersonal speech communication over long distances. A few decades later, public radio stations started transmissions, and in the middle of 1900s, also televisions became common for people. In early 1980's NMT-network (Nordic Mobile Telephone) was launched in Scandinavian, and it started the conquest of cellular networks. By that time, digitalization of telephone networks was already on the way. Soon after NMT, digital cellular system, GSM (Global System Mobile), was launched. By the end of 20th century, cellular mobile phones had found their way to everyday life in the western countries.

Concurrently with telephone networks changing towards wireless, data networks, especially Internet has blazed its trail to the desktop of people. Email and web surfing are necessary for everyday living for many people and businesses. At the moment, slow modem connections are disappearing and faster ADSL (asynchronous digital subscriber line) connections are becoming more general. Internet is also changing to wireless, WLAN (wireless local area network) networks can be nowadays found in many office buildings and homes, and even city-wide WLAN networks are available. However, the coverage of WLAN-networks is rather limited, and mobility issues are poorly supported. Already GSM system could be used for data transmission, with data rates comparable to modem connections. Improvements in GSM, like circuit switched HSCSD (high speed circuit switched data), and packet switched GPRS (general packet radio service) enhanced data transmission capability, but customer requirements for Internet connection speed were still far ahead. EDGE (enhanced data rates for GSM evolution) with new modulation technique improves the data rate. With EDGE, the GSM system can be tuned to the maximum, but always higher data rates are required.

The first version of 3rd generation (3G) system provides throughput of 384 kbps in downlink direction, and there are already standardized concepts for higher data rates, such as HSDPA (high speed downlink packet access). First mobile cellular networks using 3rd generation techniques have been launched in most sense urban areas all over the world. In the European 3G system, UMTS (universal mobile terrestrial system), WCDMA (wideband code division multiple access) technique will be used for the radio interface. New 3G networks have been launched actively during year 2004, and in a few years, WCDMA networks will most probably be available in a great part of today's GSM coverage areas. However, a lot of research work still needs to be done in the area of radio network planning, before WCDMA networks can be built in an optimal way. Proper coverage overlapping,

antenna downtilt and antenna height with well estimated capacity need make it possible to reduce iterations rounds on network optimizing.

Base station antenna downtilt can be used to direct antenna beam in desired area and therefore it is an efficient method to control coverage overlapping of adjacent base stations in the network.

In WCDMA network, interference level affects capacity very powerfully, and also coverage is affected. Base station antenna downtilt can be used to direct antenna beam in desired area, and therefore it an efficient method to control antenna radiation to the network area [1]. Thus, interference can be decreased and capacity of a network can be enhanced [2, 3]. Therefore antenna downtilt is an important and interesting radio network planning (RNP) optimizing task.

Mechanical antenna downtilt was studied in [4], and as a continuation, electrical antenna downtilt studies were considered as an important step in order to have a comprehensive understanding of WCDMA topology planning and optimization. In WCDMA, soft handovers (SHO) provide additional gain to the radio link budget. The effect of downtilt angles on probabilities of SHO connections in the network area and effect on the areas where SHO connections happen is also an interesting area to be studied as a part of downtilt studies.

The studies for the thesis are carried out by simulations with radio network simulator with Monte Carlo approach. Different site locations and antenna configurations are used in order to study downtilt in macrocellular environment, and to find optimal downtilt angles for different site and antenna configurations.

The thesis is organized as follows: Chapter 1 introduces the thesis and UMTS system is introduced in Chapter 2. In Chapter 3, basics of WCDMA cellular networks are considered, and in Chapter 4, WCDMA radio network planning aspects are considered. Simulation environment is described in Chapter 5, and simulation results are presented in Chapter 6. The thesis is concluded in Chapter 7.

Chapter 2

Introduction to UMTS System

In mobile communication systems, the capacity of air interface is usually the limiting factor of the whole system, while large geographical areas need to be covered. The UMTS system is designed to provide high data rates for users to whom existing mobile networks do not provide enough capacity. The main difference compared to previous mobile communication systems is the new radio interface, WCDMA, but also the radio access network (RAN) and the core system has been modified. In this chapter, the background of the 3G systems development and the functionality of the UMTS system is covered.

2.1 Evolution to UMTS

Analog, the 1st generation (1G) cellular mobile systems, such as NMT in Scandinavia and AMPS (advanced mobile phone system) in USA, started the conquest of wireless communications in early the 1980's. As technological development went on, digital systems, like GSM in Europe and PCS (personal communications service) in USA (2nd generation, 2G) overran the old ones. Also prices of mobiles started to go down, and in the end of 1990's mobile phones were widely distributed and commonly used everywhere in the post-industrialized countries. Furthermore, concurrently also the Internet started to expand and people started to use emails and web-browsing in their everyday life. Next step was the coalescence of these two worlds, and big steps have already been taken. Limited data transfer capacity of existing mobile systems required new techniques to be evolved. Some additions were made for the existing 2G system, like GPRS, and EDGE (also called 2.5G), but these do not totally fulfill the requirements set for the future telecommunication system. WLAN technology is approaching high data rate users from another direction, but it is not designed to cover large areas and also mobility issues are still under development.

New 3rd generation (3G) UMTS system is made to respond future requirements; provide high data rates, provide different services dynamically to large number of users, and also enable flexible mobility inside UMTS networks and easy changing to other mobile network systems. Naturally, development of mobile networks is not ending here, next generation systems for the future, called beyond 3G or 4G (4th generation), are being developed actively. However, 3G systems represent already present day and operators and mobile phone industry are waiting for breakthrough in markets. In near future, mobiles are likely to develop in such a way, that one equipment will be compatible with 2G and 3G systems all over the world, with also WLAN connectivity included.

2.2 Standardization

UMTS as one of the 3G techniques, was selected for 3G system used in Europe, and is used also in Japan and Korea. Later in this study, only UMTS is meant with the term 3G. ITU (International Telecommunication Union) has defined the name IMT-2000 (International mobile telephony 2000) for 3G systems, and 3GPP (3rd Generation Partnership Project) -organization is in charge of standardization work. WCDMA multiple access technology is chosen for the European 3G system, UMTS, and 3GPP calls WCDMA as UTRA (universal terrestrial radio access) FDD (frequency division duplex) and UTRA TDD (time division duplex). In the thesis, only UTRA FDD is covered. In Figure 2.1, the organization of 3GPP mobile network family is shown.

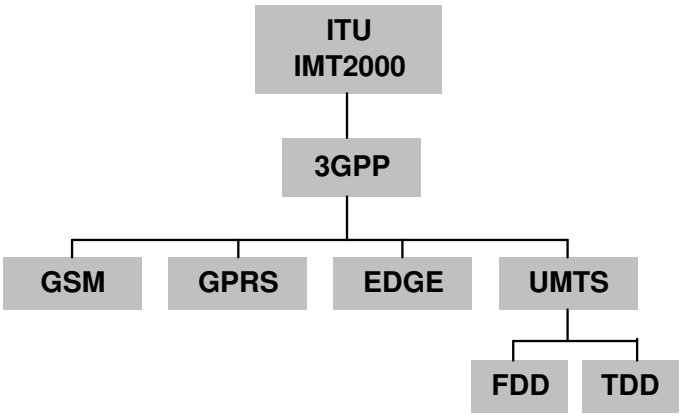

Figure 2.1: ITU 3GPP mobile network family. [5]

2.3 UMTS System

UMTS system is divided into three distinct subsystems; user equipment (UE), UMTS terrestrial radio access network (UTRAN), and core network (CN). The radio interface between UE and UTRAN (Uu), and the interface between UTRAN and CN (Iu) connect the subsystems. Iu connects RNC in packet switched (PS) or circuit switched (CS) part of core network, and so it is called either Iu-ps or Iu-cs.

Core Network

Home location register (HLR) is a database containing user service profile information and UE location information, and is located in user's home system.

MSC/VLR (mobile services switching center (MSC) / visitor location register (VLR)) works as a switch for circuit switched data , and stores visiting users' service profile information.

GMSC (gateway MSC) is a switch at the connection point to PSTN (Public switched telephone network) and other circuit switched networks.

SGSN (serving GPRS support node) works similarly in a packet switched network like MSC in circuit switched, i.e., switches packet switched connections.

GGSN functionality is similar to GMSC. It is a connection point for packet switched connections, such as the Internet.

[6, 7]

UTRAN

UTRAN consists of two parts, Node B and RNC. Node B is responsible for radio transmission and reception in air interface with UEs. The term base station (BS, or BTS in GSM) is a synonym to Node B, which is used in UMTS. RNC (radio network controller) controls radio resources of the Node Bs connected to it and radio transmission between UE and Node Bs. Iub is the interface that connects RNC Node Bs There is also an interface between RNCs, Iur, which enables soft handovers (SHO) between RNCs. [6, 7]

UE

UE is the equipment that connects user to the radio interface. UE consists of ME (mobile equipment) and USIM (UMTS subscriber identity module). ME is the radio terminal for communication over Uu interface. USIM is a smartcard that holds user information and algorithms as well as information for authentication and security. [6]

GSM elements

In UMTS system block diagram in Figure 2.2, there are also subsystems such as BSS (base station subsystem) and MS (mobile station). This illustrates how GSM is also a part of UMTS network. BSS consists of BSCs (base station controller) and BTSs (base station), like UTRAN consists of RNCs and Node Bs.

2.4 WCDMA for UMTS

2.4.1 UMTS Frequency and Channel Allocation

In WCDMA specifications, chip rate is fixed to 3.84 Mchip/s, and bandwidth of channel to 5 MHz [8]. The center frequency of the channel can be in raster of 200 kHz. Figure 2.3 illustrates the theoretical spectrum of two WCDMA channel. Frequency areas allocated for UTRA FDD are 1920 - 1980 MHz in uplink direction and 2110 - 2170 MHz in downlink. For UTRA TDD, two bands, 1900 - 1920 MHz and 2010 - 2015 MHz are allocated. [9] However, in the thesis, only UTRA FDD is covered.

2.4.2 Code Allocation

In UMTS, two different codes are used in transmission. Channelization codes are OVSF (orthogonal variable spreading factor) codes, and they are used to separate transmission to different users in downlink direction, and in uplink direction to separate data and control channels of one UE. Channelization codes are reused for every mobile and every base station, so therefore scrambling codes are needed to separate cells in downlink direction and to separate mobiles in uplink direction. [6] The principle of scrambling and descrambling is discussed in more detail in Section 3.5.

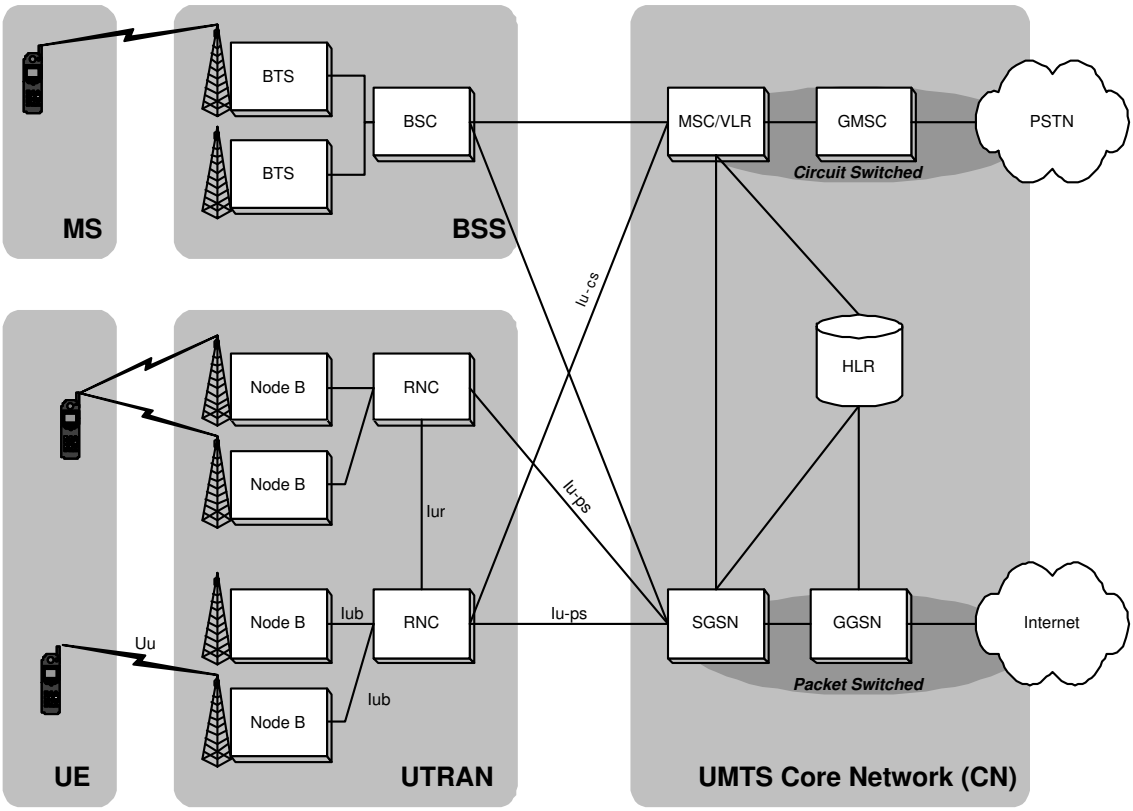

Figure 2.2: High-level UMTS system model and network elements.

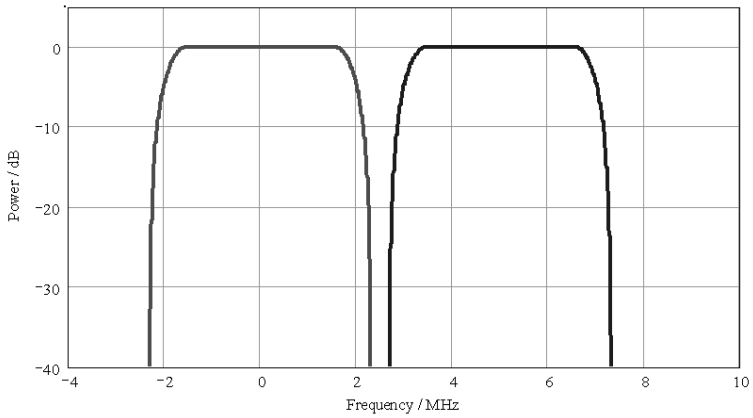

Figure 2.3: Theoretical spectrum of two WCDMA carriers with 5 MHz channel spacing. [5]

2.4.3 Channels and Signalling

The radio frame structure in UMTS is such, that in uplink and downlink, separate 5 MHz bands are used for transmission. Transmission is divided into 10ms radio frames, which consists of 15 slots, and each slot consists of 2560 chips. One slot also corresponds to one power control period. [5]

In addition to user data, also lots of signaling information need to be transmitted in the network. All channels have to share the total transmit power, and therefore adjusting the

powers of different channels is an important planning and optimization task in UMTS. The channels are divided into dedicated and common channels, and the channels are transferred in physical, transport, and logical layers.

Total description of UMTS channel structure and channel mapping is rather complex, and is not considered more deeply in this thesis, but can be found in the specifications [10] and [11].

2.5 RAKE Receiver

Multipath channel (Section 3.2.1) introduces delay and attenuation to each signal component. Traditional receiver sees only the sums of contemporaneously arriving signals. Therefore, in worst case, components having opposite phases, can cancel each others totally. Performance of such a receiver can be enhanced by algorithms like Viterbi, but the original problem still exists. In RAKE receiver used in WCDMA, each signal component can be treated separately, which improves performance of the receiver.

The principle of the RAKE receiver is presented in Figure 2.4. Before entering multipath channel, signal is spreaded (spreading and despreading are considered in Chapter 3.5) and modulated. Multipath channel is modeled by tapped delay line, that introduces delays, τ_i, and attenuations, a_i. Here, a three-tapped (capable of handling three multipath components) line is illustrated but the number of lines can be higher. Sum of multipath components is received, and demodulated. In the RAKE receiver, so-called fingers exists for each multipath component. Each multipath component is then despreaded in an individual correlator, where delay and attenuation errors are estimated and corrected. Thereafter, different fingers are summed. This is called maximal ratio combining (MRC). As multipath propagation environment changes continuously due to, e.g., mobile movement, delays and attenuations also change and the receiver needs to adjust itself when needed. Performance of the RAKE receiver depends on the number of multipath components it is capable of handling simultaneously. [12, 13]

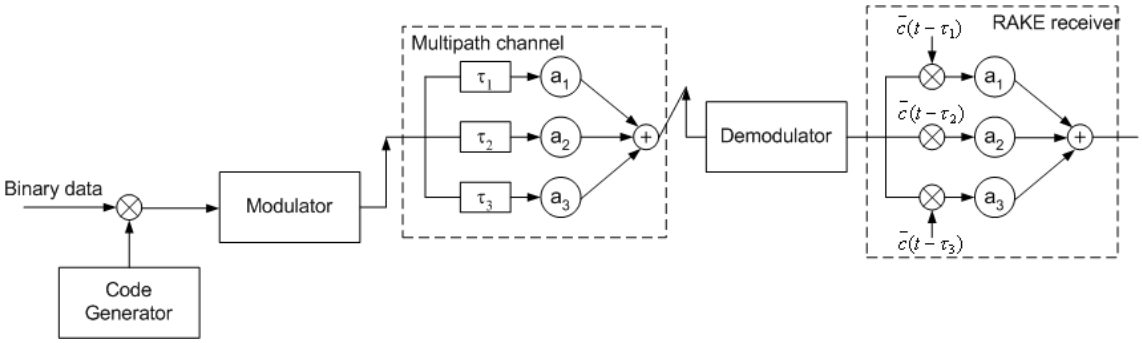

Figure 2.4: Principle of RAKE receiver. [12]

2.6 Power Control

From overall network capacity point of view, it is important that all transmission, in uplink and downlink, is done at the minimum acceptable level. This becomes critical especially in UMTS network, where frequency reuse is universal and interference plays a major role

in network capacity and coverage. If one or a few users near a base station use too high transmit powers, especially in uplink direction, they can block the whole network from the users further from the base station, because users always interfere each others due to, e.g., imperfect orthogonality of codes. Adjustment of transmit power of Node B and UE is called power control (PC), and it consists of different levels of controlling; open loop, inner loop and outer loop (Figure 2.5). [5, 7]

Open Loop Power Control

Open loop power control sets the initial power for UE or Node B, when more specific power control algorithms are not available. In uplink direction, open loop power control sets the power of first preamble of PRACH (physical random access channel) and DPCCH (dedicated physical control channel). [5, 7]

Inner Loop Power Control

In inner loop power control, received SIR (signal-to-interference ratio) is compared to SIR target at Node B, and power control commands are sent to UE. Inner loop power control commands are sent with frequency of 1500 Hz, which results in the update rate of 1500 Hz in faster power control algorithm, where Tx power is updated after every PC command. In slower power control, Tx power is updated, if five consecutive PC commands are either 'up' or 'down', which results in slower update rate. By proper usage of these algorithms in different fading environments, PC is able to compensate fast fading in most fading consequences. [5, 7]

If UE is in softer HO (handover), the PC commands are still coming from one Node B, and PC functions normally. When UE is in SHO, it is receiving PC commands from more than one Node Bs, and the commands have to be combined. [7] PC in SHO is rather complex and is explained in more detail in [14].

Outer Loop Power Control

In some cases, set SIR target is not adequate for required transmission quality. RNC monitors BER (bit error rate) or BLER (block error rate), and if quality of transmission is too low, higher SIR target is sent to Node B. Also in case of too good transmission quality, lower SIR target is sent to Node B. [5, 7]

2.7 Handovers

When UE is moving from coverage area of one cell to coverage area of another cell, a handover needs to be carried out in the area where cell coverage areas overlap in order to keep transmission going on. Hard handover is a handover where the connection to the current serving base station is first cut, and after that a connection to a new base station is established. This introduces always, if only a short, a break in the connection, which can be relevant for realtime connections, and may also be hearable in speech connection. The WCDMA technology introduces a new type of a handover, soft handover (SHO), where connection between Node B and UE can be kept up without any gaps in the transmission.

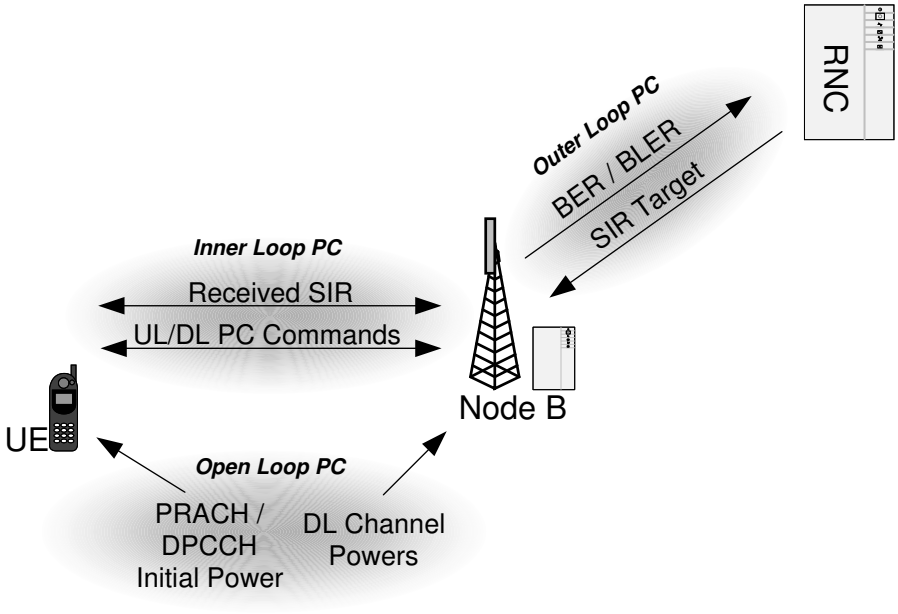

Figure 2.5: Power control in UMTS.

2.7.1 Soft and Softer Handover

In SHO, the handover is done in the same carrier, either with another Node B, or with another cell in the same Node B. When SHO is done between cells in on Node B, it is called softer handover. When UE is in SHO, it communicates with two or more Node Bs. [15]

In softer HO (Figure 2.6(a)), the same signal is sent to two sectors in the same Node B. Two air interface channels are needed because two different codes need to be used that the UE (or Node B in uplink) can separate the signals. The two signals are combined in the RAKE receiver (Section 2.4). [6]

Also in SHO (Figure 2.6(b)), two air interface channels are needed, but they are from separate Node Bs. In downlink direction, signal combining in the RAKE receiver is similar to softer HO. In uplink direction, because signals are received by separate Node Bs, the signals need to be combined in RNC. [6]

Soft Handover Gain

When UE is in soft/softer handover, macro-diversity gain exists in uplink direction, because two spatially separated Node Bs (or two spatially separated cells in same Node B) are receiving the same signal that UE is sending. [16]. The gain is proportional to the differences in path losses between the cells participating the SHO. In [17], the effect of SHO in WCDMA uplink direction with different link level differences, different channel models, and different UE speeds has been analyzed. The results show, that SHO gain is

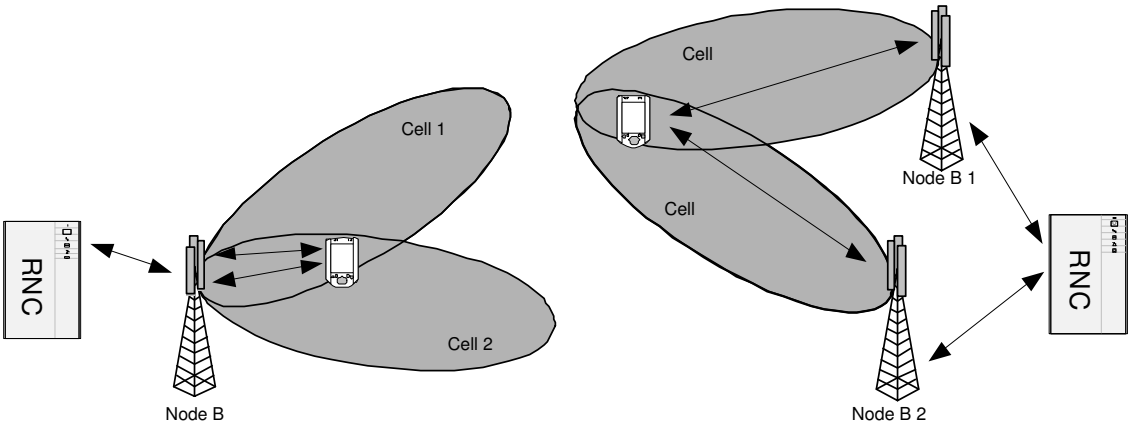

(a) Softer Handover (b) Soft Handover

Figure 2.6: Illustration of (a) softer handover and (b) soft handover. [6]

up to 4.5 dB, with slow UE speed and 0 dB level difference. SHO gain decreases below 1 dB when level difference is above 4-6 dB, depending on mobile speed. In softer HO, when combining is done in the Node B, the gain should be slightly higher [7]. In [7], also the downlink SHO gain simulation results are presented, and maximum gain of about 3 dB was observed. In uplink direction, link level difference of max. 3 dB results in gain above 1 dB. In downlink the gain can be also negative, since two (or more) simultaneous transmission lines are needed.

Soft Handover Overhead

Because in soft handover mobiles are connected to more than one cell, the mobiles consume DL transmit capacity, and introduce interference to the network. Therefore, the amount of mobiles in soft handover should be kept reasonable. [7]

Soft Handover Algorithm

An UE measures the level of all hearable CPICH (common pilot channel) pilot signals. In a normal situation, when the UE is connected to only one cell, the strongest pilot is from the cell it is connected to. Reporting range is the threshold for establishing connection to another cell, i.e. making a SHO connection. Active set (AS) means the set of cells that are simultaneously involved in the communication with UE [18]. When another pilot signal is strong enough, and AS is not full, the cell is added to the AS, if it is above *reporting range* + *hysteresis* for time to trigger (T). Similarly, a cell is removed from the AS, if the level of the pilot is below *reporting range* - *hysteresis* for time of T. A cell is replaced with another cell, if the level of the best pilot outside AS is higher than the level of the worst pilot in AS + *hysteresis for cell replacement* for time of T, and the AS is full. [15].

The operation of SHO algorithm is depicted in Figure 2.7. Reporting range is calculated from the strongest pilot in AS. First, the $Pilot1$ (red line) is dominant, and it is the only cell in AS. The level of $Pilot2$ increases, and when it reaches the upper hysteresis boundary of the reporting range, and after time T, $Pilot2$ is added to the AS. Next, level of $Pilot2$ decreases under the lower hysteresis boundary of reporting range, and is removed from AS after time T. After adding $Pilot2$ to the AS, the level of $Pilot1$ is higher than $Pilot3$ +

hysteresis for cell replacing, so *Pilot*3 is replaced with *Pilot*1. The maximum size of AS is here assumed to 2, so *Pilot*1 could not fit into AS. Otherwise *Pilot*1 would just have been added to AS.

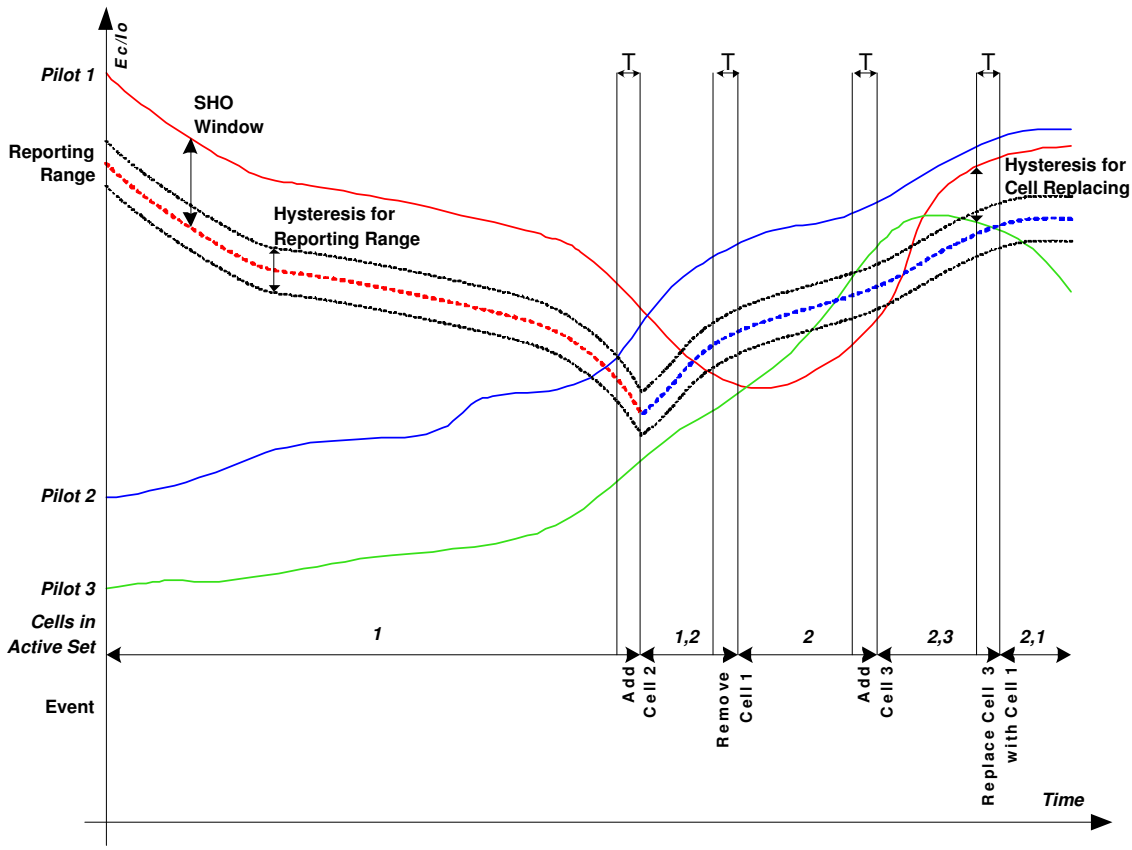

Figure 2.7: Example of soft handover algorithm [15].

2.7.2 Other Handover Types

Although SHO is the most essential handover type in WCDMA/UMTS, also other types of handovers are important to ensure seemless movement of mobiles in e.g. from pico- to micro- to macrocell when they use different frequencies, and from WCDMA to GSM. [5]

Intra-system / Intra-frequency Handover

Sometimes, when SHO can not be established, hard handovers are needed to be performed inside UMTS, even when using the same frequency. This can happen, for example, in handover between different RNCs, when Iur interface between RNCs is not established. [5] The decisions of intra-system intra-frequency HOs are made by RNC based on UE measurements. [7]

Intra-system / Inter-frequency Handover

If more than one carrier frequency is used in the network, inter-frequency hard handover can be established. Inter-frequency handover can take place for example in multi-layer

network between micro- and macrocells. Decision to perform inter-frequency handover is done by RNC, based on UE inter-frequency measurements and reports that RNC can command UE to do. [5, 7]

Inter-system Handover

Inter-system handovers are handovers between UTRA FDD and neighboring systems, such as GSM or UTRA TDD. Inter-system handovers can be made for several reasons. Capacity of GSM may not be high enough for requested services, UE may be moving outside the coverage of WCDMA network etc. Inter-system handovers can also be used to balance traffic between WCDMA and, e.g., GSM.

Chapter 3

Cellular Radio Networks

Mobile communication uses air interface in transmission. Usage of air interface enables free movement of mobile equipment, but also causes multiple things to be considered and problems to be solved. Signal attenuates rather strongly in air interface, and also multipath fading introduces challenges to signal reception.

3.1 Free Space Propagation

Fading of radio signal depends on propagation environment. Free space propagation is the simplest case, where there is no obstacles affecting the propagation. Free space propagation is described by Equation (3.1)

$$\frac{P_r}{P_t} = G_t G_r \Big(\frac{\lambda}{4\pi d}\Big)^2 \tag{3.1}$$

where P_t is transmitted power, P_r is received power, G_t is transmit gain, G_r is receive gain, λ is wavelength, and d is the distance between transmit and receive station. [19] Very often wave propagation can not be estimated with free space equation. Transmitted signal attenuates differently in different environments, and reflects and diffracts from different surfaces and obstacles. This causes different delays and distortions to signal, and more sophisticated methods need to be used to estimate radio channel. [19]

3.2 Radio Wave Propagation

3.2.1 Propagation Environment

Propagation environments are divided into macrocell, microcell, and indoor. Macrocell is thereafter divided into urban, suburban, and rural according to amount and density of built and natural obstacles. If base station antennas are over the average rooftop level, environment is considered as macrocellular, and if under the average rooftop level, microcellular. When signal is propagating inside buildings, it is treated as indoor propagation. [13] Differences between environments can be seen i.e. in varying delay spreads (3.1).

Table 3.1: Delay spread and coherence bandwidths of different environments and cellular systems [13, 20]

	Delay spread [μs]	Δf_c [MHz]	WCDMA	GSM
Bandwidth [MHz]			3.84	0.27
Macrocellular:				
Urban	0.5	0.32	WB	NB/WB
Rural	0.1	1.6	NB/WB	NB
Hilly	3	0.053	WB	WB
Microcellular	< 0.1	> 1.6	NB/WB	NB
Indoor	< 0.01	> 16	NB	NB
WB = wideband, NB = narrowband				

Multipath Propagation

When signal is propagating between a base station and a mobile station, it has many possible ways to go. In the optimal case, MS and BS are visible to each other, and signal can propagate the shortest possible way to the receiving end, which is called line-of-sight (LOS) connection. However, in typical network environment, reflections and diffractions from different obstacles enable signal to propagate via multiple paths (non-line-of-sight connection (NLOS)). This is called multipath propagation. Different paths have different lengths, and therefore the same signal arrives in separate time moments to the receiving end. These separate signals are called multipath components. Multipath propagation environment is clarified in Figure 3.1. Signals reflect typically from walls of buildings, cars etc., and diffractions occur when signal meets sharp edge, such as roofs or corners of buildings.

Delay spread, denoted as S, means the width of time window where arriving spread signal components can fit, and it is also the impulse response of channel in time domain. Typical delay spreads in different environments can be seen in Table 3.1. In Figure 3.3 (a) there is an example of impulse response of typical urban environment.

Propagation Slope

In free-space propagation, signal strength attenuation is proportional to the square of distance, r^2, which corresponds to 20 dB/decade. In macrocellular environment, propagation is not always free-space, and attenuation varies typically from 20 to 50 dB/decade, depending on the environment type (urban, rural, forest, water, open, etc). This attenuation value is called propagation slope, illustrated in Figure 3.2. Path loss between transmitting ends is strongly effected by the propagation slope. [13]

However, those pre-defined slopes are not always valid; the slope can differ although environment remains similar. For same distance from the base station, attenuation is not environment dependent, but it is proportional to inverse of distance, i.e., the attenuation is smaller. The distance from base station, where this happens, is called a breakpoint distance B, defined in Equation 3.2. [13, 21]

$$B = 4\frac{h_{BTS}h_{MS}}{\lambda} \tag{3.2}$$

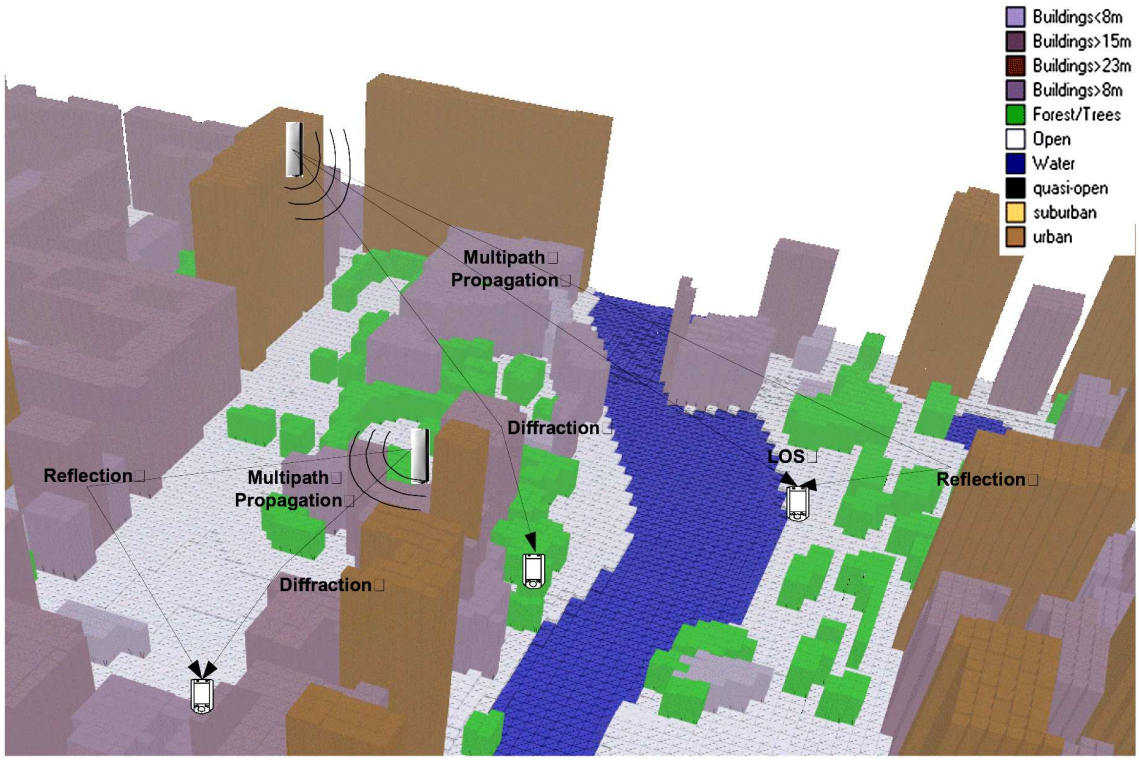

Figure 3.1: Signal propagation in multipath environment.

where h_{BTS} and h_{MS} are the heights of base station and mobile station, respectively, and λ is the wavelength of the signal.

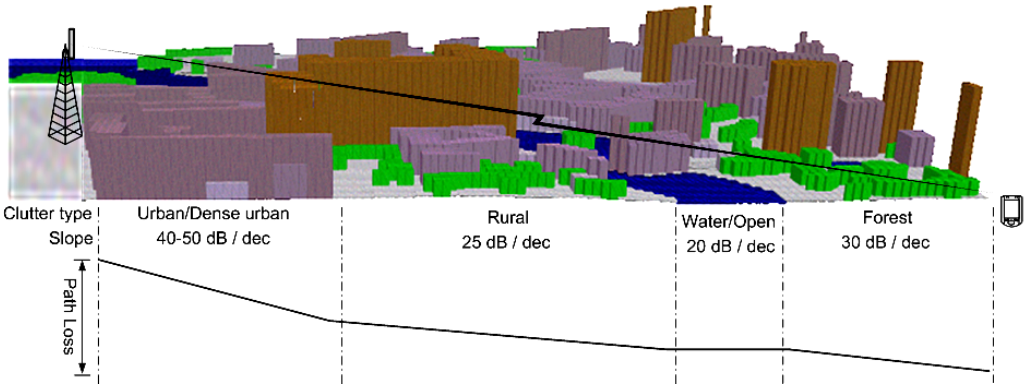

Figure 3.2: Propagation slope and path loss.

Wideband Propagation

Multipath propagation introduces fading also in frequency domain, and certain frequencies attenuate more than others. The frequency response of a typical urban channel is presented in Figure 3.3 b). Signal is considered as wideband, when coherence bandwidth of channel is much narrower than signal bandwidth. The coherence bandwidth, Δf_c, varies along different environments, and is calculated from multipath delay differences by FFT-

transforms, or from delay spread, S, shown in Equation (3.3). A WCDMA signal of 5 MHz wide is considered as narrowband only in indoor, where coherence bandwidth can be as wide as 16 MHz. [5, 12, 19]

$$\Delta f_c = \frac{1}{2\pi S} \tag{3.3}$$

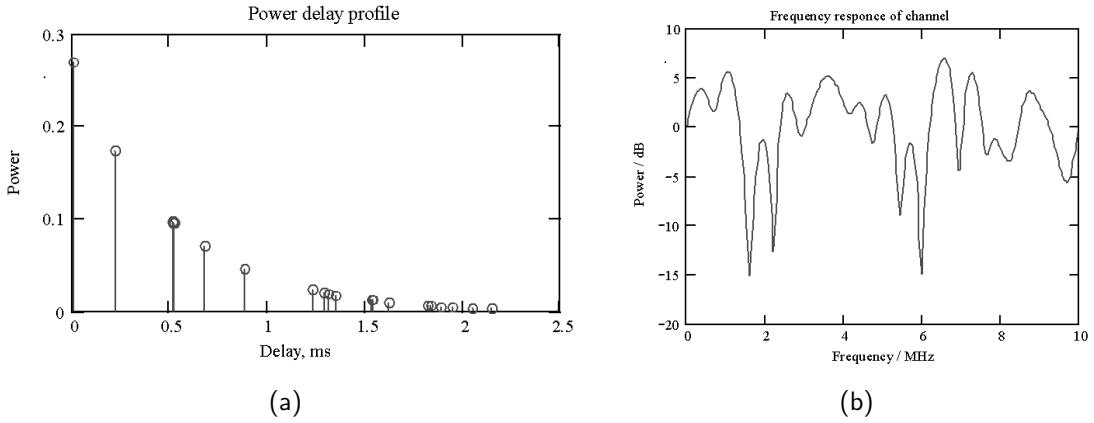

Figure 3.3: (a) Impulse response and (b) frequency response of a typical urban channel. [5]

Fast Fading

Multipath propagation causes signal strength to vary rapidly as a function of distance. This is called fast fading, and is illustrated in Figure 3.4 (solid line). Signal fluctuations are deep, and take place rapidly.

When signal has no LOS component, its components have usually uniformly and randomly distributed phases, and are Rayleigh distributed. In LOS situation, first arriving component is rather strong compared to others, and arriving signal components are Rician distributed. Fading channel signal distributions are only mentioned here, more information is available in the literature, e.g., [19] and [22].

Slow Fading

Obstacles, such as buildings, cause slow fading, which is a local mean value of fast fading. Slow fading occurs usually when mobile moves behind buildings i.e. in shadow, and is therefore called also shadowing. In Figure 3.4, slow fading is presented. It is visible, but the variations are considerably smaller and take place more slowly than in fast fading. In path loss calculation, the variation of signal caused by slow fading is taken into account by additional slow fading margin, calculated from slow fading standard deviation. Typical value for slow fading margin in UMTS frequencies is 8-9 dB. [5]

3.2.2 Propagation Models

Propagation models are typically used when path loss predictions are done in macrocellular network, and are thus an important part of radio network planning. Specific path loss

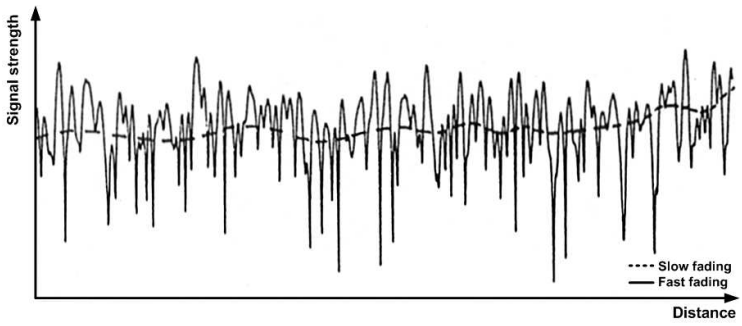

Figure 3.4: Slow fading and fast fading [19].

calculations need accurate information on the environment of the area, in order to estimate signal strength in certain area. The more information is available for predictions, the more accurate results can be achieved, but at the same time the need for computation power increases. Very accurate predictions are usually done in microcellular environment, where so called ray-tracing method can be used [23]. This "brute force" method can be used because there are usually only a few strong paths that need to be considered. [7] Accurate enough results can be achieved with less calculations with the help of models that are based on practical measurements, such as Okumura-Hata.

Okumura-Hata Propagation Model

The propagation model known as Okumura-Hata -model, is based on Y. Okumura's measurements in Tokyo [24], awhich were fitted into a mathematical model by M. Hata. The original Okumura-Hata formula is given in Equation (3.4) [25].

$$L = 69.55 + 26.16 \cdot log_{10}(f) - 13.82 \cdot log_{10}(h_{BTS}) - a(h_{MS}) + [44.9 - 6.55 \cdot log_{10}(h_{BTS})] \cdot log_{10}(d) \quad (3.4)$$

where a is defined as:

$$a(h_{MS}) = [1.1 \cdot log_{10}(f) - 0.7] \cdot h_{MS} - [1.56 \cdot log_{10}(f) - 0.8] \quad (3.4.1)$$
$$a(h_{MS}) = 3.2 \cdot [log_{10}(11.75 h_{MS})]^2 - 4.97 \quad (3.4.2)$$

Equation (3.4.1) is used for small and medium cities and Equation (3.4.2) for large cities.

Other definitions used in Equation (3.4) are:

L	Path loss (dB)
f	Frequency (150 - 1500 MHz)
h_{BTS}	Base station effective antenna height (20 - 200 m)
h_{MS}	Mobile station antenna height (1 - 10 m)
d	Distance between base and mobile station (1 - 20 km)

The original Okumura-Hata has some limitations. The most restrictive is that Okumura's measurements were made at 1920 MHz, and Hata's formulas cover only frequencies range from 150 to 1500 MHz. Also antennas have be over average rooftop level.

The original formula has been modified by COST-231 -project, which resulted in extending Okumura-Hata formula to cover frequencies from 1500 to 2000 GHz. This makes it possible to use the formula in simulations for 3G-networks for a reasonable accuracy [5]. Constants A and B are redefined, and distance dependence parameter C is recommended to be defined by measurements, but value 44.9 is still often used. The COST-231-Hata -formula is given in Equation 3.5. Constants A and B are chosen from the Table 3.2. [7] Also an additional environment dependent parameter, area type correction factor, C_m, is given. It is above 0 dB in urban areas, but in rural areas it can be even below -15 dB [13].

$$L = A + B \cdot log_{10}(f) - 13.82 \cdot log_{10} \cdot (h_{BTS}) - a(h_{MS}) + [C - 6.55 \cdot log_{10}(h_{BTS})] \cdot log_{10}(d) + C_m \quad (3.5)$$

New definitions in the formula are:

A	Constant, see Table 3.2
B	Constant, see Table 3.2
C	User defined value for distance dependence (slope factor)
C_m	Area correction factor.

Table 3.2: Constants A and B for the Okumura-Hata Equation (3.5). [13]

	150-1000 MHz	1500-2000 MHz
A	69.55	46.3
B	26.16	33.9

Model Tuning

Although accurate digital maps can be used with propagation models to enhance predictions, propagation model should be tuned in order to optimize the accuracy of coverage predictions in certain area. At first in model tuning, precise measurements need to be done in desired area with accurate location information. Thereafter, propagation predictions on same area are done. Simulation results are compared with measurement results, and then model can be tuned to fit measurements. [13]

Tuning in COST-231-Hata -model can be done by changing the distance dependent factor C in Equation (3.5), which affects to the slope. The factor 13.82, denoted as D, which affects the effect of antenna height, can also be tuned. In tuning COST-231-Hata, its incapability in handling LOS connections needs to be taken into consider, and LOS connections need to be filtered out from measurements. [13]

3.3 Cellular Network Concept

Mobile networks need to cover large geographical areas and serve large number of users, regardless where in the coverage area they are. For already decades, cellular network concept has been commercially in use in wireless networks. In cellular concept, the network area is divided into smaller areas, cell sites. Furthermore, the cell sites are split in cells.

[21] The idea of cellular network structure is illustrated in Figure 3.5. Base stations are in the middle of the cell site, and cell sites are divided into three cells.

In GSM networks, cellular structure was also the base of frequency planning; same frequency could not be used in adjacent cells, but there must be enough spacing in order to avoid interference. The smaller the spacing between two cells using the same frequency can be kept, the more effectively the frequency resources can be used. In WCDMA networks, all cells can use same frequency, but it is still important to prevent cells interfere each others too much.

The higher is the frequency used, the shorter is the range (Equation (3.1)); where the range of NMT and GSM systems (450/900 MHz) was and is up to about 25 km, the coverage of 3G systems (around 2 GHz) is typically limited to few kilometers. Thus, base stations need to be situated dense enough in order to ensure coverage on the desired area. In Figure 3.5, cell areas are shown as in hexagonal shape, but in practise terrain is not homogenous and cell areas are not that regular.

Coverage is not the only advantage of using cellular structure in networks, but also capacity can be considerably increased. Reuse of frequencies enables to fit more connections on rather small frequency range, and short distances make it possible to use low transmission powers in the mobile side and low antenna heights in the base station side.

When capacity needs in the network grow, like in, e.g., city centers, capacity may be the limiting factor in the network. This can be solved by reducing cell sizes, i.e., fitting more cells in the same area, or by using layerized cellular structure. 3G-network layer may be added to existing GSM-network layer. When considering only 3G-cells, larger cells can be used to build the coverage and smaller cells are added to ensure sufficient capacity to the network. These are called macro and micro layers, respectively. [5]

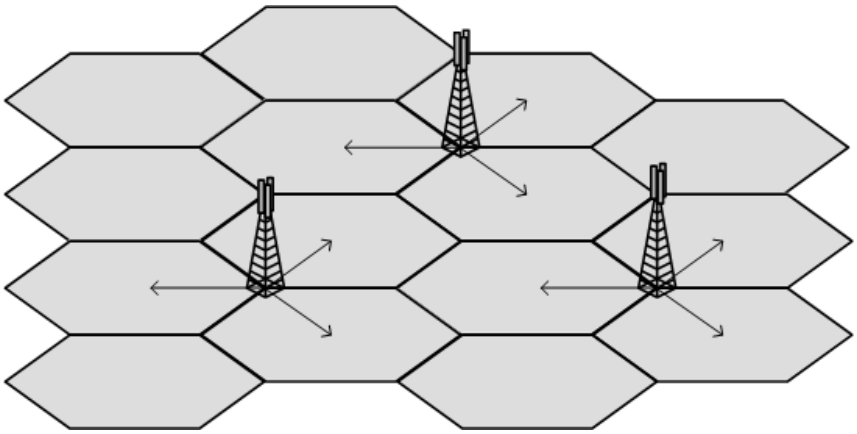

Figure 3.5: Cellular concept.

3.4 Multiple Access

TDMA (time division multiple access) and FDMA (frequency division multiple access) have been the main techniques used in mobile communication systems to separate users in air interface. Often FDMA and TDMA are combined, as illustrated in Figure 3.6(a). Different gray colors represent different connections, so in presented TDMA/FDMA solu-

tion one connection is spread in different time slots and frequencies. This technique, called frequency hopping, is in use, e.g., in GSM system.

Packet switched data communication produces more bursty and discontinuous data flows with variable bitrates. Therefore, in the 3rd generation mobile networks, new multiple access technique, code division multiple access (CDMA), which provides dynamic multiple access communication for a large number of users with high bitrates is utilized. It enables multiple connections to be established in the same frequency simultaneously with other users. The idea of CDMA is illustrated in 3.6(b), where different codes are separating users in same frequency and time space.

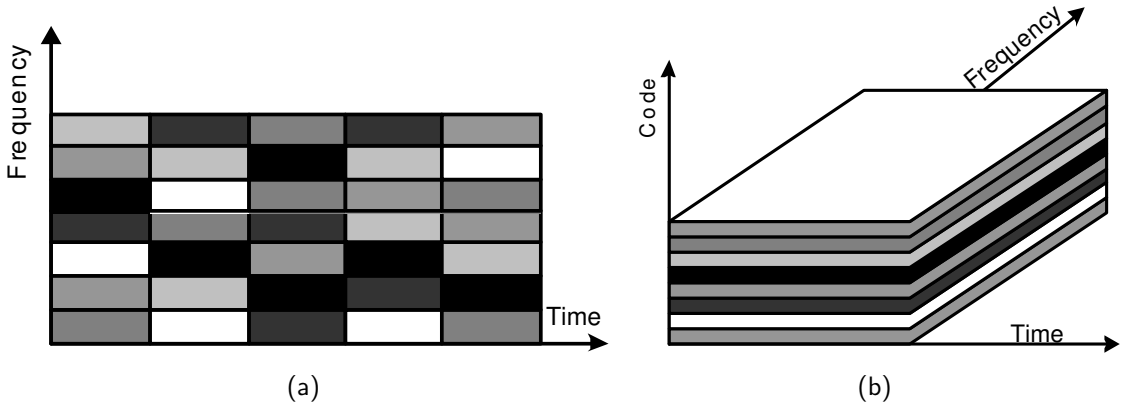

Figure 3.6: Multiple access techniques; (a) FDMA/TDMA, (b) CDMA.

3.5 Spread Spectrum Systems

The air interface used in UMTS is a wideband DS-CDMA (direct sequence code division multiple access) system. It is a spread spectrum system, where the information bandwidth is expanded to wider bandwidth. Information is spread to wider bandwidth by multiplying the data sequence with a particular spreading code. Despreading is done in a similar way; spread signal is multiplied with spreading code, which results the original data sequence.

The data rate of spreading code is called chip rate, and it is denoted by W_c, and transfer data rate is denoted with R. Ratio W_c/R is called spreading factor (SF). Using lower data rate than chip rates gives additional gain to the signal to interference ratio after despreading. Therefore the ratio W_c/R is called also processing gain (PG) presented usually in dB:s, as defined in Equation 3.6. An advantage of using spread spectrum modulation is its high tolerance to interference, unintentional or intentional (jamming). Anti-jamming capability is illustrated in Figure 3.8. Since spread spectrum signal level can be below noise level, as shown in Figure 3.8 b), it is also difficult to detect by an unintended receiver. [7, 16]

$$PG = 10 \cdot log_{10}\Big(\frac{W_c}{R}\Big) \tag{3.6}$$

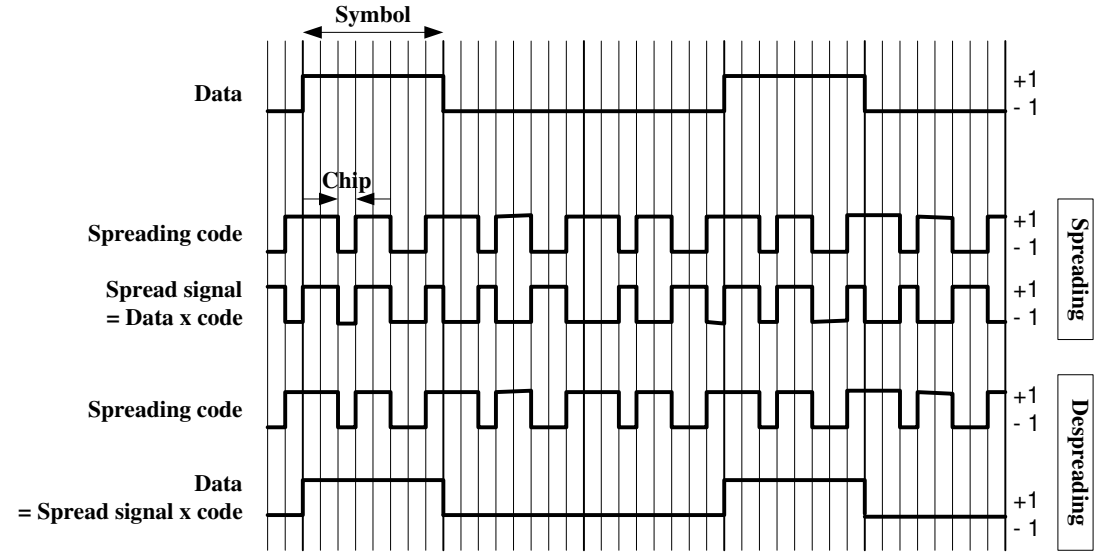

Figure 3.7: Spreading and despreading in DS-CDMA [6].

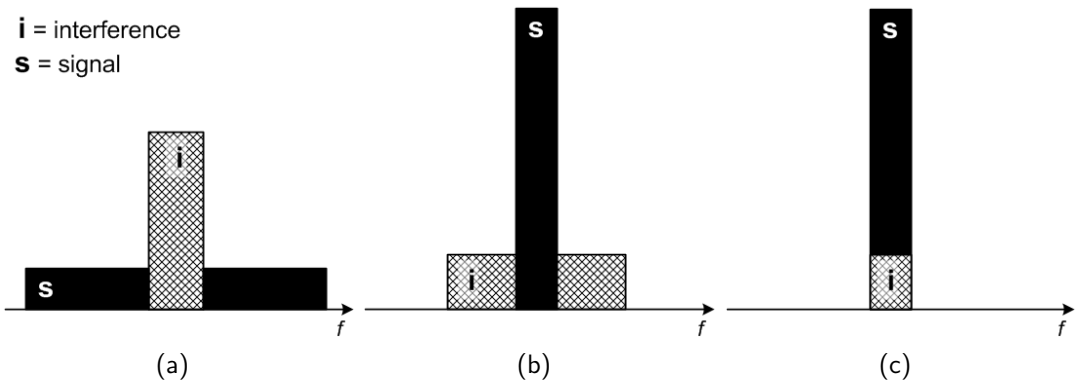

Figure 3.8: Interference tolerance of spread spectrum signal: (a) received signal and narrowband interference before spreading, (b) signal and interference after despreading, and (c) despreaded signal and interference after filtering.

Chapter 4

WCDMA Radio Network Planning

Radio network planning (RNP) in UMTS differs some from of RNP in e.g. GSM, but the basic principles of good RNP are valid in both [13]. However, GSM planning is more straightforward due to separate coverage and capacity planning. In UMTS, due to different air interface, coverage and capacity are tied together, which makes the RNP to differ from GSM and to be some more complicated.

4.1 UMTS Planning Process

Planning process in UMTS is divided into three steps; dimensioning, detailed planning, and optimization and monitoring. These steps are illustrated in Figure 4.1. Basically, the main targets of RNP are to maximize *coverage*, *capacity*, and *quality* in the network. [13]

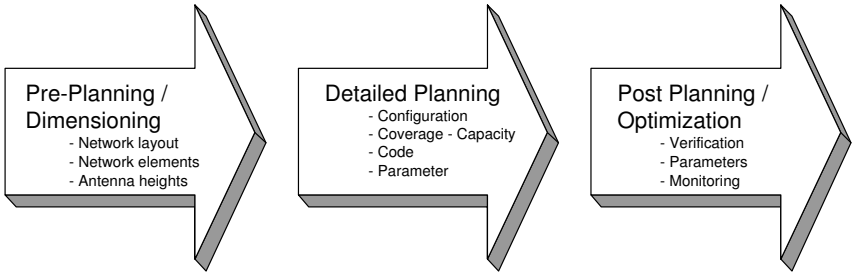

Figure 4.1: UMTS radio network planning process. [5]

4.1.1 Dimensioning

In the dimensioning phase, rough estimates on required coverage and capacity on desired area are made. Based on them, network layout is estimated, and the need of network elements is counted; amounts of needed hardware, base station sites, and antenna heights. Also the first version of link budget for each service is calculated. Link budget is a table, where the path losses between transmitter and receiver in uplink and downlink directions are calculated, taking into consideration all affecting gains, losses and noises. Dimensioning phase is also called pre-planning -phase. [5, 7]

4.1.2 Detailed Planning

In the detailed planning phase, the assumptions made in dimensioning phase are replaced with concrete values. This enables calculation of more accurate link budget; antenna gains, cable losses, slow fading margins etc. can be added to the link budget in order to get more realistic information. This is called configuration planning. [5] A practical example of link budget is given in Chapter 5, Table 5.5.

In UMTS, coverage and capacity planning have to be combined, and this combination is called topology planning. Coverage planning can be done by path loss prediction models, like Okumura-Hata, but when traffic is added, raising interference levels produce cell-breathing -effect, that shrinks coverage area of a cell. Therefore, in UMTS RNP, both coverage and capacity have to be analyzed simultaneously and together. [5] This phase requires computer simulations. Topology planning issues are described in more detail in Section, 4.2.

Code planning and parameter planning are also a part of detailed planning phase. Code planning means scrambling code allocation for cell separation in DL direction. Parameter planning includes optimizing of radio interface functionality (signaling, handover, power control, etc.). [5].

4.1.3 Post-Planning and Optimization

The post-planning and optimization phase is the final step in RNP. In this phase, the plan is verified by measurements, and by performing tests, concentrating on e.g. handovers, as well as coverage and dominance areas. Also, if needed, different parameters in, e.g., power control, handover, and signalling can be tuned. [5]

Network monitoring is also an important part of post-planning. Certain statistics, also called key performance indicators (KPI), i.e., loads, connection failures, and transfer rates in the network are being continuously monitored (with some averaging, of course), and when necessary, previous post-planning and optimization tasks can then be performed. [5]

4.2 UMTS Topology Planning

In UMTS, coverage and capacity planning are combined with topology planning introduced in Section 4.1.2, as a part of detailed planning. Multiple users share the same frequency range, and introduce therefore interference to each others. Raising interference levels require higher transmit powers to be used in the network, which then causes cell coverage to shrink when the load in the network increases. This phenomena is called cell-breathing. Networks need to be planned in such manner that the network area is covered also when the load of the network is high, and also indoor users need to be served. This results in overlapping in outdoor coverage, especially in low-loaded network, which then causes increasing interference levels in the network, and especially in the edges of cell coverage areas. In order to guarantee good network behavior, interference issues need to be controlled. Proper topology planning is one key point in controlling the interference levels in the network, and maintaining the coverage and capacity as desired.

4.2.1 Topology Planning Process

Topology planning process can be roughly divided into coverage predictions, Monte Carlo simulations, and network performance analysis. Topology planning process is illustrated in Figure 4.2.

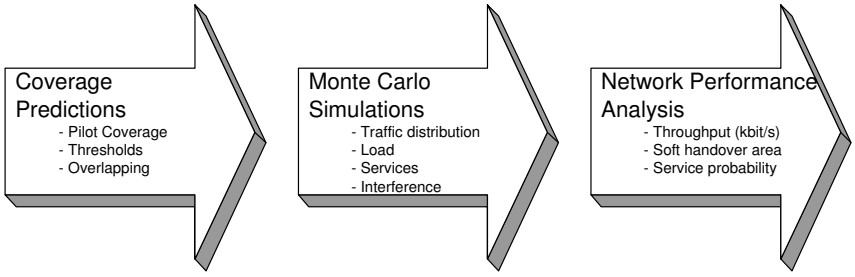

Figure 4.2: UMTS topology planning process. [5]

Coverage Predictions

The topology planning process begins with coverage predictions. In UMTS, different transmit powers are given for different signaling and traffic channels. That is, channel estimation, HO measurements, and cell selection and reselection are based on the level of common pilot channel (CPICH), and therefore it is used in coverage predictions [5]. The path loss from all cells in network area to all points in map is calculated with the help of a digital map and propagation model. Thereafter, the pilot coverage can be estimated after calculating the maximum path loss in link budget. After the coverage of pilot signal is predicted, coverage thresholds can be used to estimate coverage overlapping and cell dominance areas [5].

Monte Carlo Simulations

Statistical system-level Monte Carlo simulations are used to estimate load in the network with given traffic. Desired traffic distribution is defined, all mobiles and Node Bs are given transmit powers, and UL and DL directions are analyzed with also interference included. As a result, an analysis of system parameters and variables, such as needed Tx powers, cell loads, interferences, throughputs, service probability, SHO areas etc. is given. Monte Carlo process in the simulator used is described in Section 5.1.2.

Network Performance Analysis

The results of Monte Carlo simulations can be used to analyze network behavior. The site configuration, by means of site locations, antennas, antenna directions, antenna heights, antenna tiltings etc., can be changed and optimized. After changing the configuration, coverage predictions and Monte Carlo simulations need to be rerun in order to see the changes in network behavior. [5]

4.2.2 Load Equations

As mentioned, increasing load in the network raises the interference, and it is modeled by interference margin (IM), described in Equation 4.1 (also called noise rise). In Figure 4.3, the interference margin is plotted as a function of load. As the load reaches it's maximum value, the interference margin approaches infinity. The load can not be higher than 100 %, because it is relative to the maximum capacity of the cell. [5, 13].

$$IM = -10log_{10}(1 - load) \tag{4.1}$$

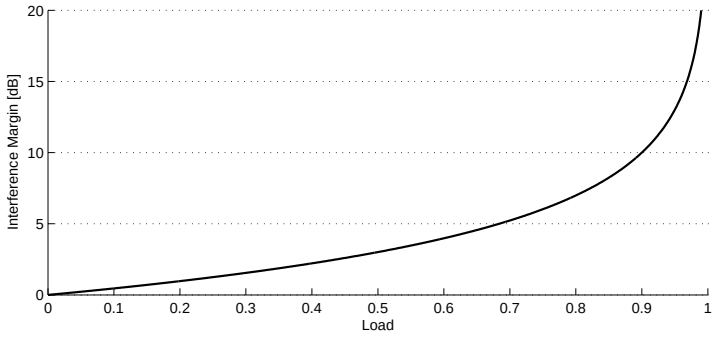

Figure 4.3: Interference margin as a function of load.

Uplink and downlink directions need to be considered separately, since the loads in uplink and downlink directions are not identical. In uplink direction, mobiles share the same radio interface, and interference in the receiving end is the same. In downlink direction, the data sent to different users consumes the shared transmit power of Node B, and also the interference that users suffer from is different in different locations. In the uplink direction, the load factor is defined as follows [5, 26]:

$$\eta_{UL} = \sum_{j=1}^{N} \frac{1}{1 + \frac{W_c}{(E_b/N_0)_j R_j \nu_j}} (1 + i) \tag{4.2}$$

where N is the number of users in the network connected to Node Bs, W_c is the chip rate, $(E_b/N_0)_j$ is the (E_b/N_0) requirement of user j, R_j is the bitrate of user j, and ν_j is the activity factor of user j. i is the other-to-own-cell interference.

In downlink direction, the load factor is defined as follows [26]:

$$\eta_{DL} = \sum_{j=1}^{N} \frac{1}{\frac{W_c}{(E_b/N_0)_j R_j \nu_j}} [(1 - \alpha_j) + i_j] \tag{4.3}$$

where α_j is the orthogonality factor, which describes the orthogonality of the codes used in the network. In optimal case, when codes are fully orthogonal, α_j equals to 1, but multipath fading deteriorates orthogonality. i_j is the other-to-own-cell interference, which is in this case different for each users due to different location.

After the loads in uplink and downlink direction have been calculated, can the interference margins in uplink (IM_{UL}) and downlink (IM_{DL}) direction be calculated. Equations 4.2 and 4.3 also show how raising interference level raises the load in the network.

4.2.3 Site Configuration

Site density, site location, and site configuration are important issues in coverage and capacity optimization. First, site placing needs to be decided, then the number of sectors and sector orientation have to be defined. These all have a strong effect on network performance. [5]

Site Location Selection

If homogenous user distribution in the network could be presumed, and also environment was approximately homogenous, a regular hexagonal site placing would be optimal. In real network, user distribution is not homogenous, but centered in certain areas, such as office buildings and shopping malls etc., while in the forests and such areas there are less users. It is also presumable that user distribution will change during the day.

In the selection of site locations, some practical limitations may occur. Building of antenna masts is not always allowed, especially in city centers. It may also be more economical to use building roofs as a base for antenna installation. Suitable buildings are not always in optimal locations, so non-optimal site locations need sometimes be used. The impact of non-optimal site locations in WCDMA network was studied in [27], where the error in site location was maximum one quarter of site spacing. The error was found to have a rather small effect on network performance. Therefore, although site location selection is an important part of planning, it is not that crucial to have sites located exactly in planned places. Instead, more effort should be directed to site configuration planning [5].

Site Sectoring and Sector Orientation

In base station site, there are normally three cells/sectors in use. 2-sectored configuration is typical when road coverage is builded, and 1-sector sites are usually used in small micro-cell configurations. In one sector, an antenna is radiating to the direction of desired cell coverage area. In 3-sectored site, antenna directions are usually divided into intervals of 120°.

Also more than 3 sectors can be used: sectors can be added if higher capacity is needed. [5] The capacity increase when adding new sectors is not proportional to the amount of sectors, but is still significant. Sectorization gain from omni- (1 sector) to 3-sectored site is close to 3, but from 3- to 6-sectored site configuration the gain is ”only” about 1.7. The more sectors are added to the cell, the more difficult is to control the interference leakage between sectors. Also the amount of softer HO connections needs to be kept at a reasonable level. Therefore, antenna beamwidth selection is an important issue in controlling sector overlapping when increasing the amount of sectors in site. [28]

Also the orientation of sectors needs to be considered. It is not always possible to install antennas in a way that the directions are the desired ones. Bringing sectors closer to each others increases sector overlapping and thus increases also the amount of softer handover connections. In [5] and [27], the effect of antenna orientation on the behavior of UMTS network was studied. The results show that small (9.1°) deviation in antenna directions is almost invisible in network behavior, and also effects of larger deviation (18.2°) are rather small, but small decrease in service probability and sector throughput is already visible.

4.3 Antenna Configuration

The duty of an antenna is to radiate and receive radiation in the 3-dimensional space. It ultimately defines how the power is transmitted in the air, and therefore plays a very important role in radio network planning. For RNP purposes, an antenna is typically characterized by frequency band, gain, and vertical and horizontal radiation pattern, but it has also multiple of other electrical and mechanical characteristics. Gain is usually expressed in dB:s compared to isotropic radiating antenna or to half-wave dipole antenna, and the used units for the gains are dBi and dBd, respectively. Vertical and horizontal radiation patterns describe how much antenna strengthens or attenuates the signal in each angle, and combining these results in the information on antenna radiation in each solid angle. The antennas used in the simulations are described more specific in Section 5.2.3.

4.3.1 Sectoring and Antenna Horizontal Beamwidth

Site sectoring was considered in Section 4.2.3, where the importance of antenna selection and antenna beamwidth was emphasized. Typical antenna horizontal beamwidths in commercial UMTS antennas are omnidirectional (360°), 90°, 65°, and 33° [29, 30]. In order to optimize cell capacity and minimize interference, antenna of 65° horizontal beamwidth is optimal for 3-sectored site configuration and antenna of 33° horizontal beamwidth for 6-sectored configuration [28, 31].

4.3.2 Antenna Vertical Beamwidth

In the literature, only a few studies on effects of different antenna vertical beamwidths on planning and performance of UMTS networks can be found. In [4] it was shown, that antenna vertical beamwidth has a considerable affect on optimal downtilt angle, and the effects of downtilt are more gentle with wider antennas. If other properties of antenna remain constant, and vertical beamwidth is widened, the gain of the antenna decreases. For comparison, Kathrein UMTS-antenna with horizontal beamwidth of 65° has gain of 18 dBi when vertical beamwidth is 6°, and gain of 15dBi in wider 12° antenna [29]. This affects already the coverage of cell, if transmit powers are kept constant.

4.3.3 Coverage Overlapping and Soft/Softer Handover Areas

Overlapping of cell coverage areas in outdoors results from requirements for indoor coverage, and unhomogeneous propagation environment produces unintentional coverage overlapping. Coverage overlapping also helps to cope with signal level fluctuation caused by slow fading. Coverage overlapping is needed also to ensure seamless handovers and to take full advantage of WCDMA technology by means of soft handover gain [7]. Soft and softer handovers occur in the areas where the coverage of two sectors (softer HO), or two cells (SHO) overlap. Site spacing, antenna height, antenna direction, antenna beamwidth, antenna downtilt etc. affect the amount of sector coverage overlapping, and therefore soft/softer handover areas. If pilots from too many cells are hearable in a certain area, they cannot be added to the active set and they only introduce interference (SHO algorithm was considered in Section 2.7.1). This is called pilot pollution, and the amount of pilot polluted areas should be minimized in the network. Also soft handover gain is said to be higher, when less disturbing pilots are hearable [32]. The number of hearable pilots

in a certain area can be controlled by adjusting the coverage overlapping areas. In Figure 4.4, an example of areas of a single cell connection, a soft handover, and a softer handover in 3- and 6-sectored network is shown. Single cell connections occur in the antenna mainbeam direction, softer handover connections in a narrow area between the sectors, and soft handover in a rather wide area between the sites.

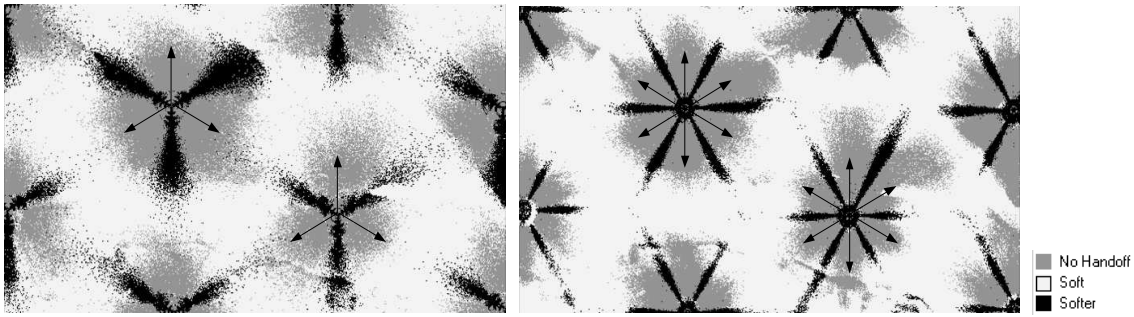

(a) 3-sectored (b) 6-sectored

Figure 4.4: Example of most probable handover types in (a) 3-sectored and (b) 6-sectored network layout.

4.4 Antenna Downtilt

Base station antenna downtilt is known to be an efficient method to control antenna radiation and direct it to the network area [1, 33]. Downtilting means directing the base station antenna of some angle, ν, towards ground, aiming at focusing the mainbeam of the antenna to cover the required area in a desired way. The idea of downtilting is illustrated in Figure 4.5. Lighter gray corresponds to a non-tilted and darker gray to a tilted antenna beam. If antennas are directed towards horizon the, the main part of the radiation power does not meet the desired coverage area of a cell. In addition, this causes interference to adjacent cells. As capacity and coverage of a WCDMA network are highly dependent on the amount of interference, and antenna downtilt can help controlling the interference levels. Antenna downtilt in was used already in GSM, and evident capacity enhancements in network were shown in literature already then (i.e. almost 20 % in [34]). Antenna downtilt in WCDMA cellular networks has been studied in literature, and similar gains in capacity have been announced (e.g. [2], [3]), but no straight rules for antenna downtilt in different site and antenna configurations have been presented.

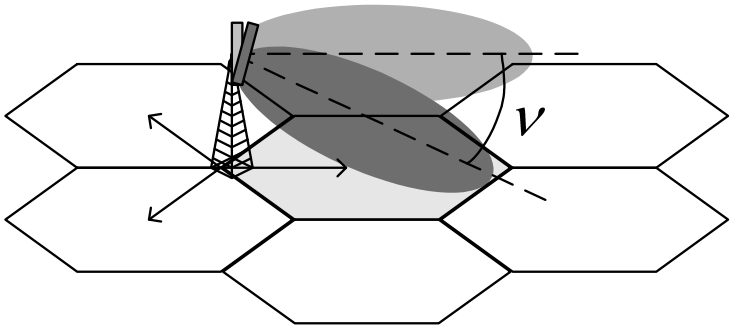

Figure 4.5: Illustration of antenna downtilt.

Antenna downtilt requires usually site visit, if there is a need to change the downtilt angle. Since the best suitable antenna downtilt angle in the network may change in process of time, possibility to continuously adjust antenna's downtilt angle is considered as one optimization and performance improvement method in WCDMA networks. [35] However, remote electrical tilt (RET) and continuously adjustable electrical downtilt (CAEDT) require hardware investments and is a rather expensive solution compared to fixed mechanical or electrical antenna downtilt.

4.4.1 Antenna Mechanical Downtilt

In antenna mechanical downtilt, the antenna element is simply physically turned towards ground in mainbeam direction. Therefore, mechanical antenna tilting is quite inexpensive solution to be implemented in the network. The idea of mechanical antenna downtilt is illustrated in Figure 4.6(a), where lighter gray and dashed line corresponds to a non-tilted, and darker gray and solid line corresponds to tilted scenario. In mechanical downtilt, while mainbeam of antenna is tilted down, the back lobes are turned upwards, and side lobes are not turned at all. Thus, antenna radiation is limited only in mainbeam direction . This leads to effect, where horizontal radiation pattern flattens in the mainbeam direction, and it results in widened horizontal beamwidth and sometimes even notch in the center. This is called "tilting antenna effect" [1]. The effect is illustrated in Section 5.2.3, in Figure 5.7 with the antennas used in the simulations.

4.4.2 Antenna Electrical Downtilt

In antenna electrical downtilting [1, 33], the antenna beam is turned by adjusting the phases of antenna elements without physically turning the antenna. This kind of beam adjusting requires usage of multi-element antennas, as macrocell antennas typically are. To obtain tilting, the phase of each antenna element needs to be tuned. This can be done either by adding electrical delay to each antenna element, or simply by producing delay by physically moving the antenna elements in order to generate phase difference between antenna elements.

The main difference, and also benefit in electrical antenna downtilt compared to mechanical is that, in addition to mainbeam direction, also back and side lobes are downtilted. Antenna electrical downtilt is illustrated in Figure 4.6(b). Tilting also side and back lobes downwards reduces unwanted radiation to neighboring cells in the network, and may therefore also intuitively improve network performance. However, it needs to be observed that the coverage of the cell shrinks due to downtilting. Therefore, too high downtilting angles can result in coverage problems.

4.4.3 Geometrical Antenna Downtilt Equation

Based on the geometry, an optimum electrical downtilt angle, ν_e, and an optimum mechanical downtilt angle, ν_m, can be assumed to be a function of at least antenna vertical beamwidth factor $\theta_{VER,BW}$ and topological factor θ_T:

$$\nu_e = f_e(\theta_{VER,BW}, \theta_T) \tag{4.4}$$

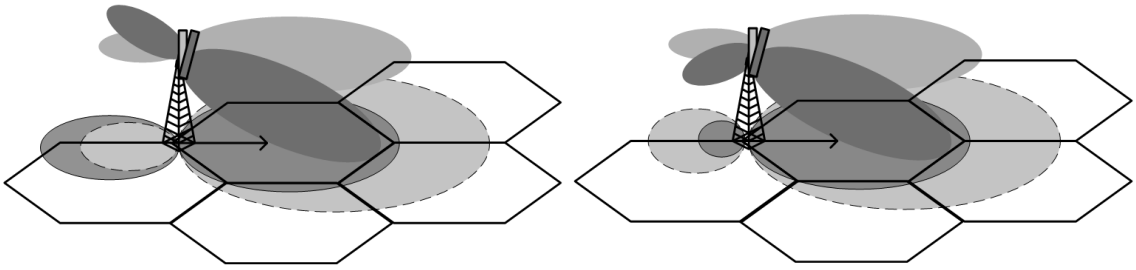

(a) Mechanical downtilt (b) Electrical downtilt

Figure 4.6: Illustration of (a) mechanical and (b) electrical antenna downtilt.

$$\nu_m = f_m(\theta_{VER,BW}, \theta_T) \tag{4.5}$$

ν_e and ν_m are separated, because it is assumed that optimal angle differs according to the tilting technique.

Antenna vertical beamwidth factor is assumed to have rather high effect. This is due to purely geometrical reasons. In Figure 4.7, different factors and variables affecting antenna downtilt are described. In case of antenna of wider vertical beamwidth, the antenna needs to be downtilted more in order to point the upper -3 dB beam towards the cell edge. The effect of $\theta_{VER,BW}$ can be calculated from the upper -3 dB point in antenna radiation pattern, or it can be simply estimated to be half of the antenna vertical beamwidth, θ_{-3dB}:

$$\theta_{VER,BW} = \frac{\theta_{-3dB}}{2} \tag{4.6}$$

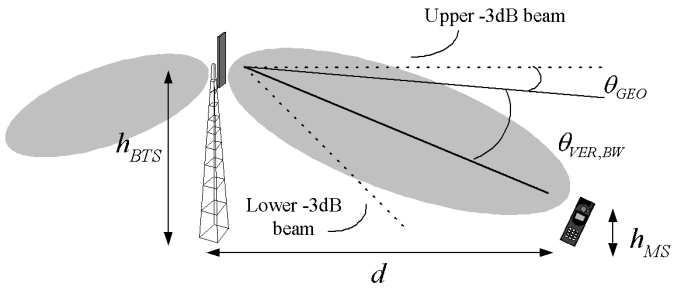

Figure 4.7: Factors in antenna downtilt angle. [36]

Of course, the upper -3 dB point does not characterize the antenna pattern perfectly; also the form of the antenna pattern affects, but it is more difficult to characterize.

The site configuration, by means of effective antenna height and the length of desired coverage area affect also optimal downtilt angle. The effective antenna height, Δh, is the difference between base station antenna height, h_{BTS}, and mobile station antenna height, h_{BTS}. The distance of cell coverage area is more difficult to define. It could be simply defined as a half of site spacing, but the desired coverage area is often larger. E.g. in hexagonal 3-sector scenario (Figure 4.8), the mainbeam of the antenna is pointing to the back lobe of other antenna in other base station. In such scenario, cell coverage area of half of site spacing would result in coverage problems near the other base station. Thus,

cell coverage distance should be longer, depending on desired overlapping. The topological factor in optimal downtilt angle can be simply simply stated as:

$$\theta_T = tan^{-1}\Big(\frac{h_{BTS} - h_{MS}}{d}\Big) \tag{4.7}$$

The distance d still needs to be defined separately. Equation (4.7) describes how the effective base station antenna height, h_{BTS}, and cell coverage distance, d, affect the required downtilt angle. Heightening the base station antenna results in a bigger downtilt angle, whereas lengthening of the cell coverage area results in smaller downtilt angle.

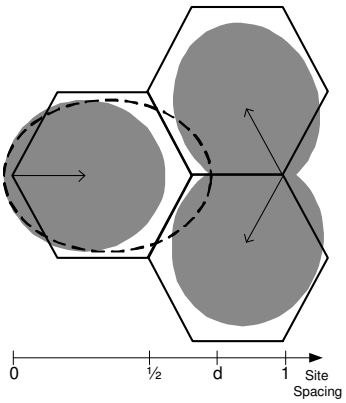

Figure 4.8: Defining optimal cell coverage area in 3-sectored network.

Combining $\theta_{VER,BW}$ and θ_T results in a simple geometrical equation which defines the optimal downtilt angle in certain site configuration:

$$\nu_{GEO} = \theta_{VER,BW} + \theta_T \tag{4.8}$$

where ν_{GEO} is the optimal downtilt angle calculated by purely geometrical information of network and site configuration. Also f_e and f_m are assumed here to be the same, but it is probable that also tilting technique has an effect on optimal downtilt angle.

Chapter 5

Simulation Environment

5.1 Simulation Scheme

A system level simulator and Monte Carlo simulations were utilized in order to study the performance of the network under different topologies and downtilt scenarios. The simulations were accomplished with Nokia NetAct WCDMA Planner Tool.

5.1.1 Coverage Calculations

In UMTS, coverage areas change dynamically depending on the load in the network. Thus, coverage calculations are more like signal propagation prediction. Radio wave propagation was considered in more specific in Section 3.2. In the simulations, COST-231-Hata propagation model was used.

Coverage prediction parameters are shown in Table 5.1. The frequency used in propagation predictions is 2140 MHz. Mobile station antenna height is fixed to commonly used 1.5 m, as BS antenna height varies from 25 to 45 m. The slope factor C in propagation model is fixed to 44.15, which result in slope variation from 35.0 to 33.3 dB/dec. An average area correction factor of -6.7 dB was used to correspond urban/suburban area. Also morphological correction factors were used to model different terrains.

5.1.2 Monte Carlo Statistical Analysis

The simulator uses statistical Monte Carlo simulations. Monte Carlo simulation procedure is described in Figure 5.1. At first, parameters for services and terminals are set, e.g., simulation resolution and fading correlations. Next, terminal arrays are created, i.e., Poisson distributed random number of terminals are placed randomly in the simulation area.

Thereafter, the snapshot procedure is started. In the beginning, Tx powers of all mobiles and BSs are set to zero, and other parameters, such as power control standard deviation, are set randomly. Also, the intra-cell and inter-cell fading correlations are generated here.

After that, the first randomly chosen mobile terminal in the array is tested for connection failure (e.g. too low E_c/I_0, or not enough Tx power to satisfy E_b/N_0 in UL or DL), and the Tx powers of MS and BS are set. Next, potential HO cells are tested for the particular

Table 5.1: Propagation prediction parameters

General parameters		
Frequency f	2140	MHz
MS antenna height h_{MS}	1.5	m
Slope factor C	44.15	
Morphological correction factors		
Open	-17	dB
Water	-24	dB
Forest/trees	-10	dB
Quasi-open	-4	dB
Suburban	-3	dB
Urban	-0	dB
Buildings $<$ 8 m	-4	dB
Buildings $>$ 8 m	-3	dB
Buildings $>$ 15 m	-0	dB
Buildings $>$ 23 m	3	dB
Average Area correction factor	-6.7	dB

mobile, and Tx powers are modified, if needed. This is repeated for all mobiles, and then repeated for all mobiles as many times as it requires to achieve convergence.

After convergence is achieved, one snapshot has been done. This is again repeated as many times as the number of required snapshots is. Snapshots are repeated so many times, that statistically reliable results can be achieved. Larger simulation area and smaller number of mobiles require more snapshots. In the simulations for the thesis, typically about 10000 snapshots for low loaded network and about 7000 snapshots for high loaded network have been done.

Definitions

E_c/I_0 is the received chip energy divided by the total power spectral density. It is used to indicate the quality of non- informative channels, e.g. CPICH channel. [7]

E_b/N_0 means the bit energy divided by noise spectral density, where noise means both noise and interference. E_b/N_0 in uplink direction can be calculated as follows:

$$\frac{E_b}{N_0} = \frac{W}{R}\frac{p_{rx}}{I - p_{rx}} \tag{5.1}$$

Where p_{rx} is received (constant) power, and I is the received noise and interference power. In downlink, E_b/N_0 is calculated as follows:

$$\frac{E_b}{N_0} = \frac{W}{R}\frac{p_{rx}}{I_{own} \cdot (1 - \alpha) + I_{oth} + P_N} \tag{5.2}$$

Where I_{own} is the total received power from the own cell and I_{oth} is the total received power from other cells. α is the code orthogonality factor, which depends on the multipath conditions. P_N is thermal and receiving end noise spectral density. [7]

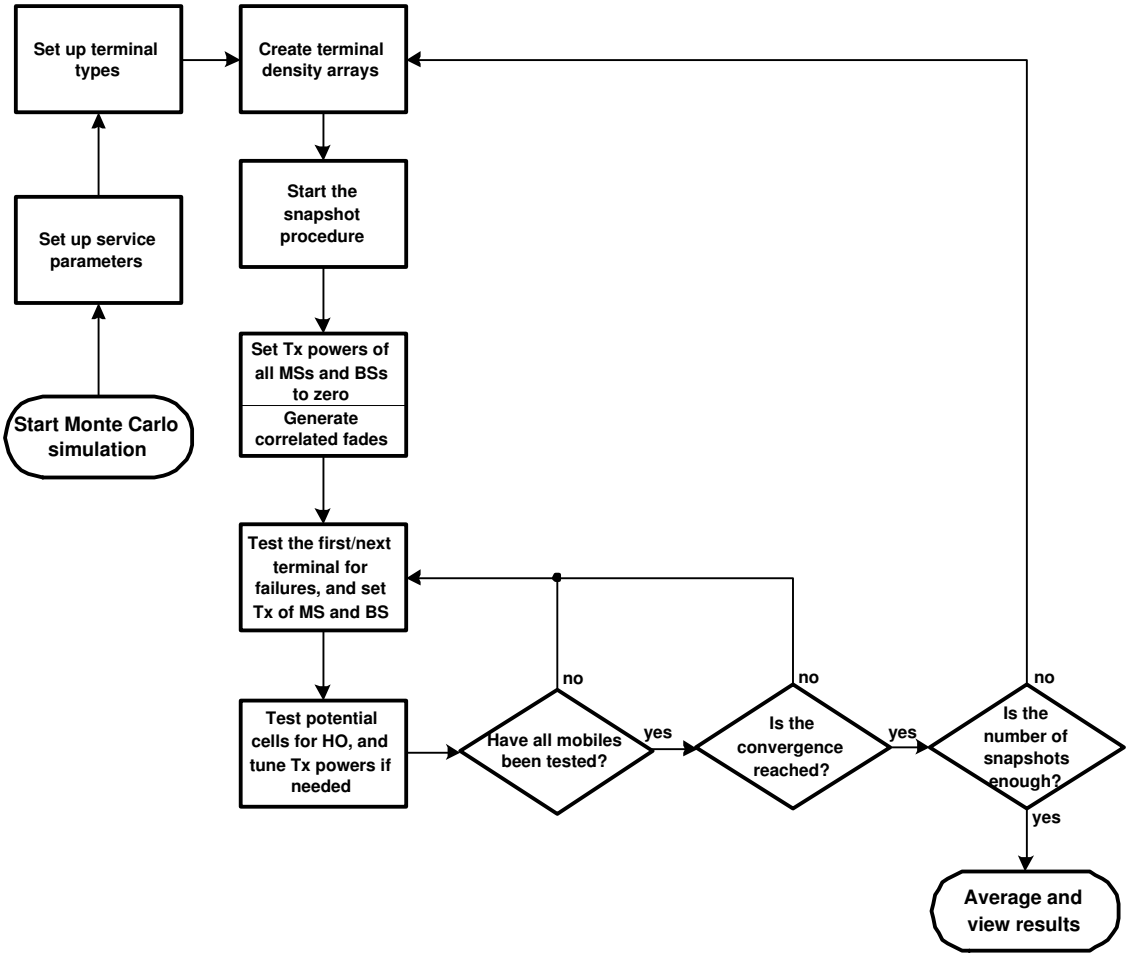

Figure 5.1: Description of Monte Carlo process.

5.1.3 Digital Maps

Digital maps are the basis of accurate propagation prediction and topology planning simulations. In the thesis, digital map with resolution of 5 meters was used. The used map covers the Tampere city area in Finland. The map area is mostly light urban / suburban area. The map includes information of terrain type (open, water, forest, buildings, etc.) with height information, building rasters with height information, and all road information in vector-like polygon format. Example of the map with sites of 2 km site spacing and the simulation area-polygon is shown in Figure 5.2

5.2 Simulation Setup

5.2.1 Site Configuration

In the simulations, there were three site location scenarios, with site spacings of 1.5, 2.0, and 2.5 km. Each scenario consisted of 19 sites situated in regular hexagonal shape. Also, the simulation area was hexagon. Simulation areas with all three site location scenarios are illustrated in Figure 5.3. Red sites have site spacing of 1.5 km, blue 2.0 km and black 2.5 km, and the black hexagons bound the simulation areas.

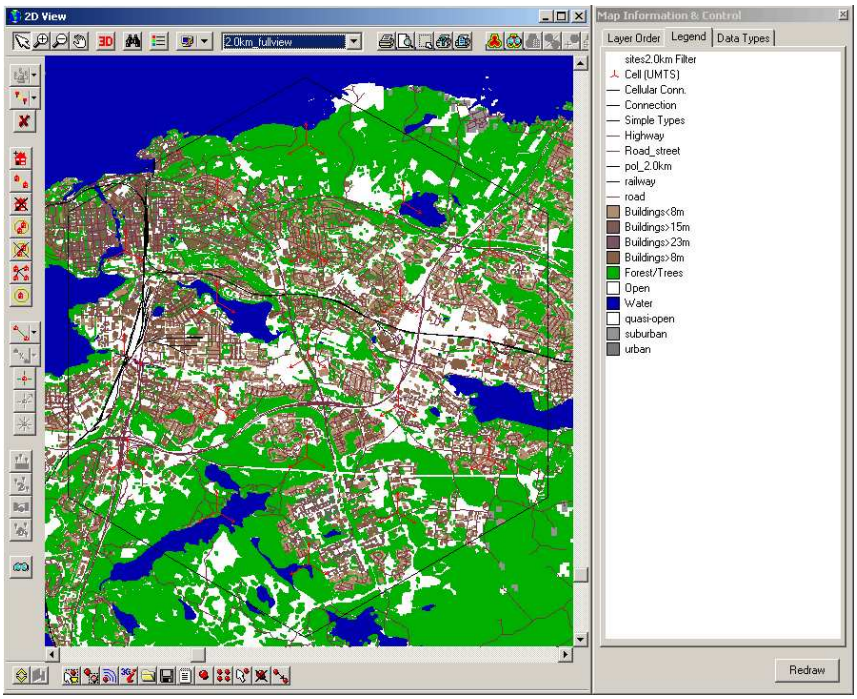

Figure 5.2: Example of 2D map view.

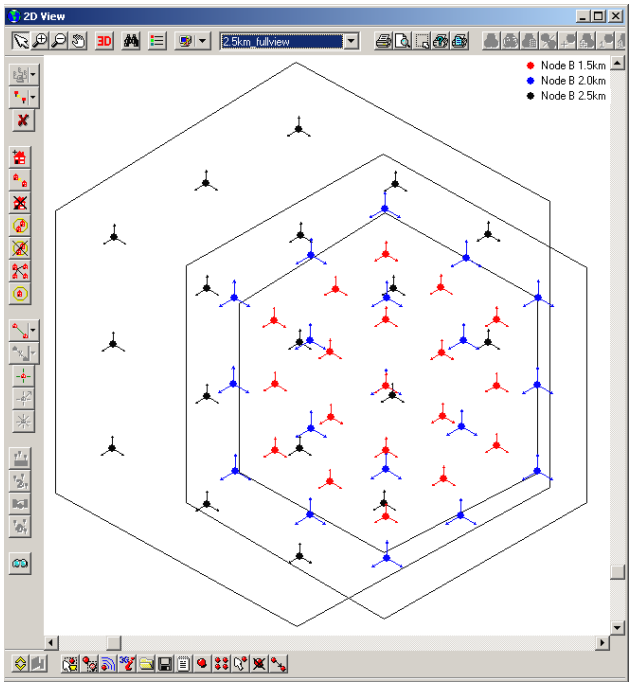

Figure 5.3: Site configuration scenarios.

In order to see the effect of antenna height, three different antenna heights; 25, 35, and 45 m, were used. Two sectoring scenarios, 3- and 6-sectored were used to emphasize the capacity enhancement by sectoring and the effect of sectoring on downtilting. Antenna directions in 3-sectored layout were 0°, 120°, and 240°, when 0° is heading up to north. In 6-sectored layout, sectors were added between the antennas used in 3-sectored layout,

therefore antenna directions in 6-sectored layout were 0°, 60°, 120°, 180°, 240°, and 300°. When in 3-sectored layout mainbeam of antenna is pointing to the back lobe of the antenna in next base station, point the mainbeams of antennas towards each others in 6-sectored network. This could be thought to raise the interference level in the network and cause coverage problems between sites. However, the results in [4] show that shifting 2nd tier antennas in regular hexagonal configuration does not affect almost at all the network performance.

5.2.2 Simulation Parameters

In the simulations, only speech users with constant 12.2 kbps bit rate was used. The users were distributed homogenously in the network area. The simulation parameters used in the simulations are described in Table 5.2. The parameters are typical values for macrocellular UMTS network, and the values are in line with, e.g., the parameters used in [5] and [7]. The maximum Tx power of the base station is used for signalling and traffic channels. Tx power of CPICH channel affects on the coverage of network and should be carefully selected. The powers of other common channels and synchronization channel are typically -3 dB from CPICH power. In order to avoid one mobile to consume all the Tx power of the base station, is the max power per connection limited to 38 dBm. Noise figure of 5 dB in base station and 9 dB in mobile station is assumed [5]. Required E_b/N_0 in base station side depends on multipath fading environment (e.g. 3GPP cases 1-4) and required transmission quality [37].

Table 5.2: General simulation parameters

Base Station (Node B)		
Maximum transmit power	43	dBm
Common pilot channel (CPICH)	33	dBm
Other common channels (CCCH)	30	dBm
Synchronization channel (SCH)	30	dBm
Maximum power per connection	38	dBm
Noise figure	5	dB
Required E_b/N_0	5	dB
Mobile Station (UE)		
Maximum transmit power	21	dBm
Tx power dynamic range	70	dBm
Power control step size	0.5	dB
Required E_c/I_0	-17	dB
Noise figure	9	dB
Required E_b/N_0	8	dB
Other		
Slow fading standard deviation	8	dB
UL IM	6	dB
DL code orthogonality	0.6	
SHO window	4	dB

5.2.3 Antennas Used in Simulations

The antennas used in simulations were UMTS-antennas, designed for frequency of 1920-2170 MHz. Horizontal beamwidths in antennas were 65° in 3-sectored scenario and 33° in 6-sectored scenario. Vertical beamwidths of antennas were 6° and 12°. Used antennas were electrically downtiltable, and for mechanical downtilt, 0° tilted electrical downtilt antenna was used. Radiation patterns for antennas used in the simulations are presented for 65°/6° antenna in Figure 5.4, 65°/12° antenna in Figure 5.5, and 33°/6° antenna in Figure 5.6. [29]

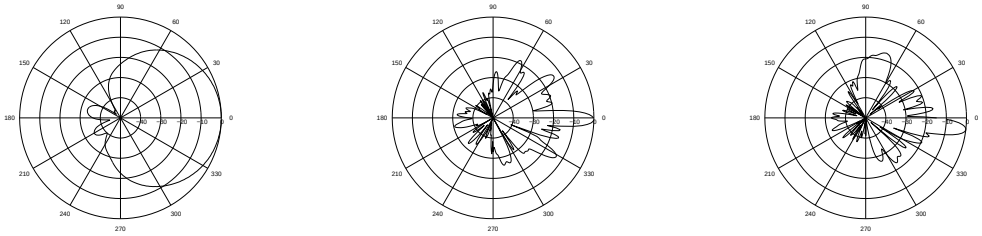

(a) Horizontal (b) Vertical 0° (c) Vertical 6°

Figure 5.4: Radiation patterns for 65°/6° antenna (Kathrein 742212): (a) horizontal radiation pattern, (b) vertical radiation pattern for 0° and (c) vertical radiation pattern for 6° electrically tilted antenna. [29]

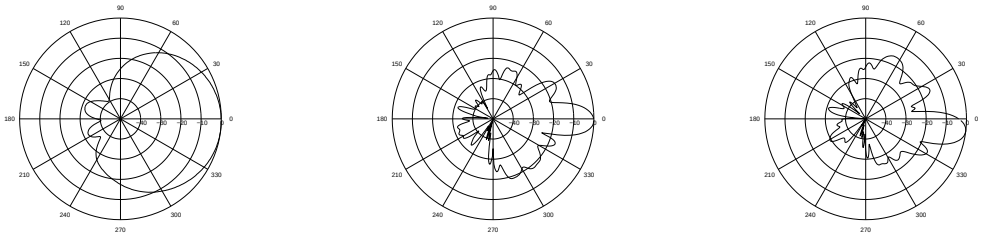

(a) Horizontal (b) Vertical 0° (c) Vertical 6°

Figure 5.5: Radiation patterns for 65°/12° antenna (Kathrein 742211): (a) horizontal radiation pattern, (b) vertical radiation pattern for 0° and (c) vertical radiation pattern for 6° electrically tilted antenna. [29]

Effects of Antenna Downtilt on Antenna Pattern

Effective horizontal beamwidth means the radiation seen in horizontal level of 0°. When downtilting antennas mechanically, the effective horizontal beamwidth changes differently than in electrical tilting; the main lobe direction flattens, and side lobe directions become more dominant. [1] This is illustrated with the antennas used in the simulations in Figure 5.7. Effective horizontal radiation patterns with different downtilt angles for mechanical downtilt are on the left side (5.7(a), 5.7(c), 5.7(e)), and for electrically tilted on the right side (5.7(b), 5.7(d), 5.7(f)). The differences of electrical and mechanical downtilting can be easily observed; with electrical downtilting, radiation attenuates equally in all horizontal angles, whereas mechanical downtilting widens the horizontal pattern significantly, and reduces the main lobe radiation up to 30 dB. Sometimes even a notch appears in the middle

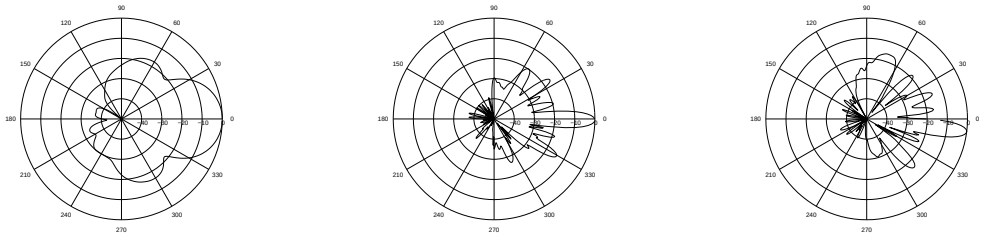

(a) Horizontal (b) Vertical 0° (c) Vertical 6°

Figure 5.6: Radiation patterns for 33°/6° antenna (Kathrein 742351): (a) horizontal radiation pattern, (b) vertical radiation pattern for 0° and (c) vertical radiation pattern for 6° electrically tilted antenna. [29]

of antenna pattern, and therefore the widening of radiation patter in mechanical downtilt is called also notch-effect. Also differences with narrow antenna (vertical beamwidth 6°) (5.7(a), 5.7(b)) are considerable clearer than with wide antenna (vertical beamwidth 12°). This leads to higher required downtilt angles to achieve the same effect of downtilting than with narrow antenna.

5.2.4 Simulation Scenarios

In order to achieve an overview on the amount of simulations run, all simulation scenarios and variables are shown in Table 5.3. Downtilt angles are the maximum used downtilt angles in a certain scenario, in some cases less simulations are performed if the direction is visible earlier. The amounts of traffic in the network differ by the load scenario and site spacing, as shown in Table 5.4, but the figures are the same in all simulated scenarios. Only 6-sectored scenario makes an exception, traffic does not vary by the site spacing.

Table 5.3: Simulated scenarios.

Downtilt technique	EDT	EDT	EDT	MDT	MDT	MDT
Sectors	3	3	6	3	3	6
Downtilt angles	0°-10°	0°-14°	0°-10°	0°-10°	0°-12°	0°-10°
Antenna configuration	65°/6°	65°/12°	33°/6°	65°/6°	65°/12°	33°/6°
Traffic	high and low load					
Antenna heights	25 m, 35 m, 45 m					
Site spacings	1.5 km, 2.0 km, 2.5 km					

Table 5.4: Amount of users in different site spacing and sectoring scenarios.

Sectoring	3-sectored						6-sectored	
Site spacing	1.5 km		2.0 km		2.5 km		all	
Load	low	high	low	high	low	high	low	high
Amount of users	1700	3700	2000	4000	1800	3800	3000	7000

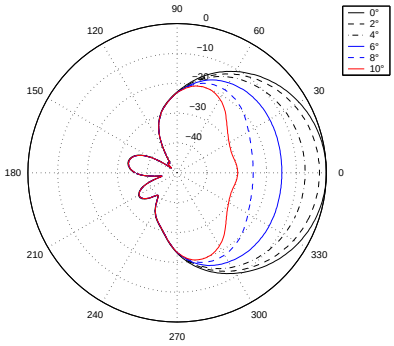

(a) MDT 65°/6°

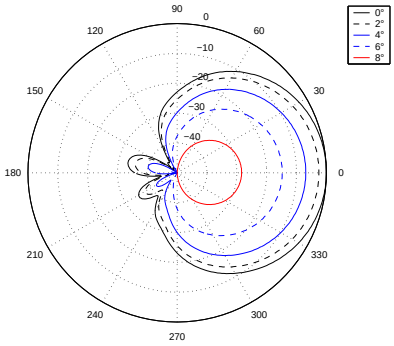

(b) EDT 65°/6°

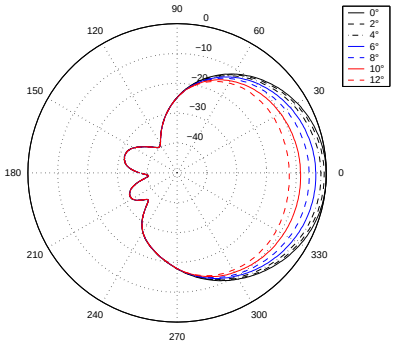

(c) MDT 65°/12°

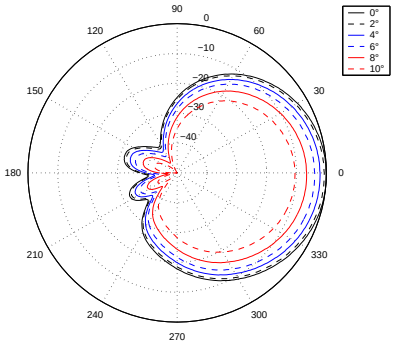

(d) EDT 65°/12°

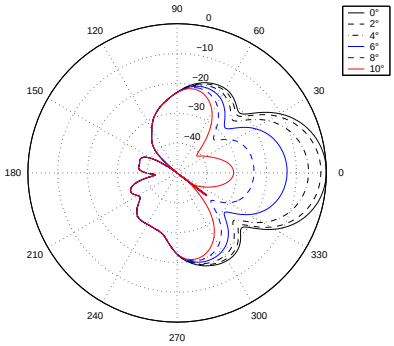

(e) MDT 33°/6°

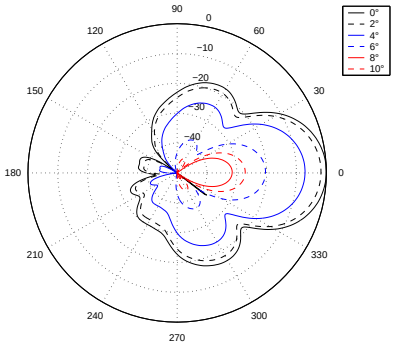

(f) EDT 33°/6°

Figure 5.7: Impact of different mechanical (a,c,e) and electrical downtilt (b,d,f) angles on the effective radiation pattern in the horizontal direction.

5.3 Link Budget

In Table 5.5, an example of a link budget for the configuration used in simulations is given. Network load is assumed to be 75 % and speech users with 12.2 kbps bitrate are observed. Thermal noise density at 20 °C is calculated in Equation 5.3. Noise figure of Node Bs is

set to 5 dB and of UE to 9 dB.

$$N = kT = 1.380658 \cdot 10^{-23} \frac{Ws}{K} \cdot 293.15K = 4.04739... \frac{W}{Hz}$$
$$N = 10log_{10} \frac{N}{mW} = -173.93 \frac{dBm}{Hz} \quad (5.3)$$

where
N = thermal noise density
k = Boltzman's constant
T = temperature in Kelvin

Receiver noise density is receiver noise figure (F) added to thermal noise density. Noise power is the total noise within the chip rate (B), and it is calculated in Equation 5.4

$$P_N = NBF = 4.047 \frac{W}{Hz} \cdot 3.84MHz \cdot \begin{bmatrix} 5 \\ 9 \end{bmatrix} dB = \begin{bmatrix} -103.08 \\ -99.08 \end{bmatrix} dBm \quad (5.4)$$

Interference margin IM is calculated from cell load level, as described in Equation 4.1. The load 75 % results in interference margin of 6.02 dB. The total interference level is the interference margin added to the noise power.

Processing gain was discussed in Section 3.5, and PG for speech traffic used in simulations (12.2 kbps) can be calculated by Equation 3.6, which results in PG of 24.98 dB.

E_b/N_0 was explained in Section 5.1.2. Typical E_b/N_0 values for speech connection, 5 dB in UL and 8 dB in DL direction are used. Receiver sensitivity is the lowest signal level that base station hardware is capable to receive with acceptable quality.

Rx antenna gain is the receiving antenna gain compared to isotropic radiator (An antenna that radiates equally in all 3D-directions). Typically antenna gains in base station are high, i.e., antennas are directional. Base station antennas used in the simulations are discussed in Chapter 5.2.3. Antennas used in the mobiles are presumed omnidirectional and therefore their gain is assumed to be 0 dBi. The cable loss in the base station side is assumed to be 0.07 dB/m, and the figure 2.5 dB results from the mean feeder cable length (antenna heights vary from 25 m to 45 m). LNAs (low noise amplifiers) and antenna diversity are not used in the simulations. Also SHO diversity gain is not treated as a separate gain in link budget calculations. Power control headroom is treated as an extra margin for network to cope with deep fast fading notches, especially at cell border areas. Adding these gains results in required signal power in the receiving end.

In the transmitting end, cable losses are subtracted and antenna gains are added to transmit power to get the peak EIRP (effective isotropic radiated power). The difference between the required signal power and the peak EIRP is the maximum allowed path loss.

Table 5.5: Example of link budget used in simulations

Service Info	**Uplink**	**Downlink**	
Load	75	75	%
Bitrate	12.2	12.2	kbps
Receiving End			
Thermal noise density	-173.93	-173.93	dBm/Hz
Receiver noise figure	5.00	9.00	dB
Receiver noise density	-168.93	-164.93	dBm/Hz
Noise power	-103.08	-99.08	dBm
Interference margin	6.02	6.02	dB
Total interference level	-97.06	-93.06	dBm
Processing gain	24.98	24.98	dB
Required E_b/N_0	5.00	8.00	dB
Receiver sensitivity	-117.05	-110.05	dBm
RX antenna gain	18.00	0.00	dBi
Cable loss	2.50	0.00	dB
LNA gain	0.00	0.00	dB
Antenna diversity gain	0.00	0.00	dB
Soft handover diversity gain	0.00	0.00	dB
Power control headroom	0.00	0.00	dB
Required signal power	-132.54	-110.04	dBm
Transmitting End			
TX power	21.00	38.00	dBm
Cable loss	0.00	2.50	dB
TX antenna gain	0.00	18.00	dBi
Peak EIRP	21.00	53.50	dBm
Isotropic Path Loss	153.54	163.54	dB

Chapter 6

Simulation Results

The results of antenna downtilt simulations are considered in this chapter. Results are first reviewed by introducing the manner of presentation in Section 6.1; different indicators in the network and presentation of the figures are analyzed. The actual simulation results are analyzed in Section 6.2, where all variables and essential simulation results are examined by means of illustrative examples of simulation results. The total collection of simulation results is presented in figures in Appendix A. Possible errors in simulation results are considered in Section 6.3, and on the basis of the simulation results, guidelines for radio network planning are given in Section 6.4

6.1 Representation of Simulation Results

In this section, the structure of simulation results is covered, and the manner of representation of different figures shown in simulation result in Section 6.2 is illustrated and analyzed.

6.1.1 Service Probability

Service probability (SP) means the probability of a mobile having a connection in the network area. In practice, if the number of users in the network is, e.g., 1000, and 950 of them can be served, is the service probability 0.95 or 95 %. In the simulations for the thesis, SP is calculated from successful speech connections, that have successfull service establishment in both uplink and downlink directions. In this respect, service probability is the most important indicator in the network, because when all mobiles have successful connections, the network is fulfilling its most important task.

The service probability values in the simulation results are presented as shown in Figure 6.1,and the values are shown as a function of downtilt angle. The left Y-axis is for the SP and X-axis is downtilt angle. The solid red line is the SP in low-loaded network, and solid black line is the SP in high-loaded network. In low-loaded network, when capacity is not the limiting factor, SP illustrates the coverage limitation caused by too high downtilt angle. When the load is higher, SP with low downtilt angles show capacity limitations due to high interference levels when antennas are directed to the horizon, and also coverage limitations with higher downtilt angles.

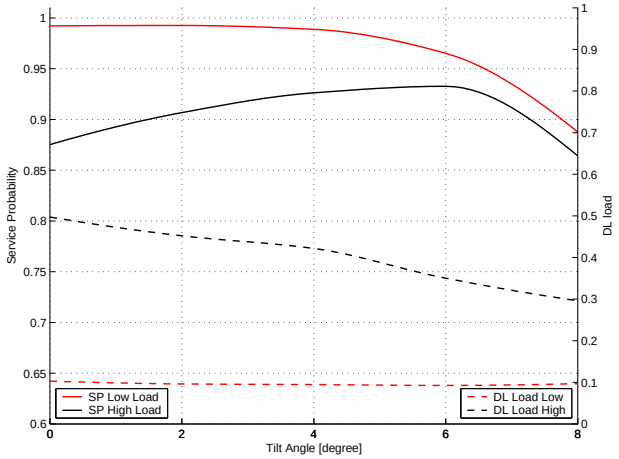

Figure 6.1: Service probability as a function of downtilt angle (EDT, 6 sectors 33°/6° antenna, antenna height 25m, and site spacing 2.5 km).

6.1.2 Uplink and Downlink Load

The origin of uplink and downlink loads was considered in Section 4.2.2 Hence, the load defines the amount of resources used in the network. Since the loads in uplink and downlink are not the same, and the lack of either uplink or downlink resources can limit the capacity and coverage, both directions have to be considered separately.

The downlink loads are presented in same figures with service probability. In Figure 6.1, the solid lines are SP values, and dashed lines describe the downlink load as a function of downtilt angle. Again, red line corresponds to low load and black line to high load scenario. In low loaded scenario, the DL load remains almost constant in all cases. It decreases slightly as downtilt angle decreases. Only in high downtilt angles the DL load begins to increase due to coverage problems in the cell edge areas. In high loaded scenario, the DL load is at rather high level in non-tilted scenarios. This depicts high interference levels due to the antennas pointing towards horizon.

The uplink direction is shown in separate figures, and the load is reviewed by average UL transmit power over the network area. In Figure 6.2, the uplink transmit powers are presented as a function of downtilt angle. Since the changes in high loaded scenario are more significant, low loaded scenario is not analyzed. When downtilting antennas, with low downtilt angles the UL Tx powers decrease a bit due to decreasing interference levels, and with higher downtilt angles the powers begin to increase towards higher values due to coverage problems. With high EDT angles, uplink power is typically limiting factor, since DL load remains at low level.

6.1.3 Connection Failures

When an error in connection occurs, there can be different reasons for that. Main failures in the simulations were E_c/I_0, DL and UL E_b/N_0 and noise rise. Too low E_c/I_0-level indicates too weak signal level, i.e., coverage problems or interference problems. E_c/I_0 can be treated as a common indicator for coverage and capacity in the network, whereas E_b/N_0 values are defined separately for each service. Therefore, too low E_b/N_0 values

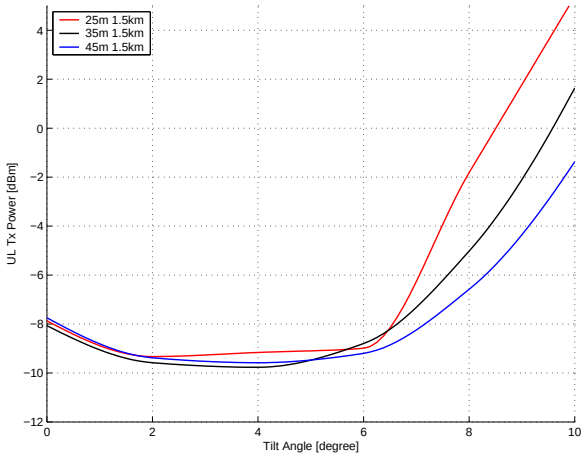

Figure 6.2: UL transmit power as a function of downtilt angle (EDT, 3 sectors 65°/6° antenna, antenna heights 25 m, 35 m, and 45 m, and site spacing 1.5 km).

mean that there is no coverage for the particular service, When downlink E_b/N_0 gets too low, it indicates too high interference levels in downlink direction, and uplink E_b/N_0 in uplink direction. Noise rise represents increase in noise level in uplink direction.

Reasons to failure in connection in different simulation scenarios with EDT and MDT are shown in Figure 6.3. Figures show what are the contributions to failure, if such occurred, without telling anything about the amounts of failures, that can be gathered from service probability figures. Multiple failures can take place simultaneously, therefore the sum of contributions to failures in certain scenario can be above one.

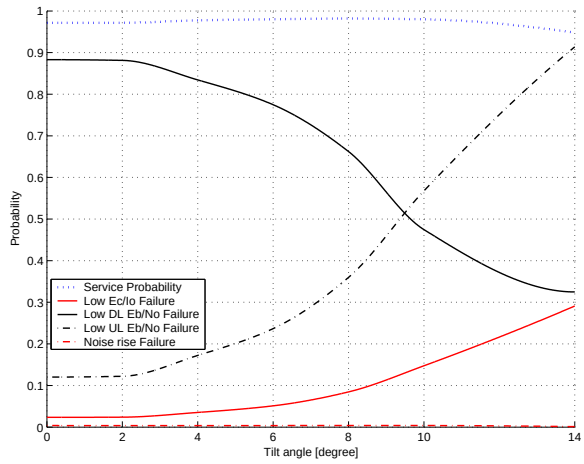

Figure 6.3: Main contributions to failure in 65°/12° electrical downtilt scenario with antenna height of 25 m and site spacing of 1.5 km.

6.1.4 Optimal Downtilt Angle

Optimum downtilt angle is defined from service probability. First, the maximum service probabilities from the low (grey/red line) and high (black line) load scenarios are collected.

Secondly, the lower and upper boundaries are searched. The lower boundary is the point where the service probability of high loaded scenario has decreased 0.5 % of its maximum value. This lower boundary describes the point where the interference level is low enough. The low load scenario does not affect the lower boundary because interferences are at low level. Coverage limitations define the upper boundary, and it is searched from both the low and high load scenarios. The upper boundary is the point where the service probability at the low load scenarios has dropped 1 % or at high load scenarios 0.5 %. An optimum tilt angle is then assumed to exist between these boundaries, and reported optimum angle is the mean value of the boundary points. Defining of an optimal downtilt angle is illustrated in Figure 6.4

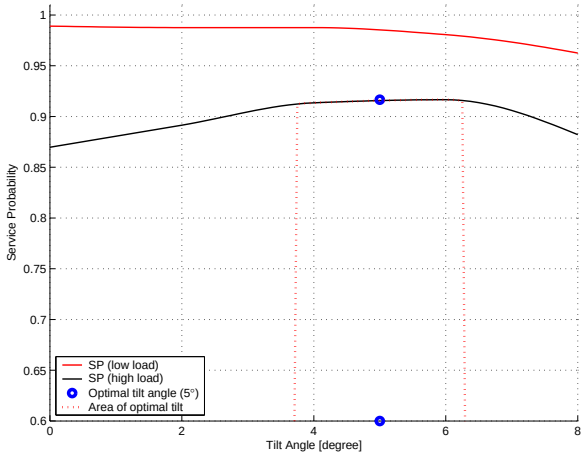

Figure 6.4: Defining the optimal downtilt angle.

6.1.5 SHO Area Analysis

The importance of controlling SHO areas in the network was considered in Section 4.3.3. The effects of downtilting on SHO areas and hearable pilots in certain area of the network are illustrated in Figure 6.5. In Figure 6.5(a), the probability of SHO connection in network area is shown. Site locations are in the middle of the dark area, where the probability SHOs is very low, and between sites there is an area, where the probability of SHO connections is high.

The blue lines in Figure 6.5(a) describe the area from where the Figure 6.5(b) is generated. The average probability of SHOs (solid black line) and softer HOs (dashed black line) are shown from main lobe to back lobe direction, and in 6-sector scenario from main lobe to main lobe direction. Also, the total SHO probability (soft+softer) is shown (solid thick black line). SHO probability is on the left axis. On top of the SHOs, also the levels of 4 first pilots are shown. Red solid line is the level of first (i.e., the strongest) pilot. Red dashed line is the 1st pilot minus reporting range, that defines the area where SHOs should occur. Also the levels of the 2nd (blue line), the 3rd (green line) and the 4th (cyan line) are drawn. Since size of the active set is 3, the 4th pilot introduces always interference and causes pilot pollution. 0° downtilt, as well as MDT and EDT from the closest simulated point to the optimal angle are shown in order to see the effect of downtilting on SHOs and pilot levels.

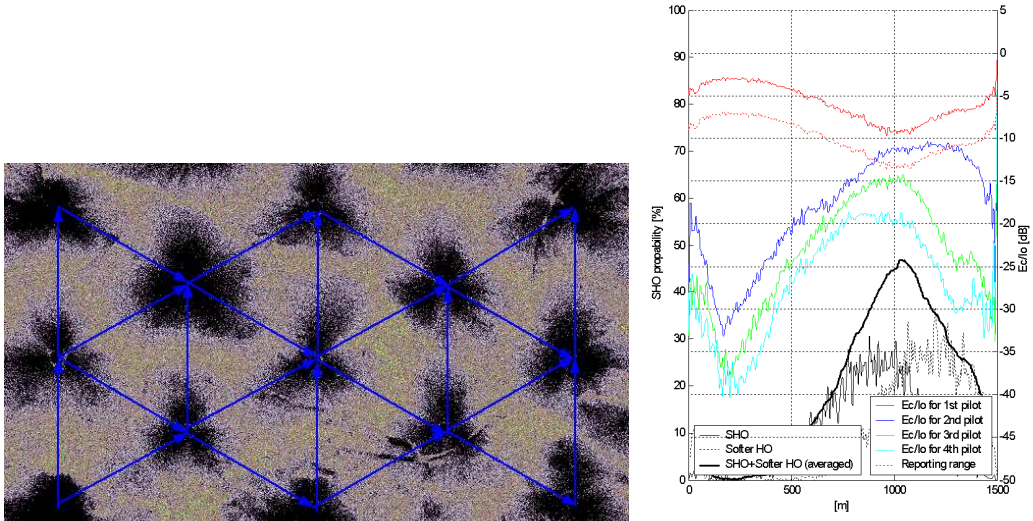

Figure 6.5: (a) SHO probability in the simulation area. (b) SHO and softer HO probabilities and the levels of 1st - 4th pilots from main lobe to back lobe direction.

6.1.6 Capacity Gain

Downtilting antennas decreases interference levels in the network, which in WCDMA network enables use of higher data rates, or greater amount of users in the network. The amount of capacity increase is called capacity gain. In the thesis, capacity gain is calculated from the amount of successful speech connections as follows.

First, the mean DL transmit power of low-loaded non-tilted scenario is calculated. Thereafter, the mean served -value of optimally tilted scenario for the same DL Tx power is estimated by linear interpolation from low and high loaded points. Then the corresponding mean served -values are gathered and capacity gain is calculated. This method is intentionally pessimistic in order to avoid too optimistic results, since only two load scenarios were simulated. If capacity gains were calculated from highest difference, the gains would be significantly higher. However, since the exact determination of capacity gain would have required simulations with several different loads, the most pessimistic values are presented to make sure not to overestimate the advantage of downtilting.

The calculation of capacity gain is illustrated with an example in Figure 6.6. Low load non-tilted DL mean Tx power is 34.5 dBm, and corresponding mean-served value 105 users. Estimated mean served value for same the DL mean Tx power is 122 users in an optimally tilted scenario. Hence, capacity gain can be calculated as follows:
$Capacity\_Gain = (\frac{122}{104.5} - 1) \cdot 100\ \% \approx 17\ \%$

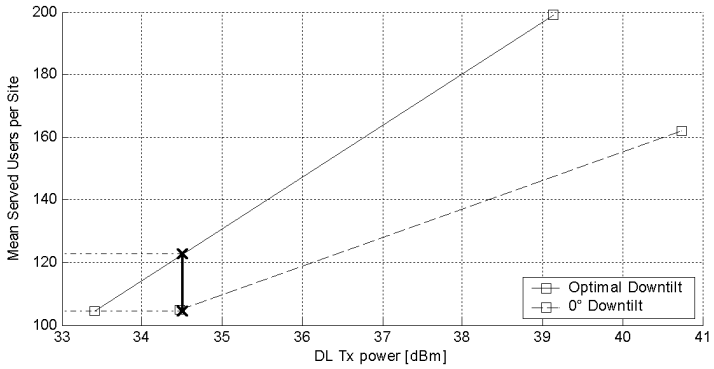

Figure 6.6: Example of capacity gain calculation: EDT 6°/65° antenna, antenna height 35 m, and site spacing 2.0 km.

6.2 Downtilt Simulation Results

6.2.1 Service Probability

Effect of Antenna Height and Site Spacing

In Figure 6.7, the effect of antenna height and site spacing is illustrated in EDT 3-sectored 65°/6° scenario. With low antenna height and small site spacing (Figure 6.7(a)), low loaded network results in about 100 % SP with reasonable downtilt. High-loaded non-tilted scenario results in SP of 87 %, and after downtilting, SP of about 98 % can be achieved.

In case of low antenna height and large site spacing (Figure 6.7(b)), SP increases when antennas are tilted, but coverage begins to limit, and only about 92 % SP can be reached in high loaded network. Also the SP in low loaded network is dropped to about 98 %.

Increasing antenna height (Figure 6.7(c)) results in high interference levels in case of small site spacing, when network is high loaded. Due to interference, SP is only about 62 % with non-tilted antennas. Downtilting antennas increase the SP dramatically, and with 6° downtilt angle SP is already almost 100 %.

Effect of Antenna Vertical Beamwidth

The effect of antenna vertical beamwidth on the network behavior is shown in Figure 6.8. Only MDT 3-sectored 65°/6° and 65°/12° scenarios with antenna height of 25 m and site spacing of 1.5 km are considered, but the effects are rather similar in overall. With narrow antenna beamwidth, downtilting increases SP about 11 %, but with wide antenna beamwidth, the increase is only about 2 %. With wider beamwidths, the advantage of tilting is not that significant, but on the other hand, optimizing the downtilt angles in the network is not that essential.

Effect of Antenna Tilting Technique (EDT / MDT)

In this section, the effect of electrical and mechanical downtilting technique on network behavior are compared. The main theoretical differences of the tilting techniques were

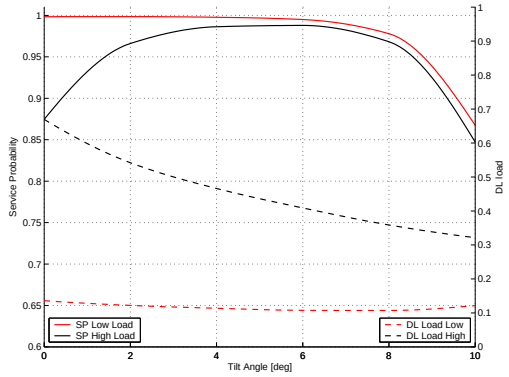

(a) 25 m 1.5 km

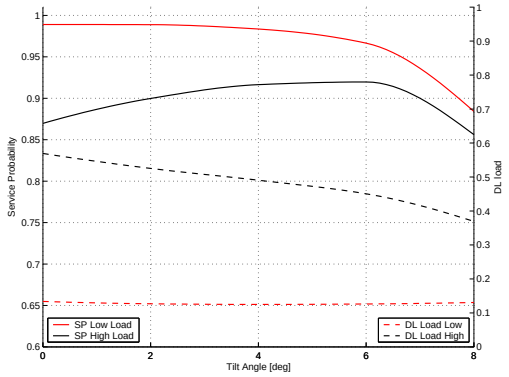

(b) 25 m 2.5 km

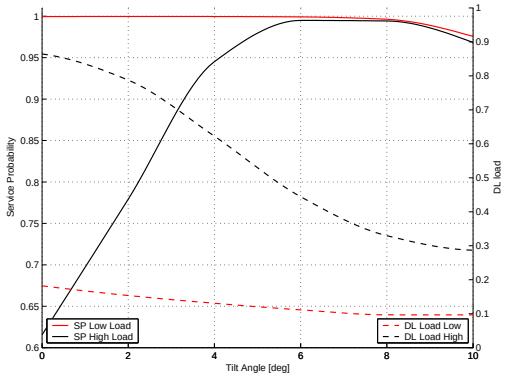

(c) 45 m 1.5 km

Figure 6.7: Comparison of the effect of antenna height and site spacing on the service probability as a function of downtilt angle. EDT 3-sectored 65°/6° scenario, antenna heights and site spacings: (a) 25 m 1.5 km, (b) 25 m 2.5 km, and (c) 45 m 1.5 km, respectively.

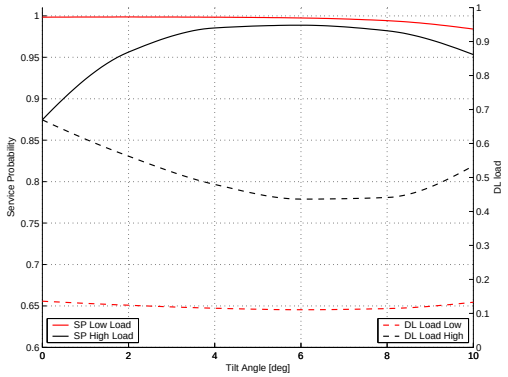

(a) Narrow antenna (6°)

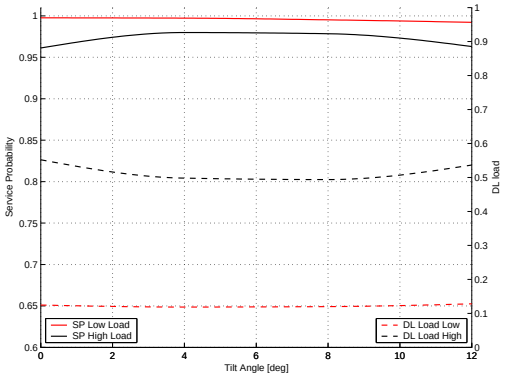

(b) Wide antenna (12°)

Figure 6.8: Comparison of the effect of antenna vertical beamwidth on the service probability as a function of downtilt angle. MDT 3-sectored (a) 65°/6° and (b) 65°/12° scenario, antenna height 25 m and site spacing 1.5 km.

discussed in Section 4.3. In Figure 6.9, results of optimal electrical and mechanical tilting are compared with non-tilted scenario. With narrow (65°/6°) antennas in 3-sectored scenario (Figure 6.9(a)), the advantage of tilting is quite obvious, but difference between EDT and MDT is almost invisible, and only 45 m / 2.5 km site configuration results in slightly better service probability with EDT. With wide (65°/12°) antennas (Figure 6.9(b)), the advantage of tilting is the smallest, due to reasons discussed in Section 5.2.3, (Figure 5.7(c) - 5.7(d)). Also here, EDT differs from MDT only in 45 m / 2.5 km site configuration. In 6-sectored (33°/6°) scenario (Figure 6.9(c)), EDT results in overall, about 1 % better service probability, and differences between optimal tilting and non-tilting are similar to (65°/6°) scenario.

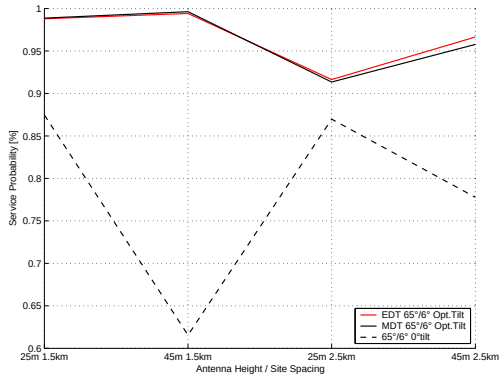

(a) 65°/6°

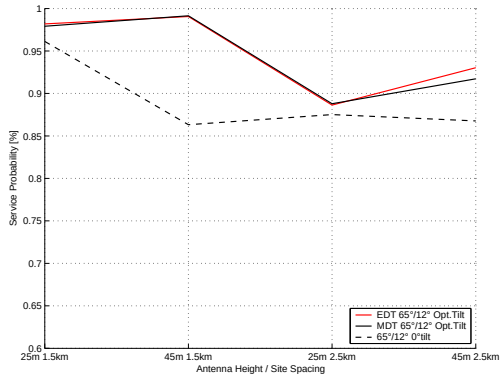

(b) 65°/12°

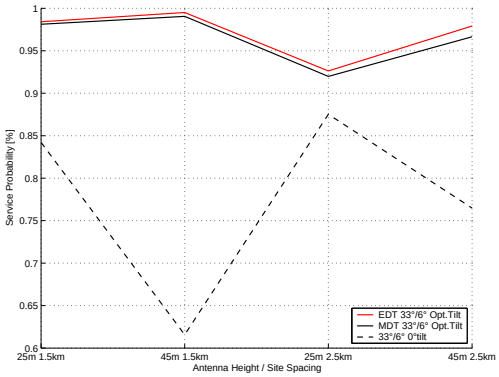

(c) 33°/6°

Figure 6.9: Comparison of service probability with non-tilted and optimally tilted antennas in different electrical and mechanical downtilt scenarios.

Effect of Sectoring

The results in 6-sectored 33°/6° scenario (Figure 6.10) are rather similar to 6-sectored 65°/6° scenario (Figure 6.7(a)), only the changes caused by downtilting are slightly stronger. Compared to the 3-sectored MDT (Figure 6.7(a)), downtilting in 6-sectored MDT (Figure 6.10(a)) scenario causes more abrupt changes, also with high downtilt angles. Changes with EDT between 3- and 6- sectors (Figures 6.7(a) and 6.10(b)) are not so great, but 6-sectored network results in slightly lower SP than 3-sectored. However, it needs to be

remembered that there is almost double amount of users in 6-sectored network.

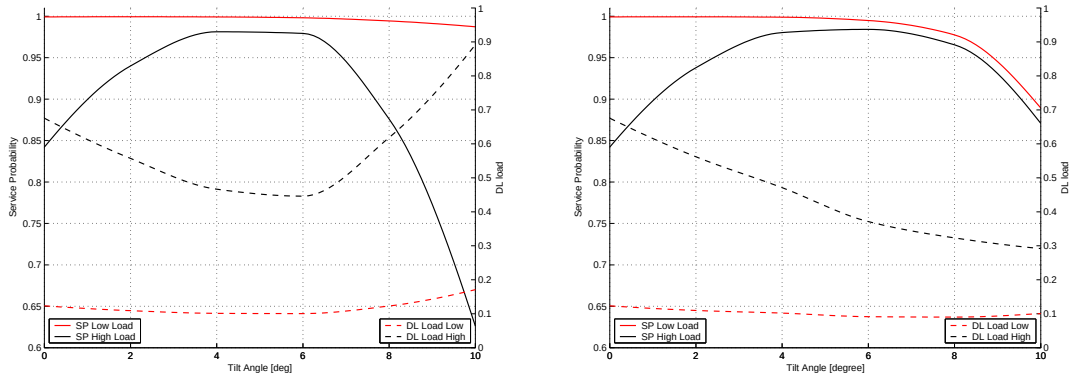

(a) 6-sectored MDT (b) 6-sectored EDT

Figure 6.10: Comparison of the effect of sectoring on the service probability as a function of downtilt angle. (a) MDT 6-sectored 33°/6° and (b) EDT 6-sectored 33°/6° scenario, antenna height 25 m and site spacing 1.5 km.

6.2.2 Uplink and Downlink Load

The basic behavior of uplink and downlink load while downtilting antennas was described in Section 6.1.2. DL load decreases in all simulation scenarios more or less linearly as a function of downtilt angle. MDT 33°/6° scenarios with high downtilt angles make an exception; the increase of softer handover connections after about 6° downtilting introduces so much Softer HO overhead, that it is clearly visible also in DL load, and especially in MDT 33°/6° scenario. In Figure 6.11, the differences in DL load (blue lines) between different EDT and MDT scenarios with antenna height of 25 m and site spacing of 1.5 km are shown. EDT results always a few percentages lower DL load than MDT at optimal downtilt angle, and differences between 0° and optimal downtilt are again smallest with wide antennas.

Also the respective UL transmit powers are shown in Figure 6.11 (black lines). In 65°/6° scenario EDT results in slightly lower average UL Tx power, but in other scenarios (65°/12° and 33°/6°), EDT results in higher UL Tx powers than MDT. This together with opposite phenomena with DL load shows that EDT results in more uplink limited network, and MDT in more downlink limited network. Also one interesting note is that when using wide antennas, optimal downtilt causes average uplink Tx power to decrease compared to non-tilted network. The difference is over 1 dBm in both, EDT and MDT 65°/12° scenarios.

6.2.3 Connection Failures

Main contributions to failures in different scenarios are shown in Figure 6.12. Only results from antenna height of 25 m and site spacing of 1.5km topology are shown, but the results in different topology differ only slightly. In non-tilted scenario, low DL E_b/N_0 is always the only reason for failures, due to antennas pointing towards horizon and each other, not desired coverage area, and thus generating high levels of interference to the other sites. The

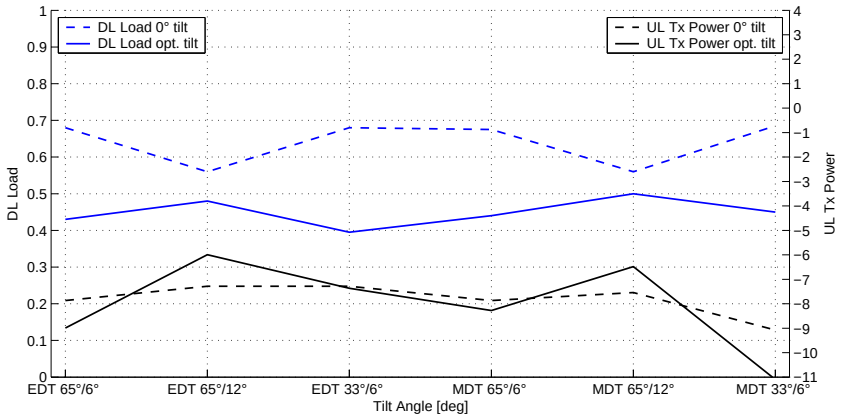

Figure 6.11: Comparison of DL load and UL average transmit power with non-tilted and optimally tilted antennas. All simulation scenarios with antenna height of 25 m, site spacing 1.5 km

differences in failure reasons in EDT and MDT are rather illustrative: when downtilting antennas mechanically, DL E_b/N_0 remains as main reason for failures, although part of UL E_b/N_0 rises a little. With EDT, state changes totally after tilting antennas; UL E_b/N_0 becomes the main reason for failure, and also E_c/I_0 -failures occur more often, which reflects coverage problems. These results confirm what was shown in previous section, that network with EDT is more uplink and network with MDT is more downlink limited. In addition, EDT results in coverage limited and MDT in interference limited network.

6.2.4 Optimal Downtilt Angle

An optimal downtilt angle was defined for all scenarios as explained in Section 6.1.4. The defined optimal downtilt angles are presented for EDT scenarios in Table 6.1 and for MDT scenarios in Table 6.2. The columns marked with S are the optimal angles gathered from the simulations, and the columns marked with G are calculated values from the geometrical downtilting Equation (4.8), presented in Section 4.4.3. The purpose of presenting the values of the geometrical equation is to compare simulated values to results of a rather simple equation, and to evaluate its suitability to be used in RNP.

The simulated optimal downtilt angles vary from 3.4° to 10.3°. For 65°/6° scenario the variation is from 4.3° to 8.1°. Antenna height has the most powerful effect on optimal downtilt angle, and site spacing has also a clear effect. The higher the antennas, the more important is proper downtilting. The difference in service probability with 45 m antenna height and 1.5 km site spacing is about 35 % between 0° and optimal downtilt. On average MDT results in 0.8° bigger optimal downtilt angles than EDT.

The simulated optimal angles in 65°/12° scenarios vary between 3.4° and 10.3°. Although the variations in optimal angle are the biggest with wide antennas, the effect of downtilting on any examined indicator in the network is rather small. With 45 m antenna height and 1.5 km site spacing, the improvement in service probability is only about 10 %, and change is smaller with other antenna height and site spacing combinations. In that sense, a system with wide antennas is rather robust for the false antenna downtilt. Average downtilt angle with EDT in this scenario is 1.4° bigger compared to MDT, so the difference is opposite compared to 65°/6° scenario.

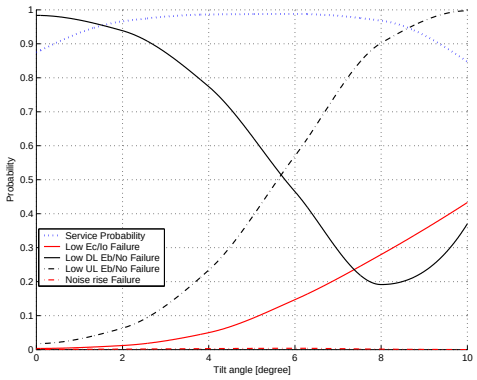

(a) EDT 65°/6°

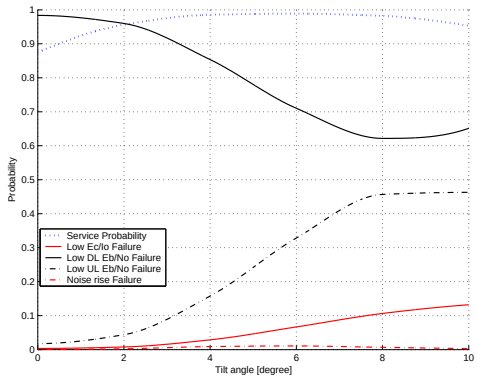

(b) MDT 65°/6°

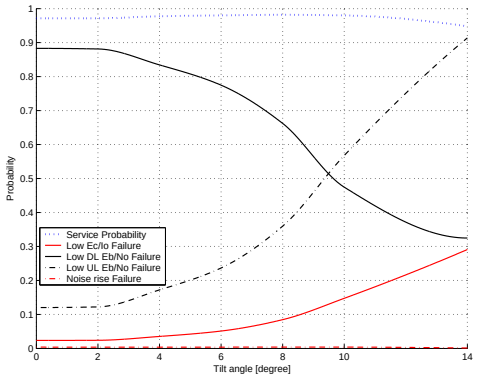

(c) EDT 65°/12°

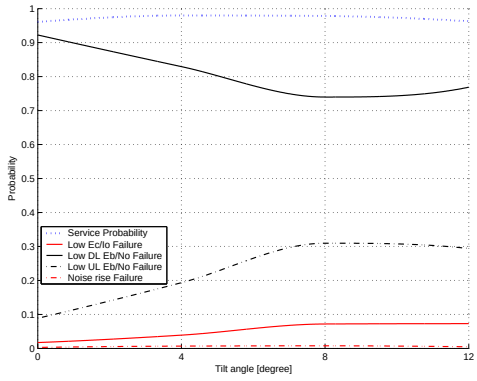

(d) MDT 65°/12°

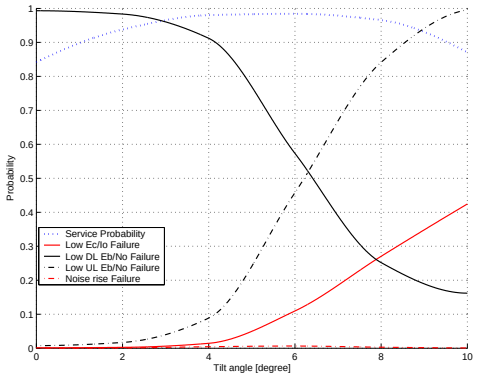

(e) EDT 33°/6°

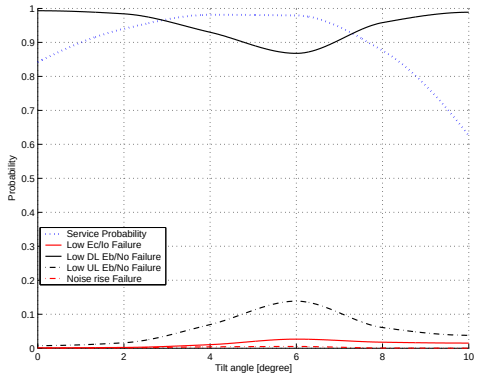

(f) MDT 33°/6°

Figure 6.12: Comparison of main contributions to failure in different electrical and mechanical downtilt scenarios (antenna height 25 m, site spacing 1.5 km).

In 33°/6° scenario, the simulated optimal downtilt angles vary from 3.7° to 7.1°. The effect of downtilt on service probability is similar to 65°/6° scenario, i.e., the higher the antennas and larger the site spacing, the greater effect downtilting has on the network behavior. Differences between EDT and MDT are slightly small, only 0.3° difference in average downtilt angle.

Simulated and geometrical optimal downtilt angles are shown in Figure 6.13, for EDT in 6.13(a) and for MDT in 6.13(b). With EDT, 65°/12° scenario follows worse the results of geometrical equation, error is almost ±1.5°. However, the influence of false downtilt angle is the smallest with wide antennas. With other EDT scenarios, simulated and geometrical downtilt angles follow each other better, and error could be easier minimized with small bias-correction. With MDT, errors in 65°/12° scenario between simulated and geometrical values are even over 3°, but still the affect of downtilt downtilt on network behavior is so small that this error would not cause major problems. In 65°/6° scenario, errors with MDT are bigger than with EDT, maximally over 2°. In 33°/6° scenario simulated and geometrical values follow each other rather well. As a conclusion for the geometrical equation, it can be used for rough estimation on the required downtilt angle for a network, but some correction factor needs to be added in order to get more realistic values. Alternatively, a more sophisticated higher order or logarithmic equation could be developed.

Table 6.1: Simulated (S) and geometrical (G) optimal downtilt angle for all simulated network topologies and site configurations with EDT.

Site spacing /	EDT 3-sec 65°/6°		EDT 3-sec 65°/12°		EDT 6-sec 33°/6°	
Antenna height	S	G	S	G	S	G
1.5 km						
25 m	5.1°	4.3°	7.3°	7.3°	5.4°	4.8°
35 m	6.1°	4.9°	9.1°	7.9°	6.3°	5.6°
45 m	7.1°	5.5°	10.3°	8.5°	7.1°	6.3°
2.0 km						
25 m	4.3°	4.0°	5.6°	7.0°	3.8°	4.3°
35 m	5.8°	4.4°	7.9°	7.4°	5.1°	4.9°
45 m	6.3°	4.9°	9.3°	7.9°	6.1°	5.5°
2.5 km						
25 m	4.5°	3.8°	5.2°	6.8°	4.6°	4.1°
35 m	5.4°	4.2°	7.6°	7.2°	5.3°	4.5°
45 m	5.9°	4.5°	8.3°	7.5°	5.7°	5.0°

6.2.5 Soft and Softer Handovers

Influence of Tilting on SHO Probability

In Figure 6.14, the behavior of soft handover (SHO) probabilities is presented with respect to the antenna downtilt angle of different simulation scenarios. In all scenarios, the probability of soft handover decreases rather linearly as a function of increasing downtilt angle. This is a direct consequence to the upper -3dB beam coming closer to the base station, and thus reducing coverage overlapping. The SHO probabilities in both 3- and 6-sectored scenarios (Figures 6.14(a) and 6.14(c), respectively) behave rather similarly with narrow antenna, but the effects of downtilting are expectedly smaller with the antennas of a wider vertical beamwidth (Figure 6.14(b)).

Intuitively, a higher antenna position creates larger coverage overlapping areas, and hence increases the soft handover probability. Moreover, larger site spacing decreases soft handover probability due to smaller coverage overlapping. With lower downtilt angles, the

Table 6.2: Simulated (S) and geometrical (G) optimal downtilt angle for all simulated network topologies and site configurations with MDT.

Site spacing /	MDT 3-sec 65°/6°		MDT 3-sec 65°/12°		MDT 6-sec 33°/6°	
Antenna height	S	G	S	G	S	G
1.5 km						
25 m	5.7°	4.3°	5.9°	7.3°	4.9°	4.8°
35 m	7.3°	4.9°	8.1°	7.9°	5.9°	5.6°
45 m	8.1°	5.5°	9.1°	8.5°	7.0°	6.3°
2.0 km						
25 m	5.1°	4.0°	4.3°	7.0°	3.8°	4.3°
35 m	6.7°	4.4°	7.5°	7.4°	4.8°	4.9°
45 m	6.9°	4.9°	8.2°	7.9°	5.9°	5.5°
2.5 km						
25 m	5.1°	3.8°	3.4°	6.8°	3.7°	4.1°
35 m	6.1°	4.2°	4.4°	7.2°	4.5°	4.5°
45 m	6.9°	4.5°	6.9°	7.5°	5.8°	5.0°

differences between topologies are emphasized, but towards higher downtilt angles, differences in soft handover probabilities are disappearing.

Influence of Tilting on Softer HO Probability

The effects of downtilting on softer HO probability are shown in Figure 6.15. With EDT (solid lines), the softer HO probability as a function of downtilt angle remains almost constant, and at about the same level, 3-5 %, in all EDT scenarios. With MDT (dashed lines), behavior is no more constant or linear, but the probability of softer HOs begin to raise after about 4° downtilt angle in all MDT scenarios; the least with wide antennas (Figure 6.15(b)), and the most with 6-sectored sites (Figure 6.15(c)). This growth of softer HO probability with MDT can be explained by the relative widening of horizontal radiation pattern in MDT, discussed in Section 5.2.3, which causes relatively more overlapping between sectors, and therefore more softer handovers. A raise of softer HOs with MDT is also visible in total HO probabilities, shown in Appendix A, Figures 16, 17, and 18.

Influence of Tilting on SHO Areas

If areas where soft handover connections happen are scattered, the active set of mobile changes all the time, causing additional signaling load and reducing the gain achieved from SHOs. Network performance could be enhanced, if the scattered areas of SHO connections could be unified. The effect of downtilting on the SHO areas were studied, and the results show that downtilting can help unifying SHO areas.

In Figure 6.16, SHO probabilities of 3-sectored 65°/6° scenario are shown. In Figure 6.16(a), the non-tilted scenario is shown. SHOs take place all over the network with rather high probability, even close to the base stations, in the antenna mainbeam direction. The effect of electrical downtilt can be seen in Figure 6.16(b), and the changes are rather evident. There is a clear single-cell connection area in the antenna mainbeam direction, where no SHOs occur. There is also a separable area between base stations where SHOs

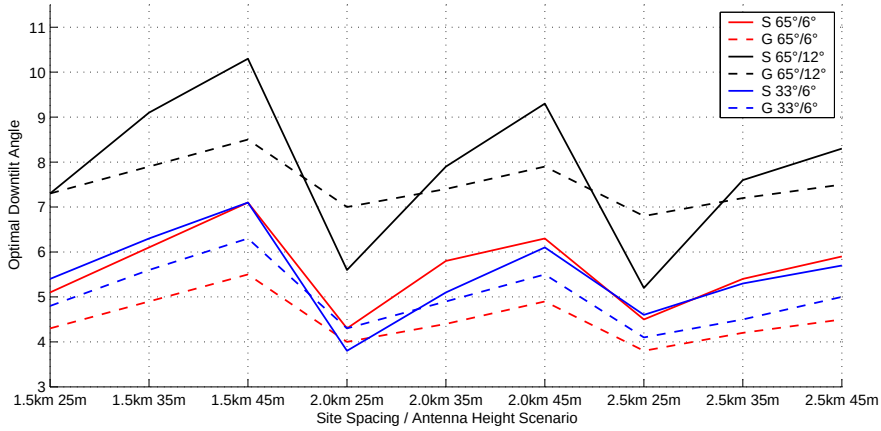

(a) EDT

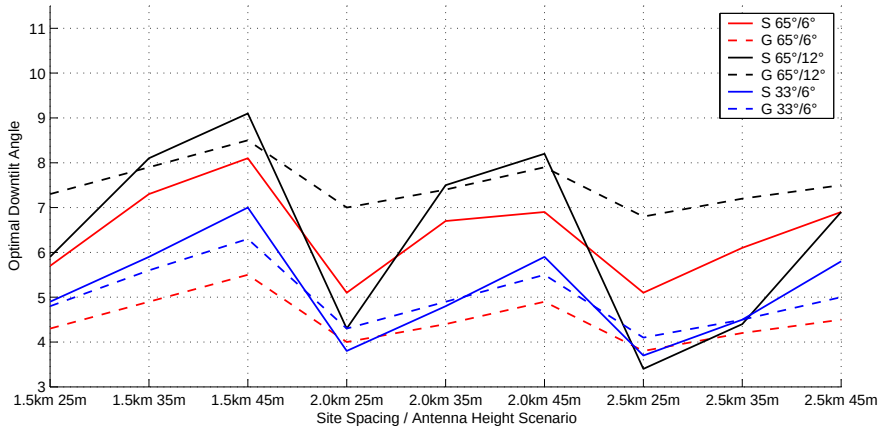

(b) MDT

Figure 6.13: Simulated (S) and geometrical (G) optimal downtilt angle for all simulated network topologies and site configurations with (a) EDT and (b) MDT.

take place. The effect of mechanical downtilt is shown in Figure 6.16(c); SHO areas distinguish similarly compared to electrical, but the edges are not that sharp. The results of 3-sectored 65°/12° scenario are similar, but the effect is not that deep. In Figure 6.17, the same results are shown in 6-sectored 33°/6° scenario. The difference between electrical and mechanical downtilting is clear. In EDT, the single-cell areas are evidently larger. Compared to 3-sectored network, areas of SHO are less continuous, which is caused by the antennas pointing towards each other.

In Figures 6.18, 6.19, and 6.20, the effects of downtilting on SHO probabilities and pilot levels are shown. In Figure 6.18(a), (3-sectored 65°/6° scenario from main lobe to back lobe direction) non-tilted antennas cause rather high level of 4th pilot (For proper functionality of the network, the modulation of only 3 best pilot signals is beneficial, and the rest can be treated as other-cell interference). Also the SHO probability close to cell in main lobe direction is rather high. Close to the back lobe, also softer HO probability gets high, which is normal between sectors. After downtilting, in both mechanical (Figure 6.18(b)) and electrical (Figure 6.18(c)), SHO probability has dropped to the zero close to the antenna main beam direction. Also the level of the 2nd - 4th pilot has dropped close the

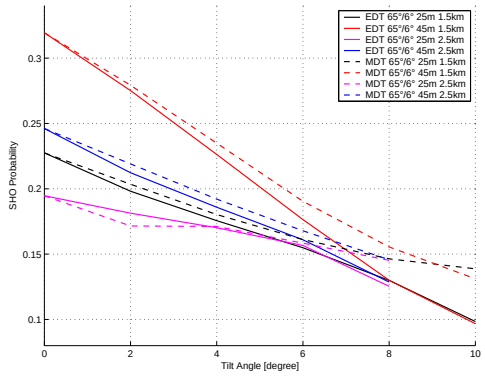

(a) EDT/MDT 65°/6°

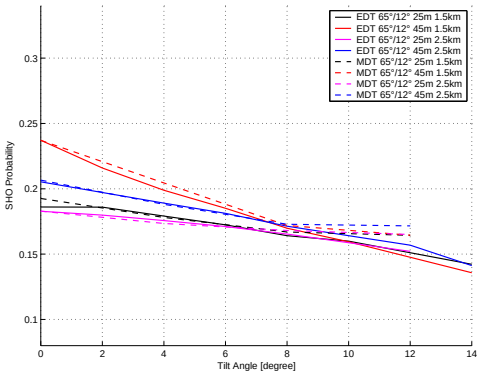

(b) EDT/MDT 65°/12°

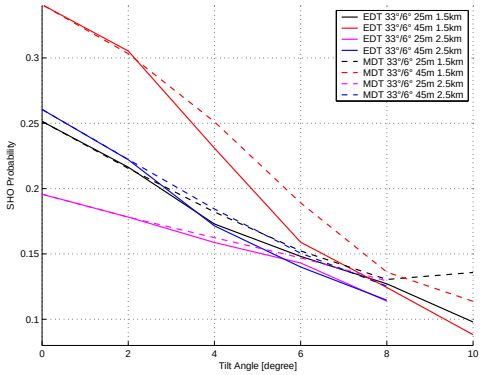

(c) EDT/MDT 33°/6°

Figure 6.14: SHO probabilities as a function of downtilt angle. in all simulation scenarios.

main beam direction. EDT results in slightly narrower SHO area. With 3-sectors and wider antenna (65°/12°), the effect of downtilting on SHO is rather minimal, but still the pilot levels drop near the base station.

In 6-sectored scenario (Figure 6.20), the situation is different since antennas point towards each other. Downtilting clearly raises the level of 1st pilot, and decreases the level of other pilots, except the level of the 2nd pilot between sectors where soft handovers occur. These results cover only a narrow area between sites. Hence, the behavior of the whole network can not be directly analyzed, but they still indicate on the effects of downtilting.

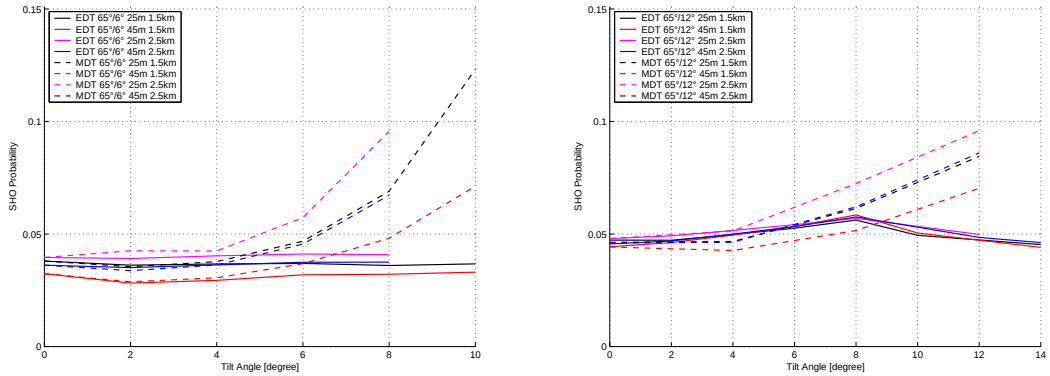

(a) EDT/MDT 65°/6° (b) EDT/MDT 65°/12°

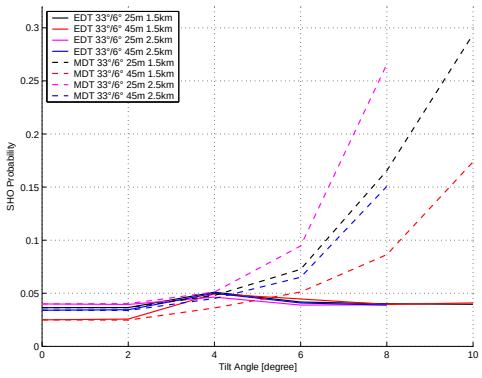

(c) EDT/MDT 33°/6°

Figure 6.15: Softer HO probabilities as a function of downtilt angle. in all simulation scenarios.

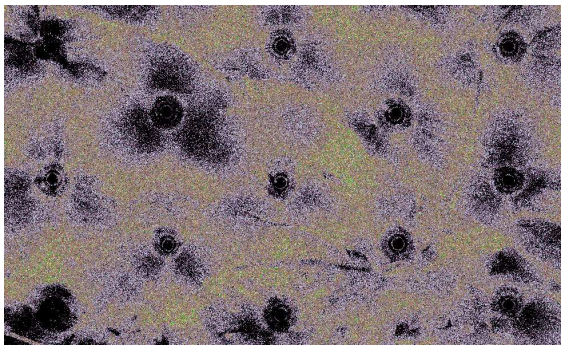

(a) 0°

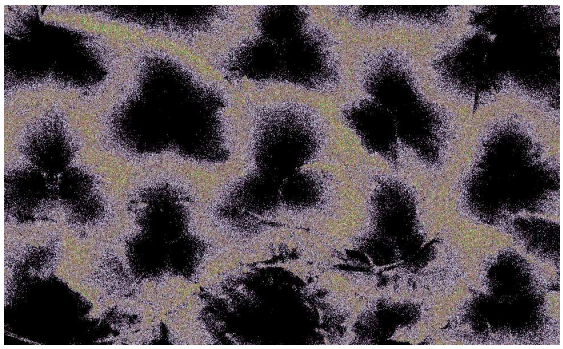

(b) EDT 8°

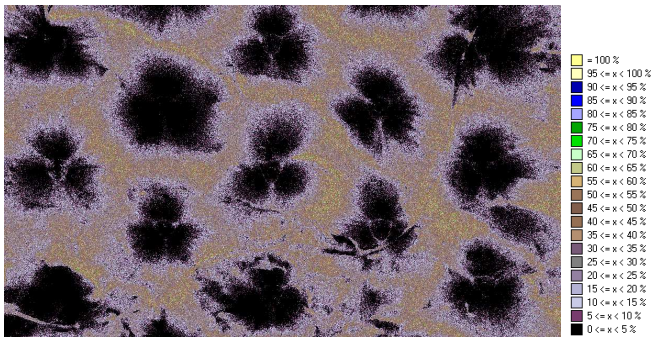

(c) MDT 6°

Figure 6.16: Comparison of SHO areas, (a) 0° downtilt, (b) EDT 8°, and (c) MDT 6° (6° / 65°, 1.5 km 25 m scenario.)

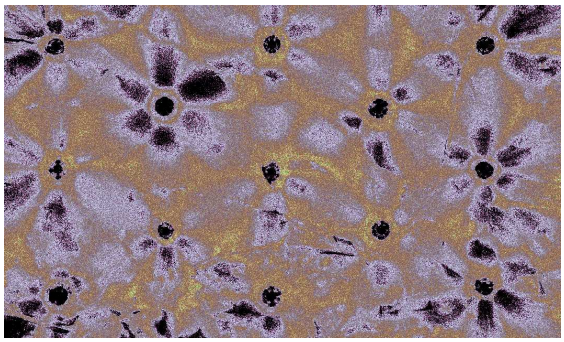

(a) 0°

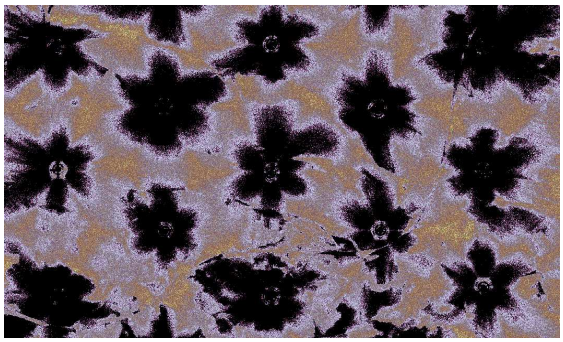

(b) EDT 6°

(c) MDT 4°

Figure 6.17: Comparison of SHO areas, (a) 0° downtilt, (b) EDT 6°, (c) MDT 4° (6° / 33°, 1.5 km 25 m scenario.)

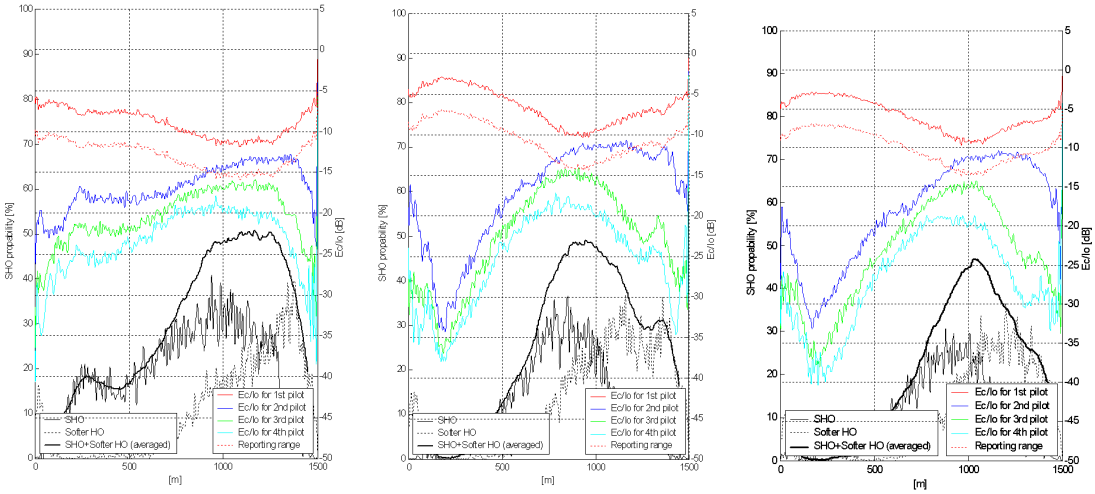

(a) 0° (b) MDT (c) EDT

Figure 6.18: SHO and softer HO probability and the level of first 4 pilots from main lobe to back lobe in 65°/6° scenario, antenna height 25 m and site spacing 1.5 km. (a) 0° downtilt, (b) optimal MDT, (c) optimal EDT

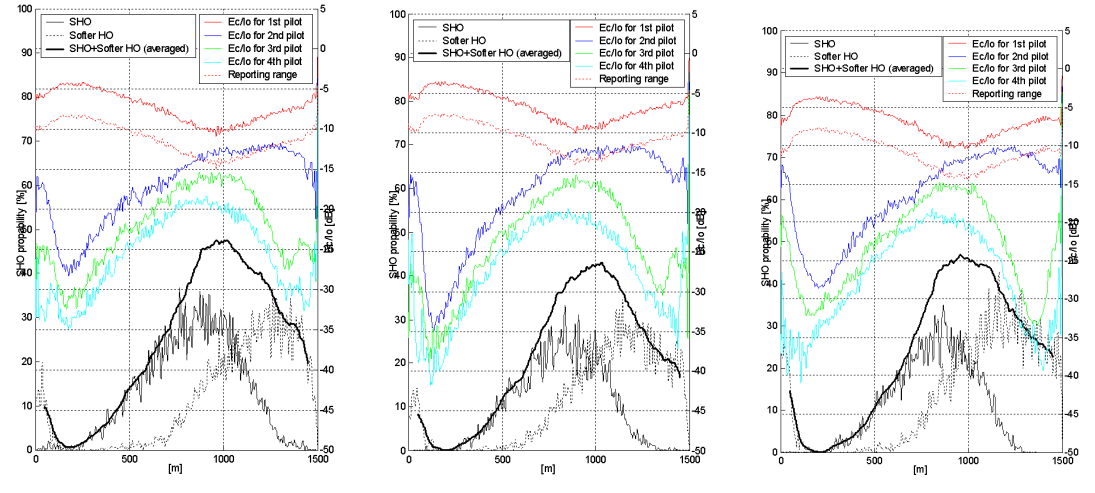

(a) 0° (b) MDT (c) EDT

Figure 6.19: SHO and softer HO probability and the level of first 4 pilots from main lobe to back lobe in 65°/12° scenario, antenna height 25 m and site spacing 1.5 km. (a) 0° downtilt, (b) optimal MDT, (c) optimal EDT

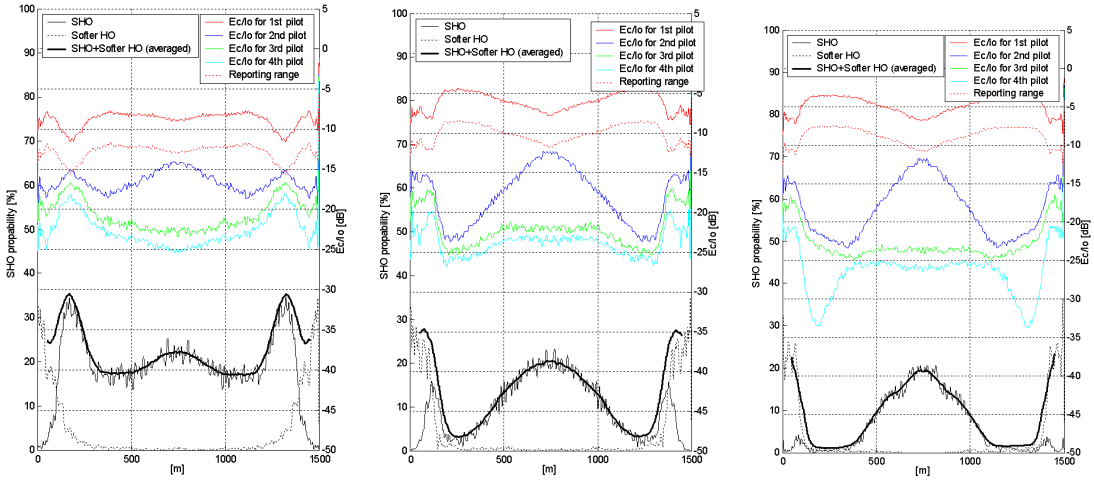

(a) 0° (b) MDT (c) EDT

Figure 6.20: SHO and softer HO probability and the level of first 4 pilots from main lobe to back lobe in 33°/6° scenario, antenna height 25 m and site spacing 1.5 km. (a) 0° downtilt, (b) optimal MDT, (c) optimal EDT

6.2.6 Capacity Gain

Capacity gains in all simulation scenarios are shown in Table 6.3. The higher the antenna positions and the smaller the site spacing, the higher is the advantage of tilting by the means of capacity gain. With antenna height of 25 m and site spacing of 2.5 km, the capacity gains are between 0.4 % and 5.5 %, but with antenna height of 45 m and site spacing of 1.5 km the capacity gains vary from 13.8 % to 53.9 %. The results also show that with wide antennas MDT gives slightly better results compared to narrow antennas. Capacity gains of EDT are higher in almost every case (0% - 10 % difference). The highest capacity gains, up to 54 % are seen in 6-sectored scenario, which indicates that greatest advantages of EDT can be achieved in 6-sectored network.

Table 6.3: Capacity gains in service probability in all simulated network topologies and site configurations.

Site spacing / Antenna height	EDT 3-sec 6°	EDT 3-sec 12°	EDT 6-sec 6°	MDT 3-sec 6°	MDT 3-sec 12°	MDT 6-sec 6°
1.5 km						
25m	18.7 %	1.8 %	21.6 %	16.6 %	3.7 %	15.4 %
35m	35.4 %	8.3 %	39.3 %	29.8 %	8.9 %	27.8 %
45m	52.3 %	13.8 %	53.9 %	42.1 %	15.7 %	36.7 %
2.0 km						
25m	7.5 %	1.3 %	6.9 %	7.6 %	1.9 %	7.4 %
35m	16.6 %	3.3 %	17.5 %	13.0 %	3.5 %	13.9 %
45m	27.7 %	6.2 %	29.7 %	24.8 %	6.6 %	22.6 %
2.5 km						
25m	4.0 %	0.4 %	5.4 %	5.5 %	0.7 %	3.6 %
35m	10.1 %	1.8 %	14.1 %	10.4 %	1.8 %	8.8 %
45m	19.5 %	2.3 %	24.6 %	17.8 %	4.1 %	17.0 %

6.3 Error Analysis

6.3.1 Impact of Different Traffic Mix Scenarios

The simulations were made with speech users only, although the 3G systems are developed mainly for data transmission purposes. However, from the capacity and coverage point of view, it should result in parallel results regardless of user types, only the total throughput matters. To verify this, a set of simulations was ran with circuit and packet switched data connections. In the traffic mix, 50 % of users were in 12.2 kbps speech connection, 25 % of users were in 64 kbps circuit switched (CS) data connection, and the rest 25 % of users were in 128 kbps non-real-time (NRT) packet switched (PS) connection. CS switched speech and data connection have higher priority than the PS switched NRT data connection. The following traffic mix scenarios (TS) were used:

TS1: Homogenous traffic mix without indoor users
TS2: Homogenous traffic mix with indoor users
TS3: 70 % / 30 % indoor / outdoor traffic mix

Two different network loadings were established. In the low-load scenario there were 1000, 500, and 500 users, and in the high load scenario there were 2000, 1000, and 1000 users for speech, CS data, and PS data connection, respectively. The characteristics for indoor users were standard deviation of slow fading 12 dB and indoor loss 15 dB. The simulations were done for 6-sec 6° scenario with antenna height of 35 m, and site spacing of 1.5 km, with both, electrical and mechanical downtilt.

In Figure 6.21 and Figure 6.22, results for traffic mix simulations with EDT and MDT, respectively, are shown. In all low loaded scenarios, the service probability is about 100 % with low downtilt angles, and starts to decrease after 6° downtilt. With MDT, the decrease is significantly lesser than with EDT. Consequently, network with EDT is more coverage limited than with MDT. In high loaded scenarios, SP in MDT drops faster compared to EDT due to increasing amount of overhead caused by softer HO connections. Due to the priorities, SP of speech or CS data connection is always the highest and SP of NRT PS data is always the lowest. Optimal downtilt angles for EDT and MDT are shown in Table 6.4 and Table 6.5, respectively. In MDT, optimal angles in different TSs vary at the maximum 0.4° from speech users only scenario, because increasing amount of softer HO connections is preventing the optimal angle to increase. With EDT, there is more variations in optimal downtilt angle: TS 1 varies at the maximum 0.8° from speech only scenario, and increasing the amount of indoor users increases the difference in optimal downtilt angle compared to speech users only scenario. However, optimal downtilt angle can be chosen by 128 kbps PS connection, since service probability of speech users still remains in high level. As a conclusion, method for defining optimal downtilt angle may cause as much error than different TS scenarios themselves.

Table 6.4: Optimal downtilt angles in different traffic mix scenarios with EDT.

TS / Service	Speech Only	TS 1	TS 2	TS 3
Speech 12.2 kpbs	6.3	6.4	6.4	6.9
64 kbps CS	-	6.6	6.7	7.1
128 kbps PS	-	7.1	7.2	7.8

Table 6.5: Optimal downtilt angles in different traffic mix scenarios with MDT.

TS / Service	Speech Only	TS 1	TS 2	TS 3
Speech 12.2 kbps	5.9	6.1	6.1	6.3
64 kbps CS	-	6.1	6.1	6.3
128 kbps PS	-	6.1	6.1	6.2

6.3.2 Simulator Errors

Simulator environment contains always some non-idealities. In the simulations for the thesis, a static simulator is used, although mobile radio network is a rather dynamic environment. The reliability of the static simulator relies on statistical analysis, and a big amount of snapshots in Monte Carlo analysis. However, the used COST-231-Hata propagation model is not perfect. It is known to work rather poorly in high-density urban environment, where building height exceeds antenna height. However, in Tampere area, which is a typical Finnish city environment, average building height is clearly below 25 m,

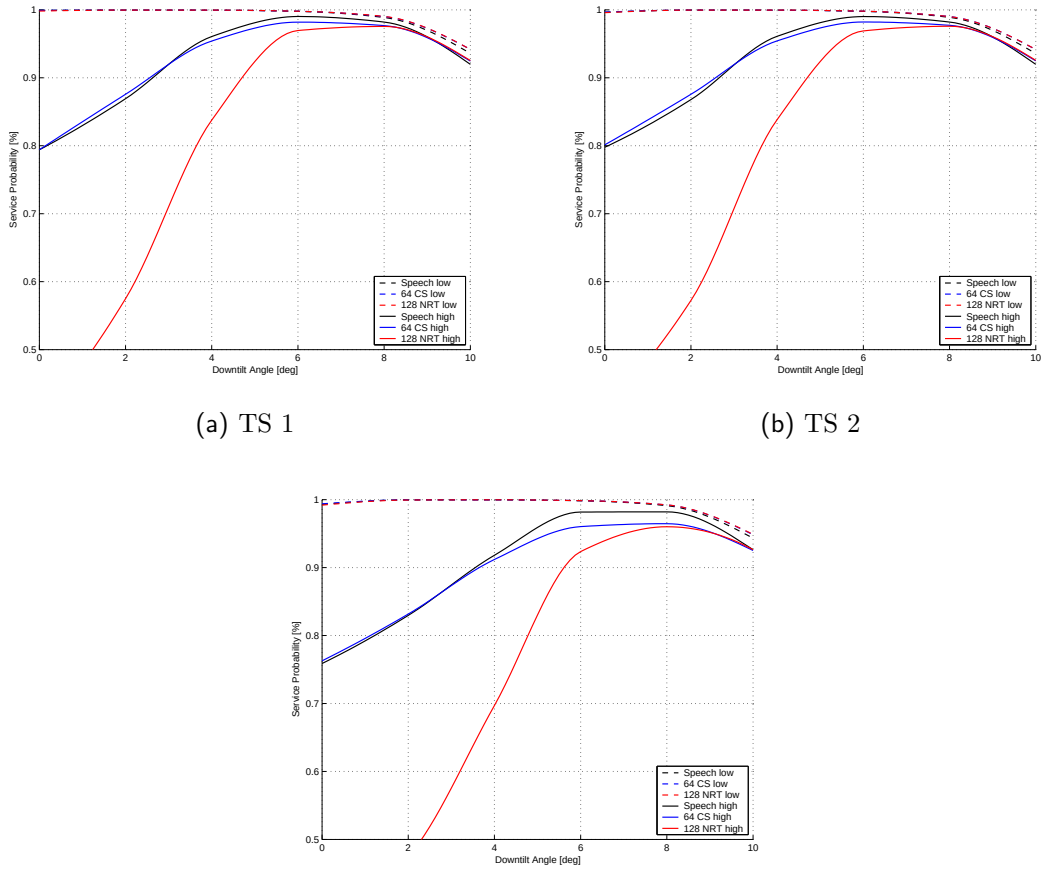

(a) TS 1

(b) TS 2

(c) TS 3

Figure 6.21: Service probability as a function of downtilt angle in different traffic mix scenarios (EDT): (a) TS 1, (b) TS 2, and (c) TS 3.

which is the lowest used antenna height in the simulations. In more urban area, with lower antenna height, usage of, e.g., ray-tracing model should be considered. The reliability of COST-231 -model is partly based on model tuning, whereafter correction factors can be set. The model tuning was not performed for the simulations, but commonly known and used correction factors for the particular environment were used. The propagation model does not take reflections into account, so in some situations, such as in city center, signal can propagate in unexpected areas. The traffic distribution in the simulator was assumed to be homogenously distributed, and the used high and low load user amounts can differ from reality, but a great number of snapshots should compensate this rather well. In the simulations, the exact validity of absolute values is not highly necessary, it is enough that they are well in line with real world. The most important is that the results of different scenarios are comparable with each others.

The definition of optimal downtilt angle may not be optimal, since it is rather simple, and is based on only service probability achieved with different downtilt angles, although service probability is a pretty inclusive indicator in the network, at least from user point of view. The results are best valid with the site and antenna configurations used in the simulations. Site spacings smaller than 1.5 km and greater than 2.5 km can result in unexpected phenomena.

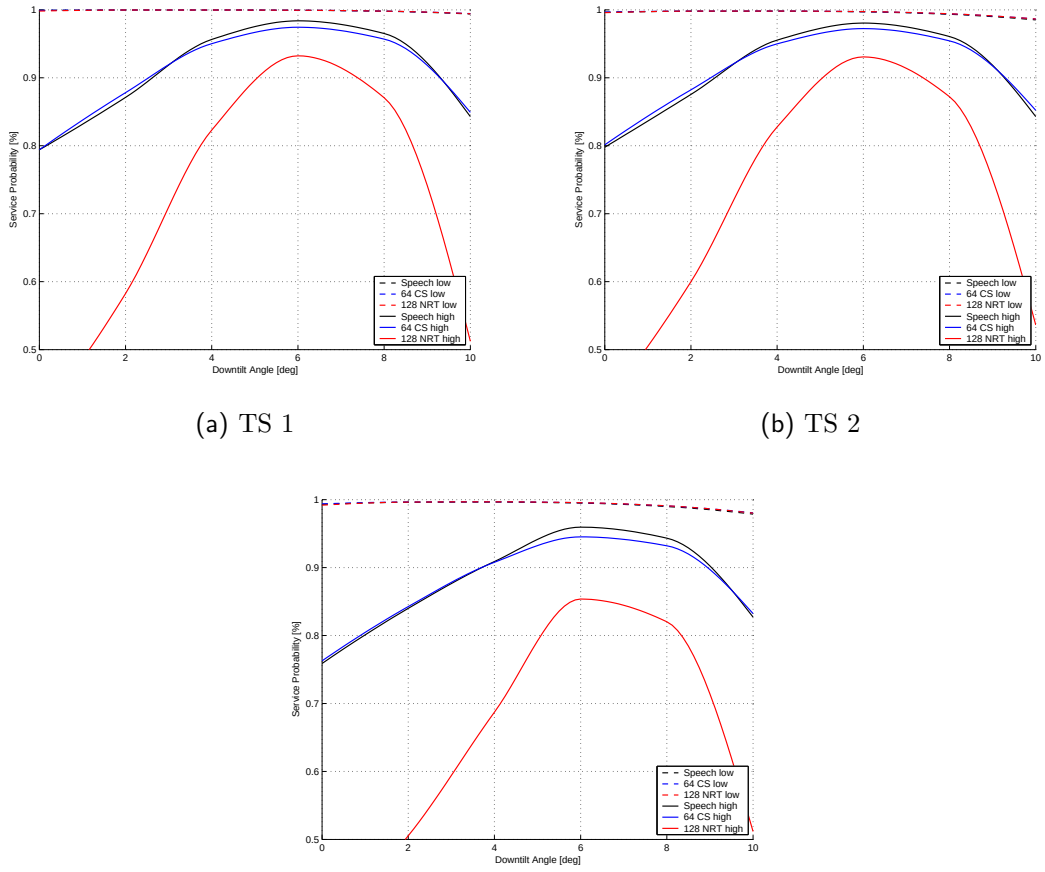

(a) TS 1

(b) TS 2

(c) TS 3

Figure 6.22: Service probability as a function of downtilt angle in different traffic mix scenarios (MDT): (a) TS 1, (b) TS 2, and (c) TS 3.

6.4 Guidelines for RNP

The simulations were carried out not only from academic interest, but also to produce valuable information to be used in RNP of real networks. The results can help radio network planners to set downtilt angles to networks with different configurations, instead of, i.e., constant 4°-6° degree downtilt angle. Of course, a real network always differs from the network layout used in the simulations, which may require manual tuning of downtilt angles on some sectors. Also higher downtilt angles near hot-spots need to be considered. Already in the used environment, e.g., water areas could have been taken into consider, and antennas pointing towards water areas should be either downtilted more or redirected. Also other similar terrain-specific details should be considered. For more precise information on particular network environment, the use of radio network simulator, such as the NetAct simulator, is recommended, although simulations in large network are very time consuming. However, proposed optimal downtilt angles can give good base-lines for antenna downtilting, and ease network tuning.

It should be taken into account, that the simulations are fully valid only with the particular antenna types used in the simulations. Differences in antenna pattern, as nulls and side and back lobes affect coverage of sector. Of course, if antennas of wider horizontal

beamwidth are used, increased amount of softer HO connection will affect network capacity. The higher the antennas are placed, the more important is it to pay attention to downtilting antennas properly. Although majority of current networks are using 3 sectors per base station, higher capacity requirements in future force operators to increase the capacity of network. Adding more sectors provides more capacity (e.g., almost double capacity from 3 to 6 sectors), and it is therefore one solution in growing network capacity. The most important rules for maximizing capacity and minimizing interference by antenna configuration are to use as high antenna positions as possible, with antennas of narrow vertical beamwidth. If there are enough resources, antennas with electrical downtilting and 6 sectors with antennas of narrow horizontal give the best capacity within the configurations considered in the thesis.

Chapter 7

Discussion and Conclusions

Topology planning is an important part of radio network planning. Antenna selection and configuration have a direct impact on signal transmission. Antenna downtilt can help to limit signal propagation outside the desired cell area, and therefore increase signal strength in cell area and decrease caused interference to adjacent cells. In the thesis, the impact of antenna downtilt on different site locations and antenna configurations was studied in macrocellular environment. The results are based on COST-231-Hata propagation model and Monte Carlo approach.

Optimal antenna downtilt angles were found for each configuration. The optimal downtilt angles vary from 3.4° to 10.3°. As expected by geometrical reasons, antenna height has a great effect on optimal downtilt angle, and also site spacing affects significantly; the higher the antennas and the smaller the site spacing, the greater the downtilt angle needs to be. Also the higher the antennas are installed, the more sensitive network is for proper antenna downtilting. High antenna positions with too small downtilt angles result in high interference levels that cause capacity of WCDMA to drop prominently.

Antenna vertical beamwidth has a significant effect on antenna downtilting. Wider vertical beamwidth requires greater downtilt angles. Narrow antennas require more precise downtilting; small error in downtilt angle can cause significant drop in service probability. Wide antennas perform quite the contrary; the changes in network behavior with downtilt angles between 4°-12° are rather minimal. However, optimal downtilt could still be found and there is no reason for not use proper downtilting also with wide antennas.

6-sectored network behaves similarly to 3-sectored network with narrow antennas. Only with mechanical downtilt, additional overhead caused by increased amount of softer handovers needs to be taken into consider. Antennas should be downtilted no more than necessary, since service probability drops fast with too great downtilt angles. Although it is obvious that MDT antennas are cheaper than antennas with EDT, it is recommended to use EDT antennas. EDT provides slightly better capacity, and clearly lower interference levels.

The errors in the simulations and given optimal downtilt angles were discussed in the end of Chapter 6. The results are valid only for macrocellular environment, which should be remembered especially when building a network in a dense city center with antennas close to average building height. The simulated optimal antenna downtilt angles can be used as a base line for antenna downtilt before final tuning of the antenna system. In addition to traditional RNP, the results could also be used as an input for automated CAEDT system algorithms.

As continuation to the work, the simulation results will be verified by a field measurement campaign in a real WCDMA network in a city environment. Also a more sophisticated equation is being developed for defining the optimal downtilt angles. The effect of downtilting on SHO areas was studied in the thesis, but more studies need to be made in order to find out can downtilt be used as a tool for optimizing SHO gain in the network. In an indoor environment, WCDMA is estimated to operate as a narrowband system. This may cause troubles for RNP, especially in optimizing parameters and SHO algorithms, and will be an interesting field for studies.

Bibliography

[1] W. C. Y. Lee. *Mobile Communication Engineering.* McGraw-Hill, 1997.

[2] I. Forkel, A. Kemper, and R. Hermans R. Pabst. The effect of electrical and mechanical antenna down-tilting in UMTS networks. In *The Third International Conference on 3G Mobile Communication Technologies*, pages 86–90, 2002.

[3] S.C. Bundy. Antenna downtilt effects on CDMA cell-site capacity. In *Radio and Wireless Conference, RAWCON 99*, pages 99–102, 1999.

[4] J. Niemelä and J. Lempiäinen. Impact of mechanical antenna downtilt on performance of WCDMA cellular network. In *Proc. 59th Vehicular Technology Conference, Milan*, 2004.

[5] J. Lempiäinen and M. Manninen, editors. *UMTS Radio Network Planning, Optimization and QoS Management.* Kluwer Academic Publishers, 2003.

[6] H. Holma and A. Toskala. *WCDMA for UMTS.* John Wiley & Sons Ltd, 2000.

[7] J. Laiho, A. Wacker, and T. Novosad. *Radio Network Planning and Optimisation for UMTS.* John Wiley & Song Ltd, 2002.

[8] 3GPP TS 25.101 V3.16.0, Release 1999. *User Equipment (UE) radio transmission and reception (FDD).*

[9] R. Prasad, W. Mohr, and W. Konhäuser, editors. *Third Generation Mobile Communication Systems.* Artech House, 2000.

[10] 3GPP TS 25.301 version 3.9.0 Release 1999. *Radio Interface Protocol Architecture.*

[11] 3GPP TS 25.211 version 3.9.0 Release 1999. *Physical channels and mapping of transport channels onto physical channels (FDD).*

[12] T. Ojanperä and R. Prasad. *Wideband CDMA for Third Generation Mobile Communications.* Artech House, 1998.

[13] J. Lempiäinen and M. Manninen. *Radio Interface System Planning for GSM/GPRS/UMTS.* Kluwer Academic Publishers, 2001.

[14] 3GPP TS 25.214 version 3.9.0 Release 1999. *Physical layer procedures (FDD).*

[15] 3GPP TR 25.922 V3.7.0 , Release 1999. *Radio resource management strategies.*

[16] A. J. Viterbi. *CDMA: Principles of Spread Spectrum Communication.* Addison-Wesley, 1995.

[17] K. Sipilä, J. Laiho-Steffens, and A. Wacker. Soft handover gains in a fast power controlled WCDMA uplink. In *Proc. 49th IEEE VTC Conf., Houston, Texas, May 1999*, pages 1594–1598, 1999.

[18] 3GPP TR 21.905 V3.7.0 , Release 1999. *Vocabulary for 3GPP Specifications.*

[19] J.D. Parsons. *The Mobile Radio Propagation Channel.* Pentech Press Ltd, 1992.

[20] 3GPP TR 25.943 V5.1.0 , Release 5. *Deployment aspects.*

[21] W. C. Y. Lee. *Mobile Communication Design Fundamentals.* John Wiley & Sons, Inc., 1993.

[22] M. K. Simon and M. Alouini. *Digital Communication over Fading Channels.* John Wiley & Sons, Inc., 2000.

[23] K.R. Schaubach, N.J. Davis, and T.S. Rappaport. A ray tracing method for predicting path loss and delay spread in microcellular environments. In *Proc. 42nd Vehicular Technology Conference, Denver*, pages 932–935, 1992.

[24] Y. Okumura, E. Ohmori, T. Kawano, and K. Fukuda. Field strenght and its variability in UHF and VHF land-mobile radio service. In *Review Electronic Communication Lab.*, pages 873–825, 1980.

[25] M. Hata. Empirical formula for propagation loss in land mobile services. In *IEEE Transactions on Vehicular Technology*, pages 317–325, 1980.

[26] J. Laiho. *Radio Network Planning and Optimisation for WCDMA*. PhD thesis, Helsinki University of Technology, 2002.

[27] J. Niemelä and J. Lempiäinen. Impact of base station locations and antenna orientations on UMTS radio network capacity and coverage evolution. In *Proc. IEEE 6th Int. Symp. on Wireless Personal Multimedia Communications Conf., Yokosuka*, pages 82–86, 2003.

[28] A . Wacker, J. Laiho-Steffens, K.Sipilä, and K. Heiska. The impact of the base station sectorisation on WCDMA radio network performance. In *Proc. 50th IEEE Vehicular Technology Conference*, pages 2611–2615, 1999.

[29] Kathrein web site [Online]. 790 - 2200 MHz base station antennas for mobile communications. <http://www.kathrein.de>, February 2004. Referred 26.8.2004.

[30] Allgon web site [Online]. <http://www.lgpallgon.com>, 2004. Referred 26.8.2004.

[31] J. Niemelä and J. Lempiäinen. Impact of the base station antenna beamwidth on capacity in WCDMA cellular networks. In *in Proc. IEEE 57th Vehicular Technology Conference, Jeju*, pages 80–84, 2003.

[32] J. Leino, M. Kolehmainen, and T. Ristaniemi. On the effect of pilot cancellation in WCDMA network. In *Vehicular Technology Conference*, pages 6–9, 2002.

[33] G. Wilson. Electrical downtilt through beam-steering versus mechanical downtilt. In *Proc. 42nd Vehicular Technology Conference, Denver*, pages 1–4, 1992.

[34] L. Zordan, N. Rutazihana, and N. Engelhart. Capacity enhancement of cellular mobile network using a dynamic electrical down-tilting antenna system. In *Proc. 50th Vehicular Technology Conference, Vancouver*, pages 1915–1918.

[35] P. Nobileau. Remote tilt benefits 2G and 3G. *Wireless Europe*, July 2003.

[36] T. Isotalo, J. Niemelä, and J. Lempiäinen. Electrical antenna downtilt in UMTS network. In *Proc. 5th European Wireless Conference, Barcelona*, pages 265–271, 2004.

[37] 3GPP TS 25.104 V3.12.0, Release 1999. *BS Radio transmission and Reception (FDD).*

Appendix A

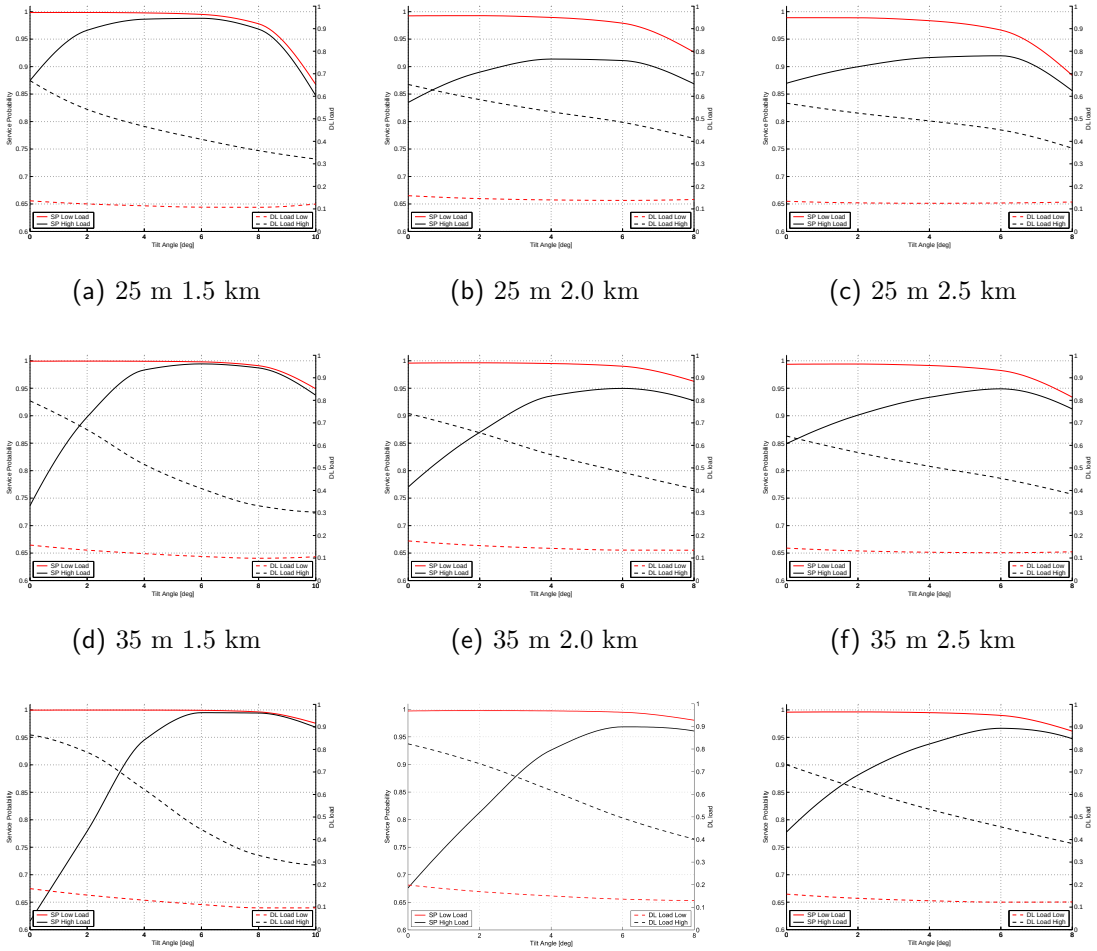

(a) 25 m 1.5 km (b) 25 m 2.0 km (c) 25 m 2.5 km

(d) 35 m 1.5 km (e) 35 m 2.0 km (f) 35 m 2.5 km

(g) 45 m 1.5 km (h) 45 m 2.0 km (i) 45 m 2.5 km

Figure 1: Impact of downtilt angle on service probability and DL load in EDT 3-sectored 65°/6° scenario for 25 m, 35 m, and 45 m base station antenna heights and 1.5 km, 2.0 km, and 2.5 km site spacing.

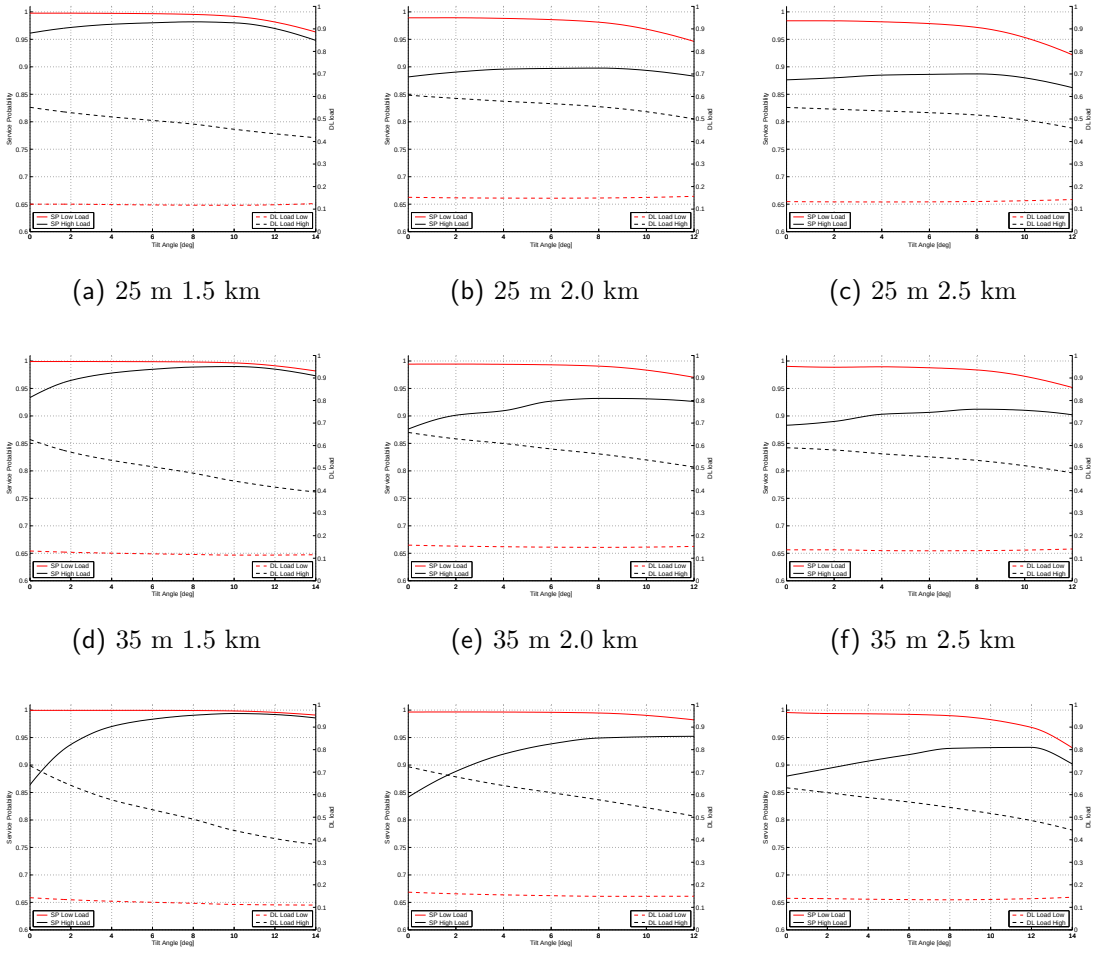

(a) 25 m 1.5 km (b) 25 m 2.0 km (c) 25 m 2.5 km

(d) 35 m 1.5 km (e) 35 m 2.0 km (f) 35 m 2.5 km

(g) 45 m 1.5 km (h) 45 m 2.0 km (i) 45 m 2.5 km

Figure 2: Impact of downtilt angle on service probability and DL load in EDT 3-sectored 65°/12° scenario for 25 m, 35 m, and 45 m base station antenna heights and 1.5 km, 2.0 km, and 2.5 km site spacing.

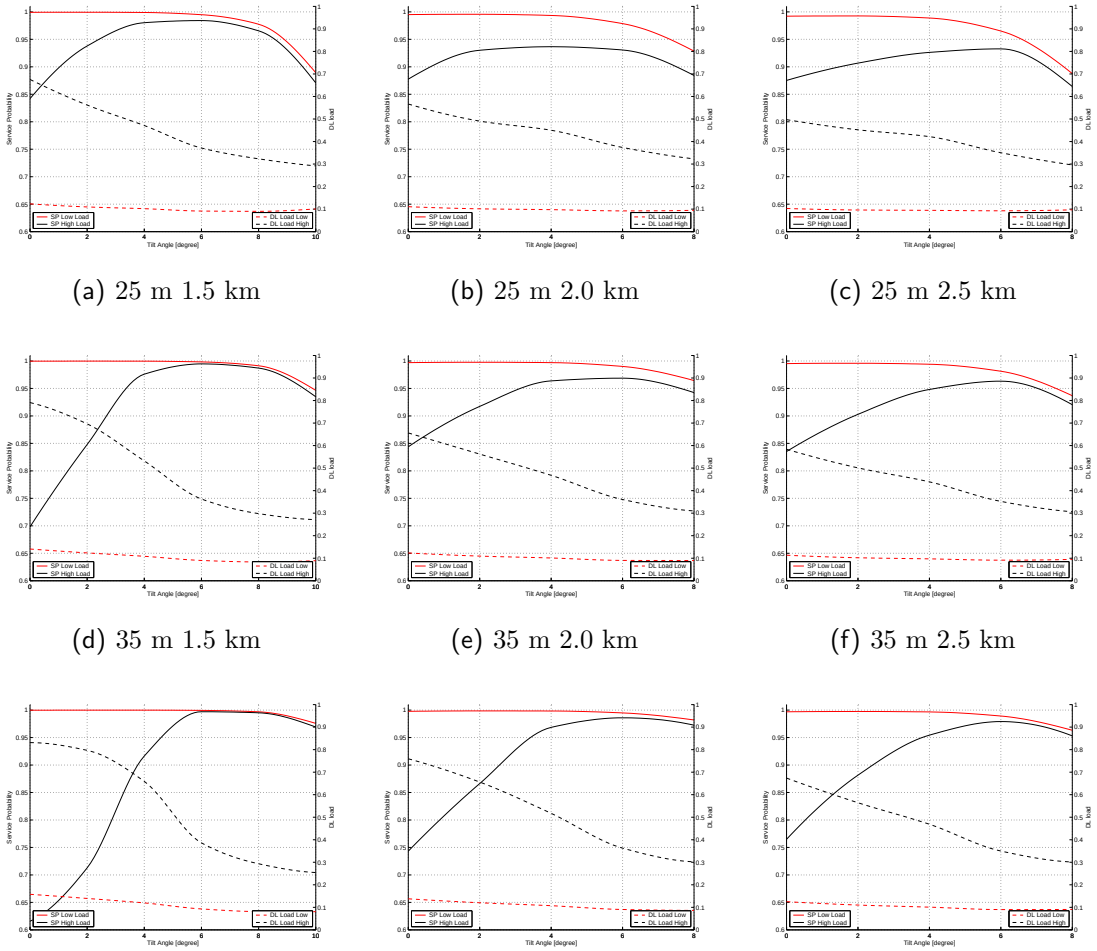

(a) 25 m 1.5 km (b) 25 m 2.0 km (c) 25 m 2.5 km

(d) 35 m 1.5 km (e) 35 m 2.0 km (f) 35 m 2.5 km

(g) 45 m 1.5 km (h) 45 m 2.0 km (i) 45 m 2.5 km

Figure 3: Impact of downtilt angle on service probability and DL load in EDT 6-sectored 33°/6° scenario for 25 m, 35 m, and 45 m base station antenna heights and 1.5 km, 2.0 km, and 2.5 km site spacing.

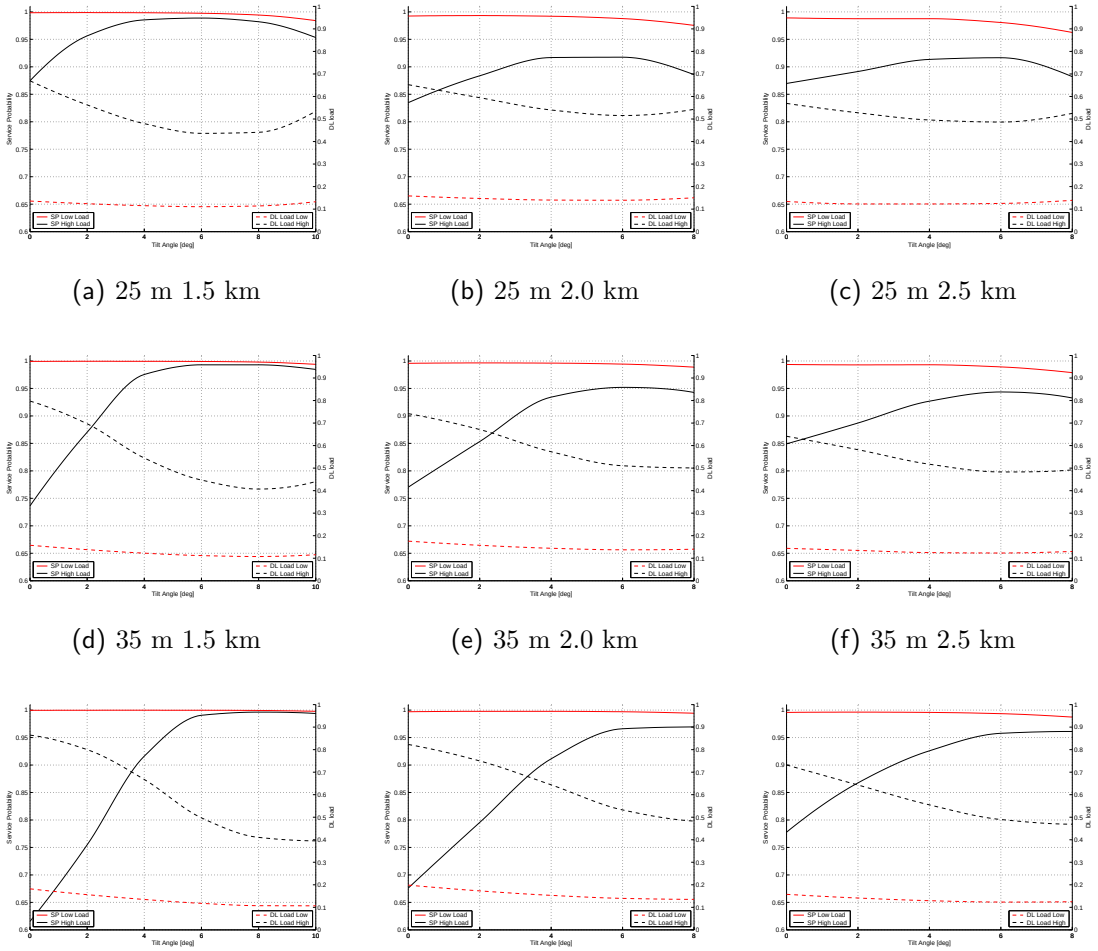

(a) 25 m 1.5 km (b) 25 m 2.0 km (c) 25 m 2.5 km

(d) 35 m 1.5 km (e) 35 m 2.0 km (f) 35 m 2.5 km

(g) 45 m 1.5 km (h) 45 m 2.0 km (i) 45 m 2.5 km

Figure 4: Impact of downtilt angle on service probability and DL load in MDT 3-sectored 65°/6° scenario for 25 m, 35 m, and 45 m base station antenna heights and 1.5 km, 2.0 km, and 2.5 km site spacing.

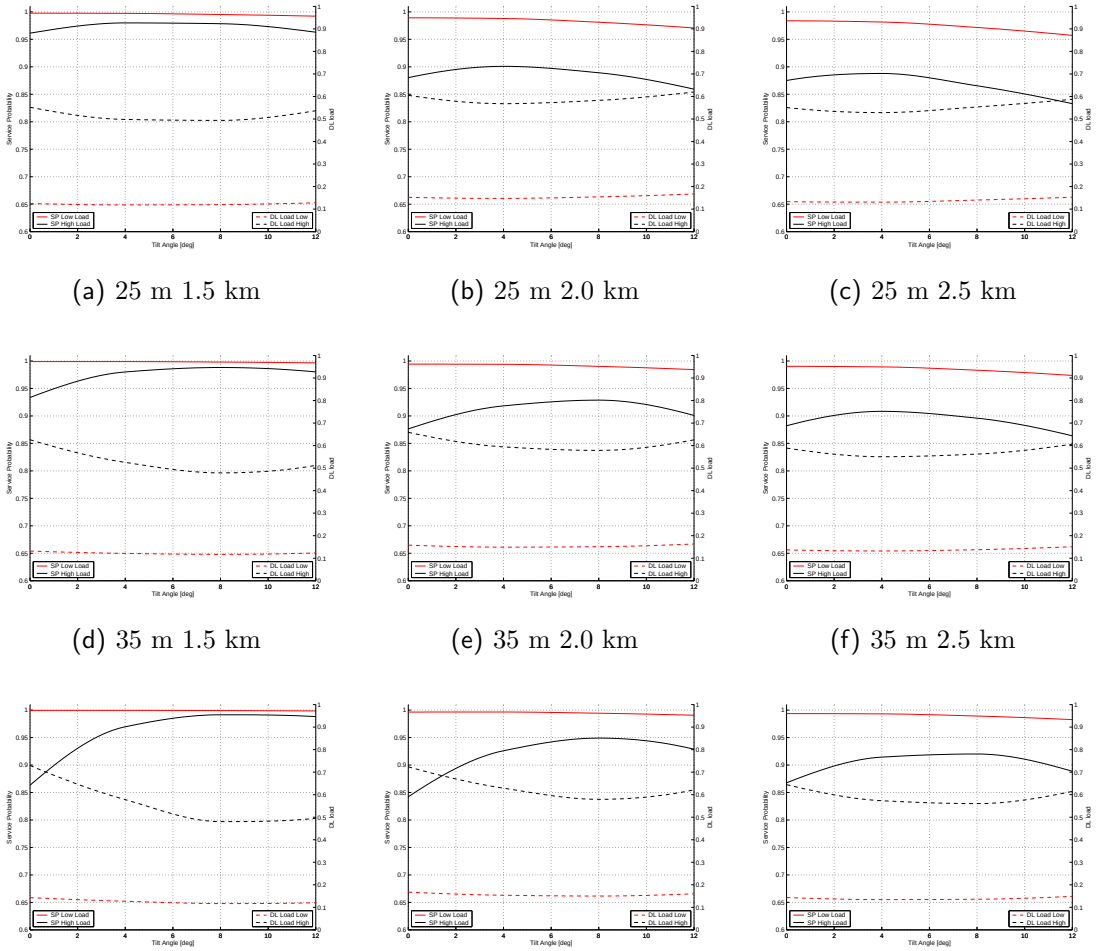

(a) 25 m 1.5 km (b) 25 m 2.0 km (c) 25 m 2.5 km

(d) 35 m 1.5 km (e) 35 m 2.0 km (f) 35 m 2.5 km

(g) 45 m 1.5 km (h) 45 m 2.0 km (i) 45 m 2.5 km

Figure 5: Impact of downtilt angle on service probability and DL load in MDT 3-sectored 65°/12° scenario for 25 m, 35 m, and 45 m base station antenna heights and 1.5 km, 2.0 km, and 2.5 km site spacing.

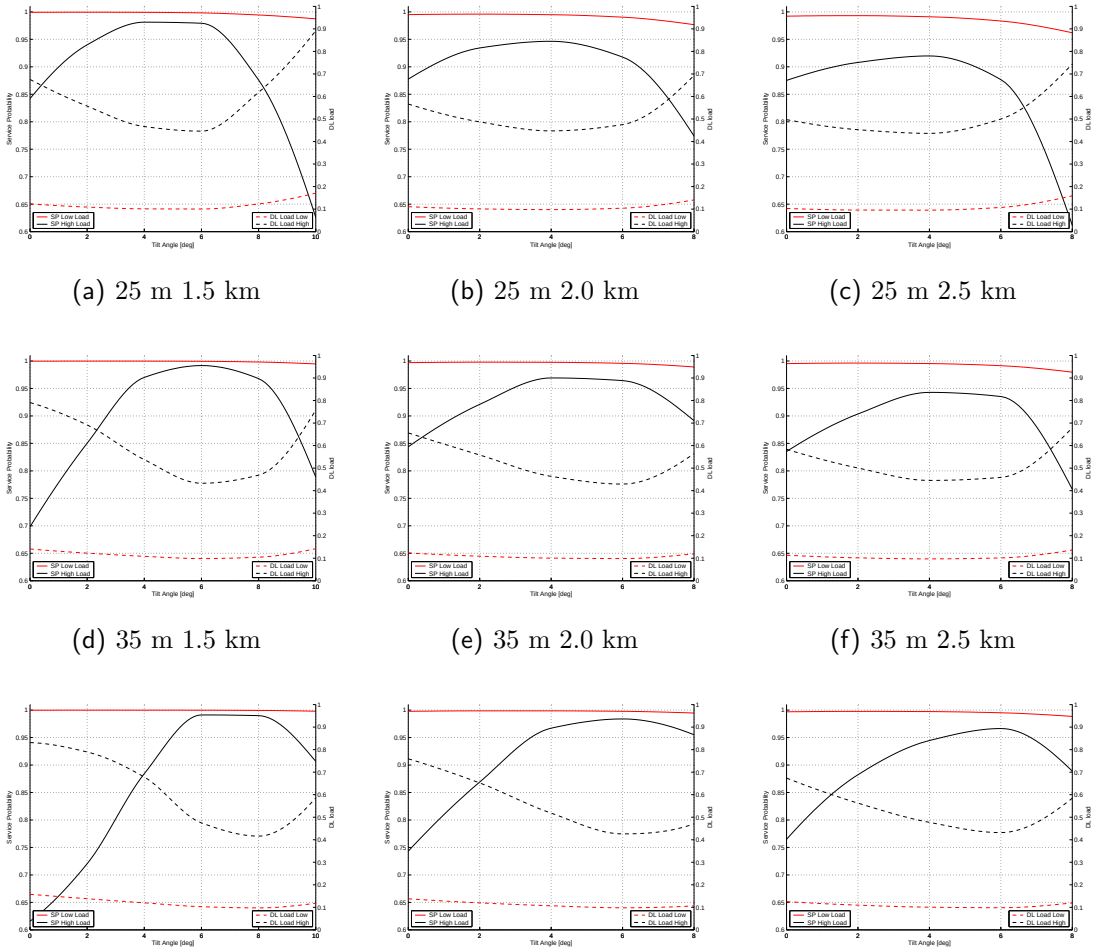

(a) 25 m 1.5 km (b) 25 m 2.0 km (c) 25 m 2.5 km

(d) 35 m 1.5 km (e) 35 m 2.0 km (f) 35 m 2.5 km

(g) 45 m 1.5 km (h) 45 m 2.0 km (i) 45 m 2.5 km

Figure 6: Impact of downtilt angle on service probability and DL load in MDT 6-sectored 33°/6° scenario for 25 m, 35 m, and 45 m base station antenna heights and 1.5 km, 2.0 km, and 2.5 km site spacing.

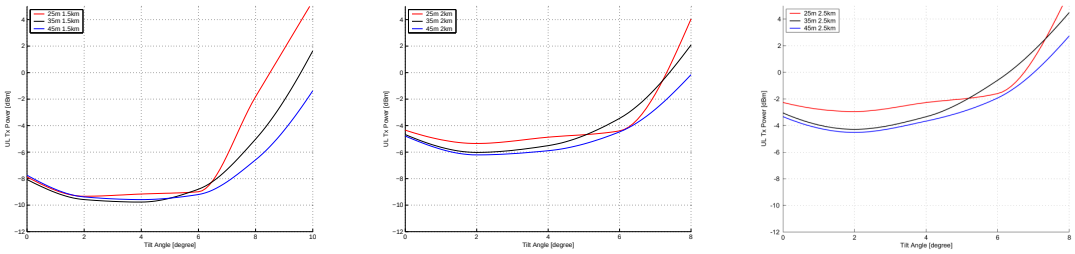

(a) 1.5 km (b) 2.0 km (c) 2.5 km

Figure 7: Impact of downtilt angle on average UL transmit power in EDT 3-sectored 65°/6° scenario for 25 m, 35 m, and 45 m base station antenna heights and 1.5 km, 2.0 km, and 2.5 km site spacing.

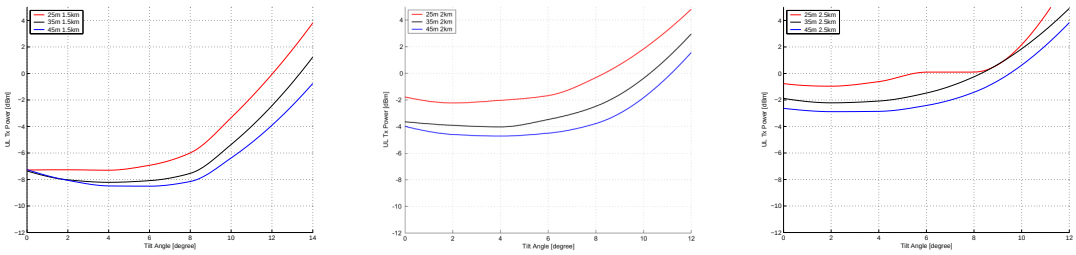

(a) 1.5 km (b) 2.0 km (c) 2.5 km

Figure 8: Impact of downtilt angle on average UL transmit power in EDT 3-sectored 65°/12° scenario for 25 m, 35 m, and 45 m base station antenna heights and 1.5 km, 2.0 km, and 2.5 km site spacing.

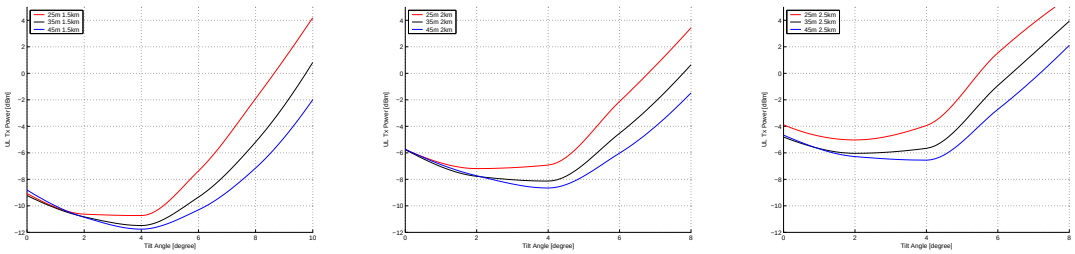

(a) 1.5 km (b) 2.0 km (c) 2.5 km

Figure 9: Impact of downtilt angle on average UL transmit power in EDT 6-sectored 33°/6° scenario for 25 m, 35 m, and 45 m base station antenna heights and 1.5 km, 2.0 km, and 2.5 km site spacing.

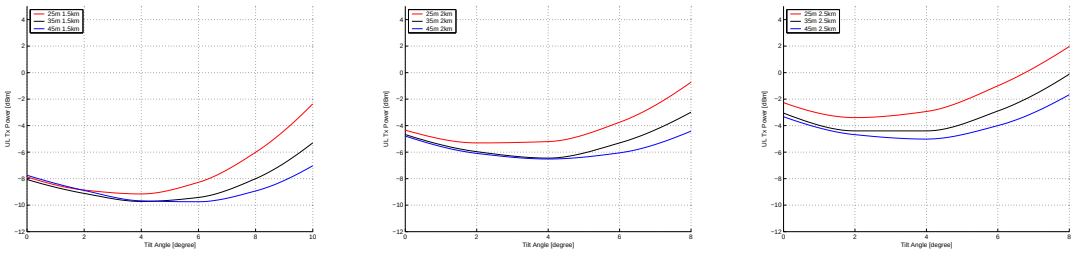

(a) 1.5 km (b) 2.0 km (c) 2.5 km

Figure 10: Impact of downtilt angle on average UL transmit power in MDT 3-sectored 65°/6° scenario for 25 m, 35 m, and 45 m base station antenna heights and 1.5 km, 2.0 km, and 2.5 km site spacing.

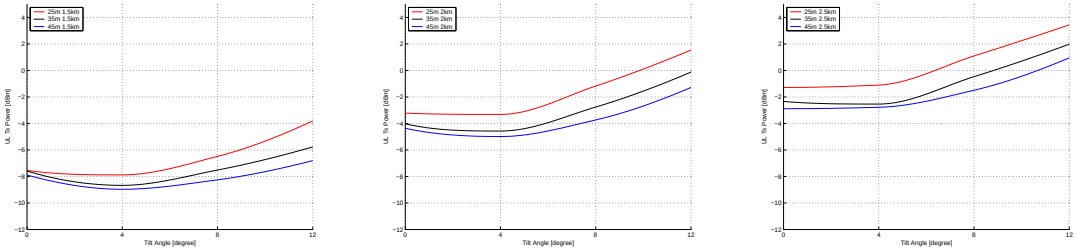

(a) 1.5 km (b) 2.0 km (c) 2.5 km

Figure 11: Impact of downtilt angle on average UL transmit power in MDT 3-sectored 65°/12° scenario for 25 m, 35 m, and 45 m base station antenna heights and 1.5 km, 2.0 km, and 2.5 km site spacing.

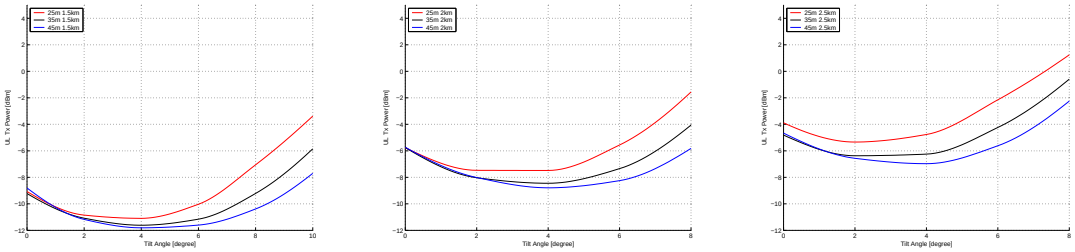

(a) 1.5 km (b) 2.0 km (c) 2.5 km

Figure 12: Impact of downtilt angle on average UL transmit power in MDT 6-sectored 33°/6° scenario for 25 m, 35 m, and 45 m base station antenna heights and 1.5 km, 2.0 km, and 2.5 km site spacing.

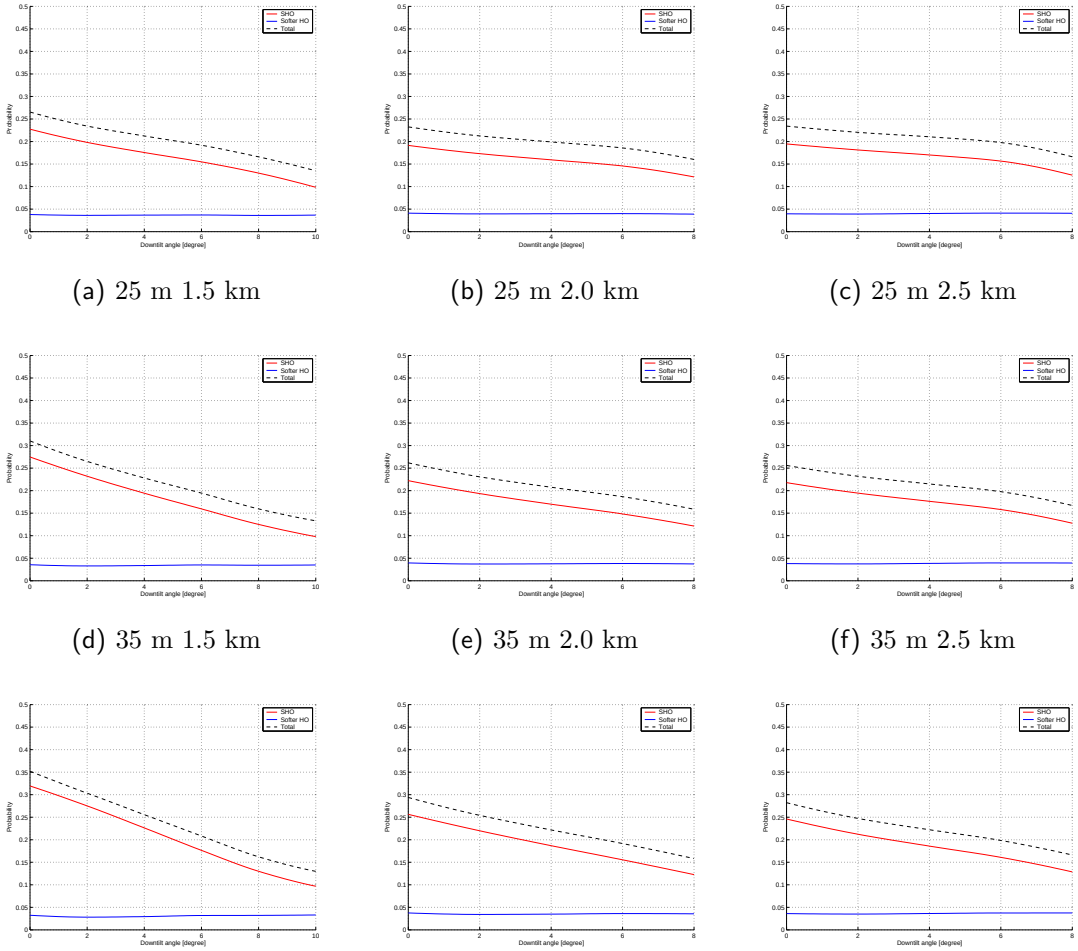

(a) 25 m 1.5 km (b) 25 m 2.0 km (c) 25 m 2.5 km

(d) 35 m 1.5 km (e) 35 m 2.0 km (f) 35 m 2.5 km

(g) 45 m 1.5 km (h) 45 m 2.0 km (i) 45 m 2.5 km

Figure 13: Impact of downtilt angle on SHO and softer HO probability in EDT 3-sectored 65°/6° scenario for 25 m, 35 m, and 45 m base station antenna heights and 1.5 km, 2.0 km, and 2.5 km site spacing.

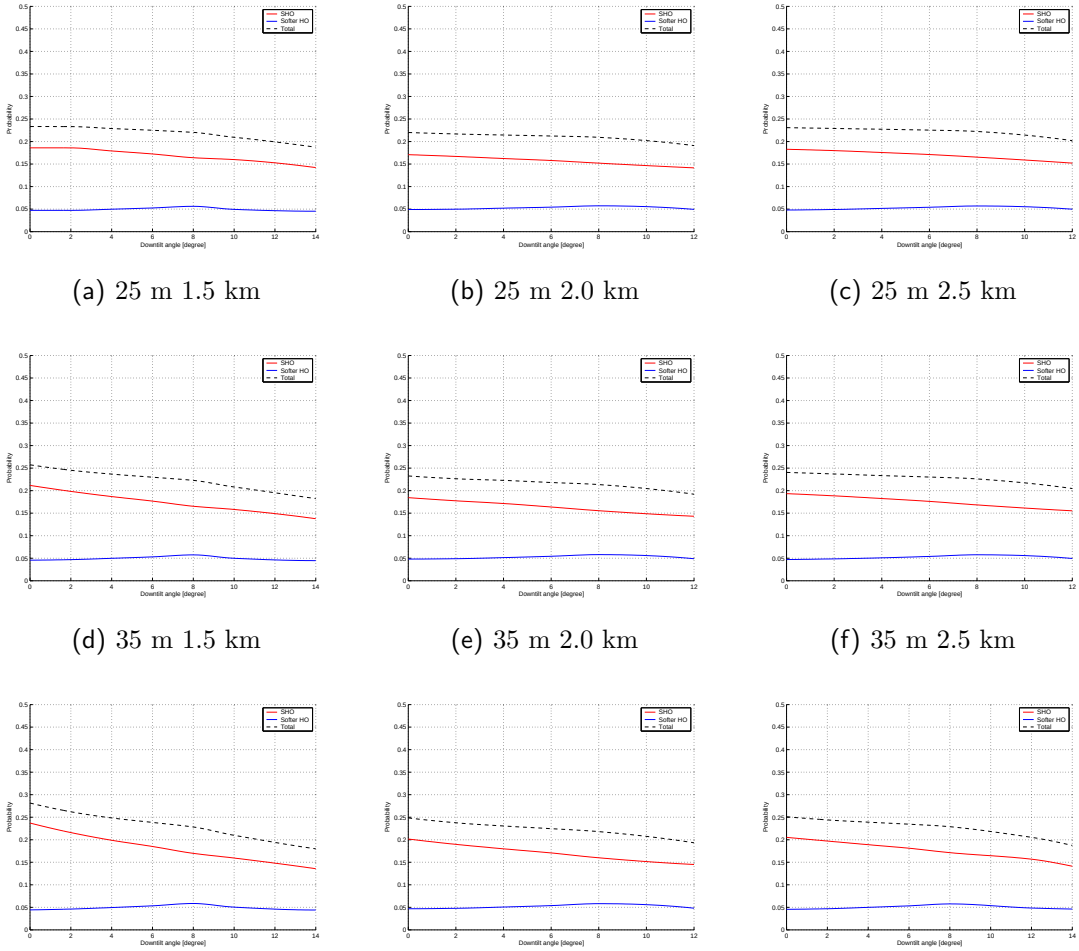

(a) 25 m 1.5 km (b) 25 m 2.0 km (c) 25 m 2.5 km

(d) 35 m 1.5 km (e) 35 m 2.0 km (f) 35 m 2.5 km

(g) 45 m 1.5 km (h) 45 m 2.0 km (i) 45 m 2.5 km

Figure 14: Impact of downtilt angle on SHO and softer HO probability in EDT 3-sectored 65°/12° scenario for 25 m, 35 m, and 45 m base station antenna heights and 1.5 km, 2.0 km, and 2.5 km site spacing.

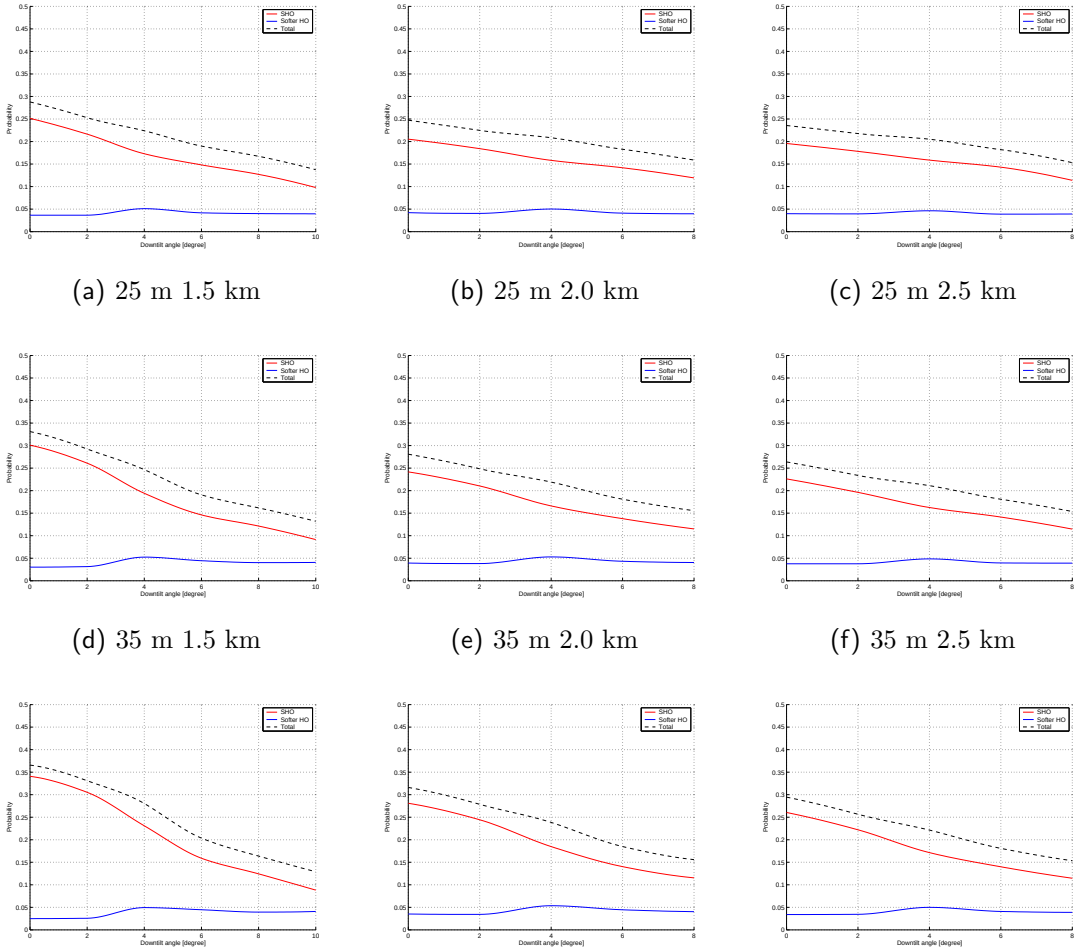

(a) 25 m 1.5 km (b) 25 m 2.0 km (c) 25 m 2.5 km

(d) 35 m 1.5 km (e) 35 m 2.0 km (f) 35 m 2.5 km

(g) 45 m 1.5 km (h) 45 m 2.0 km (i) 45 m 2.5 km

Figure 15: Impact of downtilt angle on SHO and softer HO probability in EDT 6-sectored 33°/6° scenario for 25 m, 35 m, and 45 m base station antenna heights and 1.5 km, 2.0 km, and 2.5 km site spacing.

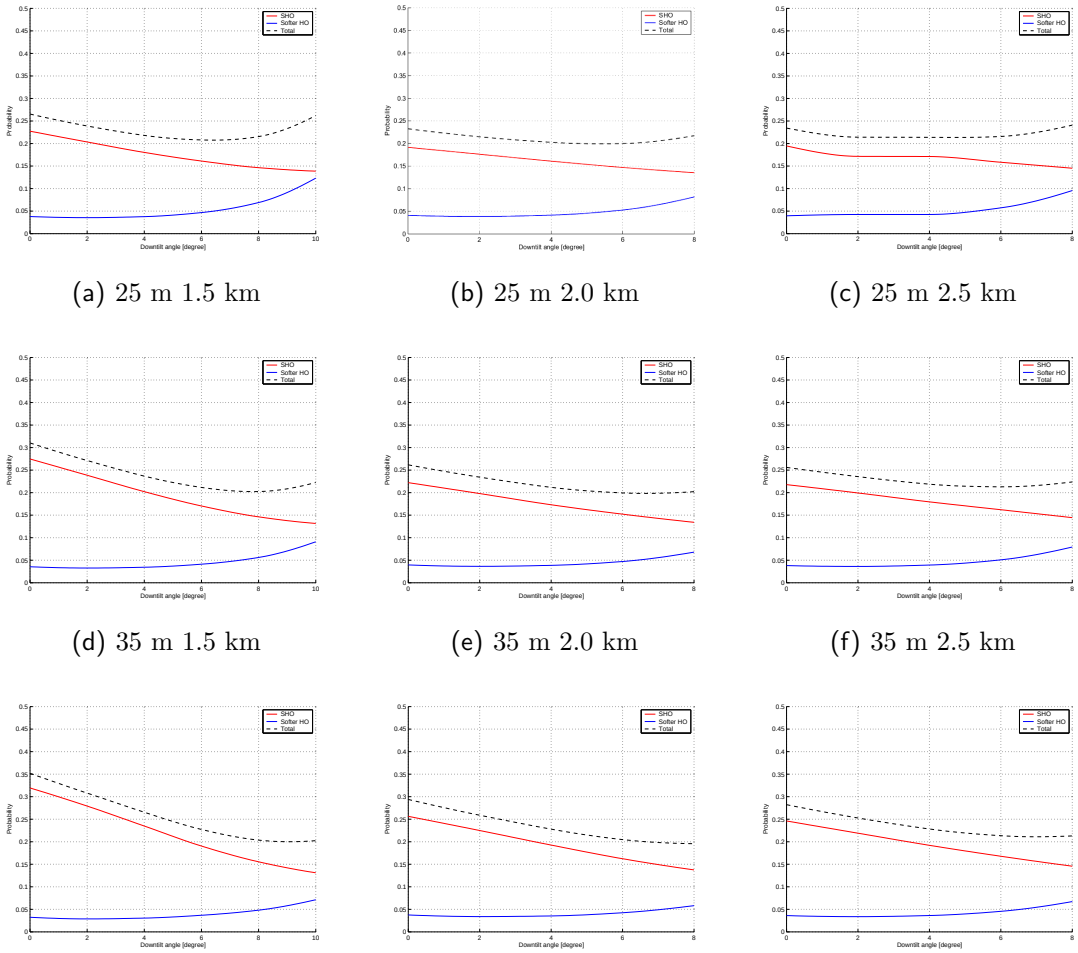

(a) 25 m 1.5 km (b) 25 m 2.0 km (c) 25 m 2.5 km

(d) 35 m 1.5 km (e) 35 m 2.0 km (f) 35 m 2.5 km

(g) 45 m 1.5 km (h) 45 m 2.0 km (i) 45 m 2.5 km

Figure 16: Impact of downtilt angle on SHO and softer HO probability in MDT 3-sectored 65°/6° scenario for 25 m, 35 m, and 45 m base station antenna heights and 1.5 km, 2.0 km, and 2.5 km site spacing.

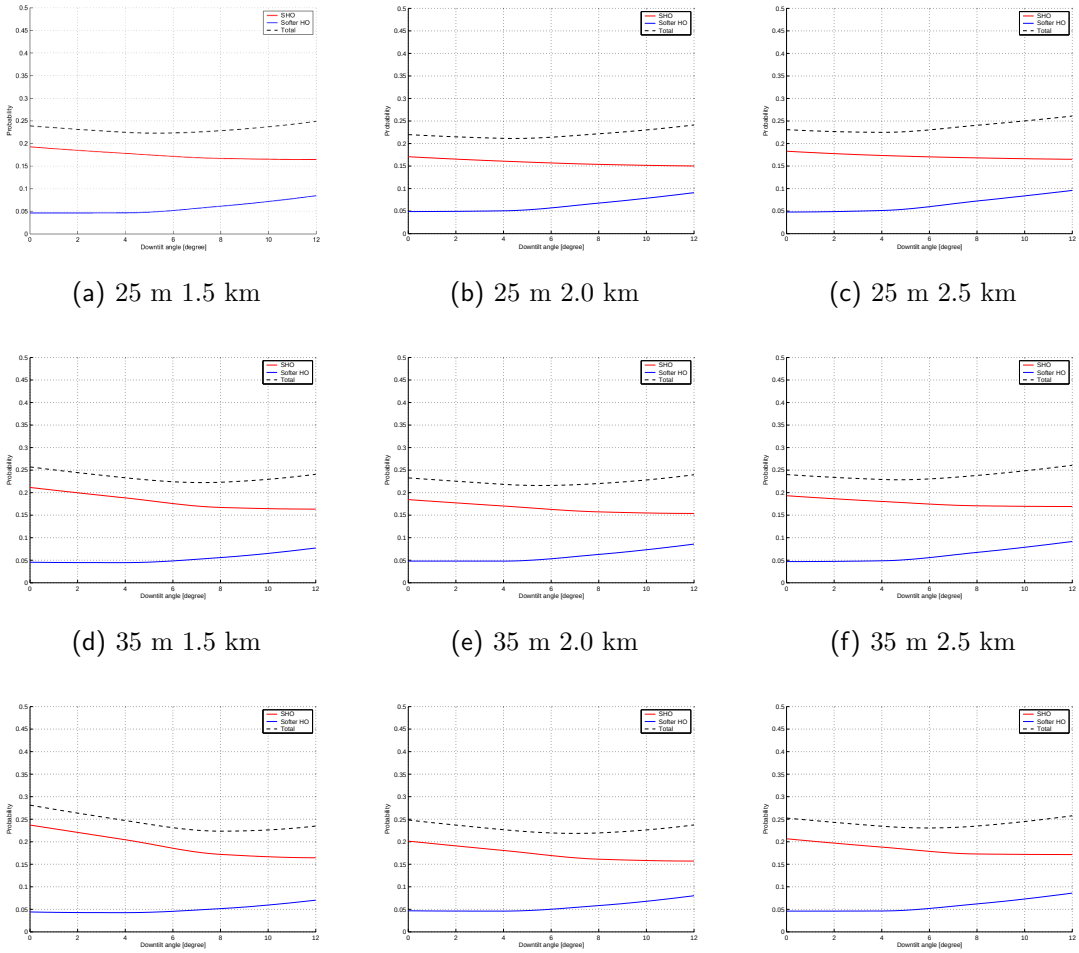

(a) 25 m 1.5 km (b) 25 m 2.0 km (c) 25 m 2.5 km

(d) 35 m 1.5 km (e) 35 m 2.0 km (f) 35 m 2.5 km

(g) 45 m 1.5 km (h) 45 m 2.0 km (i) 45 m 2.5 km

Figure 17: Impact of downtilt angle on SHO and softer HO probability in MDT 3-sectored 65°/12° scenario for 25 m, 35 m, and 45 m base station antenna heights and 1.5 km, 2.0 km, and 2.5 km site spacing.

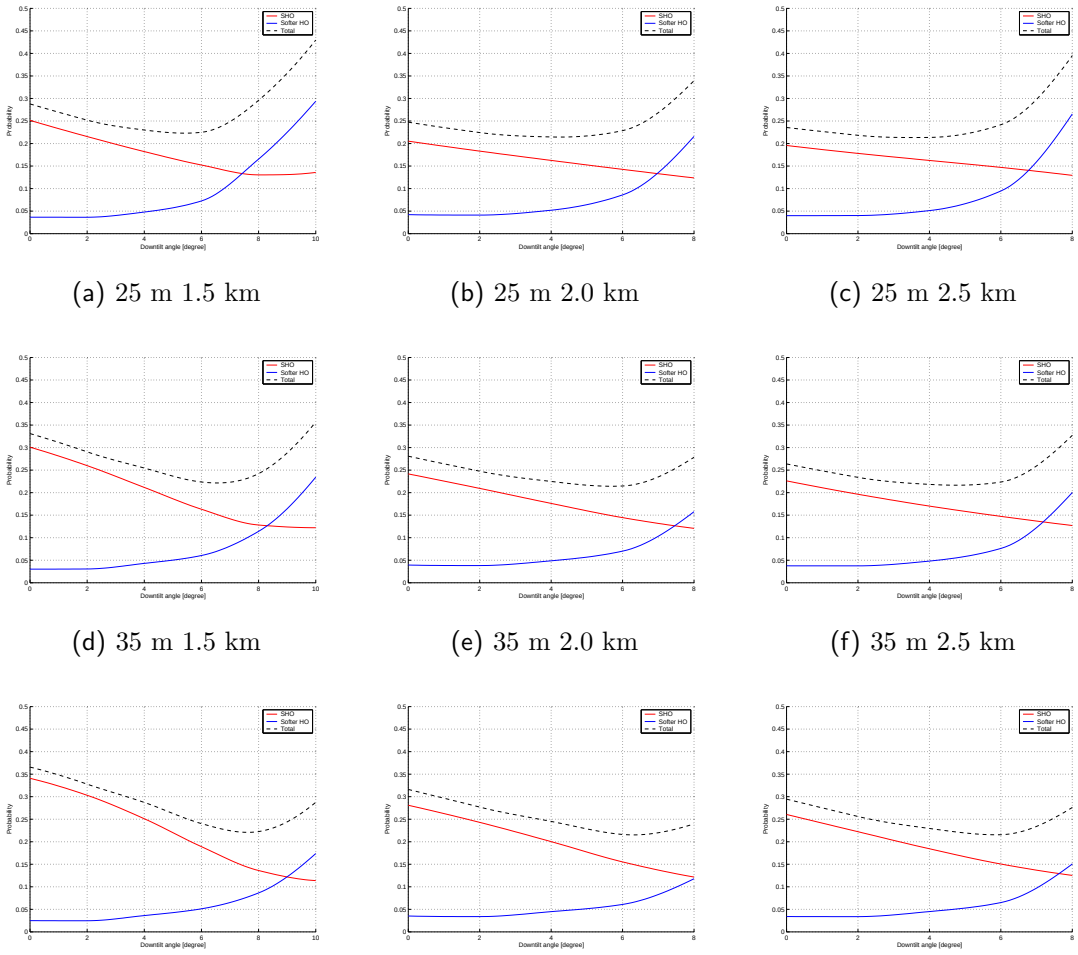

(a) 25 m 1.5 km (b) 25 m 2.0 km (c) 25 m 2.5 km

(d) 35 m 1.5 km (e) 35 m 2.0 km (f) 35 m 2.5 km

(g) 45 m 1.5 km (h) 45 m 2.0 km (i) 45 m 2.5 km

Figure 18: Impact of downtilt angle on SHO and softer HO probability in MDT 6-sectored 33°/6° scenario for 25 m, 35 m, and 45 m base station antenna heights and 1.5 km, 2.0 km, and 2.5 km site spacing.